K/SUB/93-XJ947 /1

K-25

OAK RIDGE
K-25 SITE

LOCKHEED MARTIN

TECHNICAL DOCUMENTATION OF HGSYSTEM/UF_6 MODEL

S. R. Hanna
J. C. Chang
J. X. Zhang
The Earth Technology Corporation
196 Baker Avenue
Concord, MA 01742

Prepared October 1994
under Subcontract 1AK-XJ947C for
MARTIN MARIETTA ENERGY SYSTEMS, INC.
managing the
Oak Ridge K-25 Site
Oak Ridge National Laboratory
Oak Ridge Y-12 Plant
under contract DE-AC05-84OR21400
and managing
Environmental Restoration and Waste Management
Activities
at Paducah Gaseous Diffusion Plant
Portsmouth Gaseous Diffusion Plant
under contract DE-AC05-76OR00001
for the
U.S. DEPARTMENT OF ENERGY

MANAGED BY
LOCKHEED MARTIN ENERGY SYSTEMS, INC.
FOR THE UNITED STATES
DEPARTMENT OF ENERGY

UCN-13671 (16 6-95)

K/SUB/93-XJ947

Gaseous Diffusion Plant
Safety Analysis Report Upgrade Program

TECHNICAL DOCUMENTATION OF HGSYSTEM/UF_6 MODEL

Date Published - January 1996

Document authored by
S. R. Hanna
J. C. Chang
J. X. Zhang
The Earth Technology Corporation
196 Baker Avenue, Concord, MA 01742
under Subcontract No. 1AK-XJ947C
October 1994

Document published by
LOCKHEED MARTIN ENERGY SYSTEMS, INC.
managing the
Oak Ridge K-25 Site
and
Oak Ridge Y-12 Plant
under contract DE-AC05-84OR21400
and managing
Environmental Restoration and Waste Management Activities
at Paducah Gaseous Diffusion Plant
and
Portsmouth Gaseous Diffusion Plant
under contract DE-AC05-76OR00001
for the
U.S. DEPARTMENT OF ENERGY

CONTENTS

CONTENTS (continued)

LIST OF FIGURES

LIST OF FIGURES (continued)

LIST OF TABLES

ABBREVIATIONS AND ACRONYMS

AFGL	Air Force Geophysical Laboratory
AIChE	American Institute of Chemical Engineers
API	American Petroleum Institute
ARAP	Aeronautical Research Associates Princeton
ATDD	Atmospheric Turbulence and Diffusion Division
BNWL	Battelle Northwest Laboratories (now PNL)
DOE	Department of Energy
EPA	Environmental Protection Agency
GDP	Gaseous Diffusion Plant
GPM	Gaussian Plume Model
HF	Hydrogen Fluoride
ISC	Industrial Source Complex
LLNL	Lawrence Livermore National Laboratory
LNG	Liquified Natural Gas
LPG	Liquified Petroleum Gas
MDA	Modelers Data Archive
NOAA	National Oceanic and Atmospheric Administration
NTIS	National Technical Information Service
ORGDP	Oak Ridge Gaseous Diffusion Plant (now Oak Ridge K-25 Site)
ORNL	Oak Ridge National Laboratory
OSTI	Office of Scientific and Technical Information
PNL	Pacific Northwest Laboratory (formerly BNWL)
RADM	Regional Acid Deposition Model
SAR	Safety Analysis Report
TIC	Technical Information Center (now OSTI)
UF_6	Uranium Hexafluoride
USAEC	United States Atomic Energy Commission
USDOC	United States Department of Commerce

EXECUTIVE SUMMARY

Objectives and Background

The U.S. Department of Energy has directed Martin Marietta Energy Systems, Inc., to upgrade the safety analyses for the gaseous diffusion plants at Paducah, Kentucky, and Piketon, Ohio. These safety analyses will require assessment of consequences of accidental releases of uranium hexafluoride (UF_6) to the atmosphere at these plants.

Energy Systems has previously conducted a review of available models and chosen the HGSYSTEM model as the basis for evaluating UF_6 releases. HGSYSTEM includes state-of-the-art dispersion algorithms for dense gases and treats the chemistry and thermodynamics of hydrogen fluoride (HF), a major product of the reaction of UF_6 with water vapor in the air. The HGSYSTEM model has achieved credibility within the hazardous-gas modeling community in industry and government.

The objective of this project was to incorporate additional capability into HGSYSTEM: UF_6 chemistry and thermodynamics, plume lift-off algorithms, and wet and dry deposition. The resulting model was to be evaluated using field experiments with UF_6 and other dense gases.

Expected Source Scenarios

Three major source emission scenarios were foreseen:

1. A valve or pipe on a 14-ton liquid UF_6 storage tank could break. The resulting time-variable release rate could be very large for a large opening (e.g., 10 cm) or relatively small for a small hole (e.g., 0.1 cm).

2. A 14-ton, liquid UF_6 storage tank could completely rupture, causing an instantaneous release of a large cloud of UF_6 vapor and particles.

3. A high-temperature gaseous release from a pipeline could occur within a large building and might enter the atmosphere through a vent stack on the roof or side of the building.

Model Technical Components

HGSYSTEM/UF_6 is a hybrid that combines the dispersion and HF thermodynamics aspects of HGSYSTEM with the chemistry and thermodynamic aspects of UF_6. The HGSYSTEM model consists of these nearly independent modules:

- HFPLUME - for an elevated HF jet
- AEROPLUME - for an elevated general aerosol (not HF) jet

- HEGADAS - for a ground-based continuous HF or other dense gas plume
- HEGABOX - for a ground-based instantaneous HF or other dense gas puff
- PGPLUME - for an elevated passive gas plume

The model contains limited source emission algorithms that only apply to HF. During the course of the HGSYSTEM/UF_6 project, Shell has continued to develop certain parts of HGSYSTEM, and we have coordinated our development efforts with them. Results of both of our model development efforts are combined in a separate technical document prepared by Shell.

UF_6 chemistry and thermodynamics algorithms have been combined with HF chemistry and thermodynamics algorithms in the AEROPLUME, HEGADAS, and HEGABOX modules of HGSYSTEM. Solutions are obtained by solving a set of fourteen simultaneous differential equations (involving chemistry, dispersion, and thermodynamics) using a proprietary solver (SPRINT-NAESOL) developed by Shell. As the proportion of UF_6 in the release decreases and the proportion of HF vapor increases, the HGSYSTEM/UF_6 solution approaches the basic HGSYSTEM solution for pure HF vapor releases.

A two-phase UF_6 release is likely to be initially denser than air because of the presence of UF_6 particles, the high molecular weight of UF_6 vapor, and the cooling of the mixture due to sublimation. As a result, an elevated plume may sink to the ground where it spreads out, thus following the principles of dense-gas slumping. However, the reaction of UF_6 vapor with water vapor will release heat, possibly causing the plume to become buoyant (less dense than air). The new model accounts for the possibility that this buoyant plume may "lift-off" the ground.

To account for gravitational settling of solid particles that are formed after a UF_6 release, a dry deposition algorithm has been added to HGSYSTEM/UF_6. This algorithm also accounts for dry deposition of gases and for wet deposition (rain-out) of gases and particles. The dry and wet deposition algorithms are applied as post-processors.

A state-of-the-art meteorological pre-processor has been included that allows parameters such as the friction velocity and the Monin-Obukhov length to be calculated from simple measurements of wind speed, cloudiness, and surface conditions. HGSYSTEM/UF_6 uses the friction velocity and the Monin-Obukhov length to calculate Richardson numbers, entrainment rates, dispersion rates, and the speed at which the plume or cloud is being advected downwind.

Two simple effects of buildings have been included as post-processors:

1. A canyon model constrains the plume from spreading beyond the building walls when the release is in a "canyon" between two large buildings.

2. A stand-alone model calculates concentrations on the roof and sides of a building when the release is from a vent stack on the building. In the case of the vent stack, it is assumed that the initial release is inside the building and the gas is passive (i.e., no more chemical reactions or thermodynamics effects will take place) once it exits the vent.

Evaluation of HGSYSTEM/UF_6

Three types of evaluations of the new model were made:

1. The HGSYSTEM code (1994, Shell Version 3.0, without UF_6) was evaluated with data from eight field studies discussed by Hanna, Chang, and Strimaitis.[1] The findings are as follows:

   - The 1994 Version 3.0 of the code produces results that are not much different from the results produced by the 1990 Version 1.0.
   - The new HEGABOX algorithm for instantaneous dense gas releases produces results in good agreement with the Thorney Island field data.
   - Performance measures for HGSYSTEM predictions are as good as those for the three or four best models that are clustered together on the model performance graphs.

2. When compared with concentration and lateral plume width observations from three French UF_6 field experiments, the HGSYSTEM/UF_6 model shows fair agreement, in general, at downwind distances beyond about 40 m. The model does exhibit a slight tendency to overpredict concentrations and underpredict lateral plume widths at those distances. In the near-field, at downwind distances less than 40 m, the results are uncertain because observations were taken at a 1-m height, which was 2 m below the level at which the plume was released. Since these UF_6 releases were in the vapor phase and relatively small, chemistry and thermodynamics effects were not evident in the three field tests, and the HGSYSTEM/UF_6 model reduces to a passive gas Gaussian plume model.

3. The UF_6 chemistry and thermodynamics algorithms in the hybrid code were checked by comparisons with the equilibrium analytical solutions by Rodean.[2] Agreement between the two solutions is generally good. Any minor differences are thought to be caused by the time-dependent chemical reaction assumption in HGSYSTEM/UF_6.

User's Guide

A separate report by Post[3] contains a user's guide for HGSYSTEM Version 3.0, including the generic improvements described in Sect. 6 of this report. An addendum to the current report contains specific information on how to set up input files for UF_6 and run the AEROPLUME/UF_6, HEGABOX/UF_6, and HEGADAS/UF_6 modules (see Appendix C).

---

[1] S. R. Hanna, J. C. Chang, and D. G. Strimaitis, "Hazardous Gas Model Evaluation with Field Observations," *Atmos. Environ.*, 27A, pp. 2265-2285, 1993.

[2] H. C. Rodean, *Toward More Realistic Material Models for Release and Dispersion of Heavy Gases*, UCRL-53902, DE 900 12015, Lawrence Livermore National Laboratory, Livermore, CA 94551, 1989.

[3] L. Post, *HGSYSTEM 3.0 User's Manual*, TNER.94.058, Thornton Research Centre, Shell Research Ltd., 1994.

1. OBJECTIVES AND BACKGROUND OF STUDY

The primary objective of this study has been development and testing of a new or updated computer model to simulate the dispersion of UF_6 and other gases to support the Gaseous Diffusion Plant (GDP) Safety Analysis Report (SAR) Upgrade Program. Martin Marietta Energy Systems, Inc., has the responsibility for this program. The GDPs under consideration are the Paducah and Portsmouth Gaseous Diffusion Plants, located in Paducah, Kentucky, and Piketon, Ohio, respectively. Energy Systems also has the objective of including some general enhancements to the revised model, such as accounting for the effects of transient releases, averaging times, concentration fluctuations, buildings and terrain, and up-to-date meteorological parameterizations. These improvements would be valid for any type of chemical release.

Between 1978 and 1985, Energy Systems, under prime contract to the U.S. Department of Energy (DOE), developed and improved a model (PLM89A) to simulate the dispersion of uranium hexafluoride (UF_6) (Bloom et al., 1989). In 1985, an external peer review identified factors that could limit the adequacy of PLM89A and suggested an alternative approach. DOE then directed Energy Systems to stop further development of PLM89A and directed the National Oceanic and Atmospheric Administration (NOAA) to develop an alternative model (TRIAD) described by Hicks et al. (1989). PLM89A had been used intermittently since 1985, but up until the present project was begun, no significant work had been done to incorporate the comments generated by the peer review, to incorporate more recent information, or to bring PLM89A up to present quality assurance requirements.

About 1992, under subcontract to Energy Systems, Aeronautical Research Associates Princeton (ARAP) Group, Princeton, New Jersey, reviewed the models available. They identified existing computer models that possibly were adequate (or could be easily adapted) for the atmospheric dispersion of UF_6 and similar dense, reactive gases (Sykes and Lewellen, 1992). After initially examining 37 models, the authors focused on these five:

- PLM89A
- TRIAD
- HGSYSTEM, developed by Witlox et al. (1990) of Shell Research, Ltd., and available through the American Petroleum Institute (API)
- ADAM, developed by Raj and Morris (1987) and available from the U.S. Air Force
- SLAB, developed by Ermak (1990) and available from Lawrence Livermore National Laboratory

PLM89A and TRIAD were the only models specifically developed for UF_6 dispersion. HGSYSTEM and SLAB were based on widely accepted dense gas models, while HGSYSTEM and ADAM included the chemistry and phase behavior of hydrogen fluoride (HF). Having concluded that all these models needed revisions, ARAP made specific technical recommendations regarding how each model could be modified.

ARAP then recommended that Energy Systems either (1) revise PLM89A since it already included UF_6 chemistry and was most familiar to Energy Systems personnel or (2) revise HGSYSTEM because it was widely accepted and included HF chemistry. After reviewing the ARAP recommendations, Energy Systems decided that revising HGSYSTEM was the best option. The HGSYSTEM model was selected by Energy Systems for the following reasons.

- HGSYSTEM was developed to simulate dense gas dispersion and included modules for the chemistry and phase behavior involved in HF dispersion.
- The model was not proprietary, so SAR reviewers could be provided with all details used in the dispersion analyses.
- The modular nature of HGSYSTEM would allow someone familiar with the model to make the necessary changes relatively easily and timely.
- If, in the limit of pure HF releases and general dense gas and aerosol releases, the UF_6 version of HGSYSTEM could be reduced to the original HGSYSTEM, then the new HGSYSTEM/UF_6 model would be more acceptable to regulatory agencies that had extensively evaluated and recognized the basic HGSYSTEM in the past.

The HGSYSTEM/UF_6 model was required to address certain mechanisms, materials, and types of releases. These are presented in Sects. 1.1-1.4.

1.1 PHYSICAL MECHANISMS TO BE TREATED BY NEW MODEL

The HGSYSTEM/UF_6 model had to incorporate the latest technology for dense gas and atmospheric dispersion. Therefore, the new model had to accomplish the following:

- Account for the trajectory of the plume and the entrainment of ambient air into the plume in each of the regions the plume might go through: negative, neutral, and positive buoyancy.
- Account for possible transitions between an elevated and a ground-hovering plume (descent to ground) and subsequent lift-off of the plume as its buoyancy increases.
- Account for energy and mass exchanges with the ground for a ground-hovering plume, including the effects of dry and wet deposition.
- Account for gravity spreading in calculations involving the dynamics of the dense plume.
- Include turbulent dispersion algorithms to treat instantaneous, steady-state, and time-varying releases because accidental releases considered in the SARs are transient.
- Account for effects of restrictions to plume growth by canyons because the Portsmouth GDP is located in hilly terrain and both GDPs contain very large buildings that can produce a canyon-like effect.
- Include estimates of the turbulent fluctuations in the predicted concentrations in order to estimate the variations of concentration with averaging times and the probability magnitude of peak concentrations.
- Develop improved methods for parameterizing meteorological variables.

1.2 MATERIALS AND CHEMICAL REACTIONS TO BE TREATED BY NEW MODEL

Models such as HGSYSTEM can handle transport and dispersion of releases of dense gases and account for effects of plume thermodynamics. However, aside from HF, the original HGSYSTEM model did not consider any materials whose chemistry and phase behavior are important for the GDP SAR Upgrade Program. The new model had to be able to simulate (1) the chemical reactions of UF_6 with water vapor (which forms UO_2F_2 and HF) and (2) the simultaneous dispersion of two or three ideal gases of any molecular weight and of two or more materials in liquid or solid phase.

Large UF_6 releases involve simultaneous consideration of the phase behavior between solid and gaseous UF_6 and kinetics of the UF_6-water reaction. This reaction causes changes in energy and composition, which cause a change in density and therefore in the buoyancy of the plume. Kinetics of the UF_6-water reaction are determined by the amounts of UF_6 and water vapor in the plume and the degree of turbulent mixing within the plume. Kinetics are also affected by the phase composition of UF_6 in the plume. Energy Systems chemists found that UF_6 reacts relatively slowly with ***liquid*** water (Barber, 1994), so the reaction of UF_6 is assumed to take place only with water ***vapor***. UO_2F_2 and HF reaction products exist in their simplest forms: UO_2F_2 solid and HF gas. These chemical and phase transitions, along with their corresponding energy changes, had to be considered in the dispersion model.

1.3 RELEASE SCENARIOS TO BE TREATED BY NEW MODEL

Accidental UF_6 release scenarios considered in SARs are usually transient (time-varying) with durations ranging from a few seconds to a few hours. Scenarios include a rupture or leak in a 14-ton liquid cylinder, a gas jet from a pipe break or building vent, and a large initial volume resulting from complete failure of a process facility. Potential releases can be at ground level or elevated and directed at any vertical angle, occur in open areas (e.g., a storage yard), or be influenced by large nearby buildings. The model does not need to explicitly simulate all these different release types but needs to provide reasonable approximations to them with suitable initial calculations. Examples of some initial calculations used to describe the release scenarios for input to PLM89A are cited by Williams (1985a; 1985b; 1986).

1.4 INPUT, OUTPUT, LANGUAGE REQUIREMENTS OF NEW MODEL

Input to the HGSYSTEM/UF_6 model ahd to be user-friendly. Inputs should be reasonably obtained numbers. Default values must be provided for those inputs which may be difficult to estimate. Since health consequences are expressed in a variety of time-averages of concentrations, output must include concentrations as a function of averaging time for the major chemical species as functions of distance. Other quantities, such as plume height or average plume density, should be output as diagnostic aids and as aids to understanding results. Output must be in the form of tables and either graphs or data (files) that can be easily graphed. The computerized form of the model should be written in FORTRAN for a 386- or 486-compatible computer.

2. OVERVIEW OF CHARACTERISTICS OF EXISTING MODELS (PLM89A AND HGSYSTEM)

The new HGSYSTEM/UF_6 model has been developed as a hybrid model containing the best attributes of the HGSYSTEM and PLM89A models plus enhancements to account for several additional phenomena, as shown in Fig. 2-1.

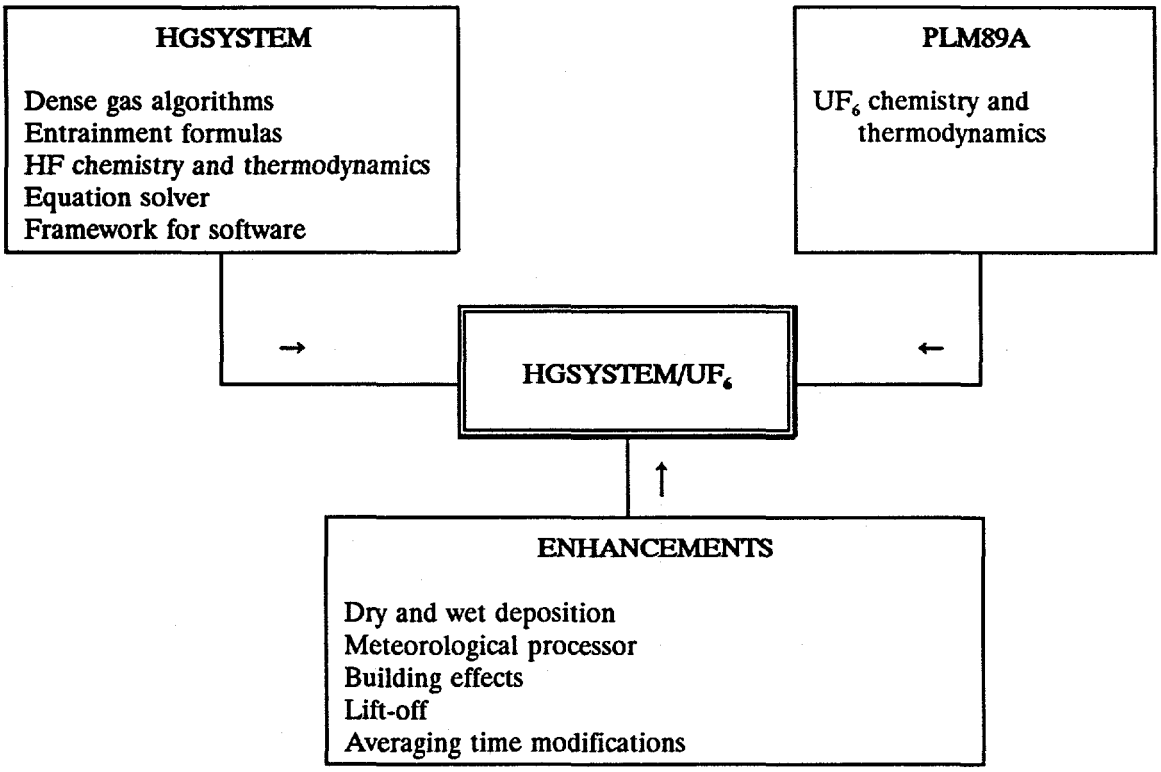

Fig. 2-1. The new HGSYSTEM/UF_6 hybrid model.

2.1 BACKGROUND ON THE SHELL HGSYSTEM MODEL

The HGSYSTEM model originated in the late 1970s and early 1980s as a dense gas area source model called HEGADAS that was primarily intended for application to liquid spills and subsequent evaporation of liquified natural gas (LNG) and liquified petroleum gas (LPG) (Colenbrander, 1980). The HEGADAS model was developed by Shell for continuous releases, and the code was made available by the U.S. Environmental Protection Agency as part of their air quality modeling guidelines. Concurrently, Shell also developed the

HEGABOX model for application to instantaneous releases of dense gases. Because of the concerns of industry with HF releases, in the mid-to-late 1980s a comprehensive research program took place in which field experiments were carried out, the data analyzed, and a new model developed for application to two-phase aerosol jets of HF resulting from ruptures of valves and pipelines on pressurized HF tanks.

The new model, developed by Shell during 1987-1990, was called HGSYSTEM. It was valid for transient or continuous releases of gases or aerosols from pressurized containers or from liquid spills (McFarlane et al., 1990; Witlox et al., 1990) but did not include instantaneous sources. HGSYSTEM was based on HEGADAS, with modifications to account for two-phase aerosol jets; was generally applicable to any dense or passive gases; and had special capabilities to handle the chemistry and thermodynamics of HF (Schotte, 1987; 1988). Some source emission characterizations were also possible for HF, including calculations of the initial flash and the jet mass emission rate.

The 1990 version of HGSYSTEM consisted of several submodels:

- HFFLASH - Calculates flashing of HF releases.
- HFPLUME - Calculates jet source emission rate for HF release and subsequent aerosol jet transport and entrainment, including effects of dense gas and HF chemistry and thermodynamics.
- PLUME - Calculates jet transport and entrainment for generalized gas of positive, neutral, or negative buoyancy.
- HEGADAS - Calculates steady-state (Version S) and transient (Version T) transport and entrainment of ground-based plume; includes HF chemistry and thermodynamics.
- PGPLUME - Calculates far-field transport and entrainment of elevated passive (neutral) plume. Has no chemistry.

Hanna, Chang, and Strimaitis (1993) evaluated the 1990 version of HGSYSTEM with data from eight field experiments, showing its performance was as good as the best of the available hazardous gas models.

The petroleum industry was not satisfied with the HGSYSTEM 1990 version and, to further improve it, API sponsored several enhancements by Shell to HGSYSTEM beginning in 1991 and extending to the present. Improvements included the addition of (1) the instantaneous dense gas model, HEGABOX, with incorporation of HF chemistry and thermodynamics and (2) a generalized two-phase aerosol jet model, AEROPLUME. Other minor enhancements included modifications to input and output files. Several draft reports by Shell describe these improvements (see Chaps. 4–6 and reports by Post [1993a, b; 1994b] and Witlox [1993a, b, c]). The new version, HGSYSTEM-3.0, is fully discussed in a recent report by Post (1994c) which includes several sections from the current report.

In November 1993, the Shell-API and The Earth Technology Corporation-Energy Systems researchers met and decided to coordinate efforts and publish a single technical report, user guide, and code describing the enhancements made to HGSYSTEM by both groups. Thus, all improvements are included in the Shell HGSYSTEM model and vice versa.

2.2 BACKGROUND ON THE ENERGY SYSTEMS PLM89A MODEL

The PLM89A model was developed under the support of DOE in the early 1980s by Energy Systems and its contractors (Bloom, Just, Williams, 1989). It was intended specifically for application to SARs at the GDPs. The strong point of PLM89A was its thorough treatment of UF_6 chemistry and thermodynamics. It had the capability of accounting for the hydrolysis of UF_6 as a time-dependent (mass-transfer-limited reaction rate) process, using parameterizations of length and velocity scales for plume entrainment developed by Varma (1982). It included an equilibrium module for the HF-H_2O system, including the effects of HF polymerizations. Although the PLM89A HF module was slightly different from the HGSYSTEM HF (Schotte, 1987; 1988) module in all aspects, the final results were similar. For example, it made little difference whether a model selected the polymer $(HF)_4$ or $(HF)_3$ as long as the total heat absorbed during the depolymerization process was simulated and the molar flux of HF was conserved.

PLM89A was unique among dense gas models because it contained algorithms for dry and wet deposition of various plume materials (solid and gaseous UF_6, solid UO_2F_2, gaseous HF, and liquid $HF{\cdot}H_2O$). No other available dense gas models (e.g., DEGADIS, SLAB, ALOHA, HGSYSTEM) included deposition. However, the PLM89A model was regarded by reviewers as relatively weak in parameterizations of transport, diffusion, entrainment, and dense gas slumping (Hicks et al., 1989; Sykes and Lewellen, 1992). These modules had not been taken from existing state-of-the-art models nor been thoroughly tested with field data. The only testing of PLM89A involved comparisons with UF_6 experiments in France in which such small amounts of UF_6 were released that the thermodynamic effects were minor (Bloom and Just, 1993). PLM89A was also capable of modeling F_2 and ClF_3, two other gases used in GDPs. The chemistry and thermodynamics of these gases were treated in the model.

3. SUMMARY OF TYPICAL EXPECTED UF_6 SOURCE SCENARIOS

The GDPs store and process many tons of UF_6. At atmospheric pressure, UF_6 can exist only as a gas or solid (similar to CO_2), with a sublimation point of 56°C. The liquid phase exists only at pressures exceeding about 1.6 atmospheres and at temperatures exceeding 64°C. Any solid UF_6 will evaporate rapidly in the ambient atmosphere, so the UF_6 tends toward the gas phase. For *storage* purposes, it is preferable that UF_6 be in the solid or liquid phase because it then occupies about a thousand times less volume than in the gas phase. For *safety* purposes, storing UF_6 in the solid phase rather than in the liquid phase is preferable. This is because a ruptured tank of *solid* UF_6 will evaporate relatively slowly from its exposed surface; but a ruptured tank of *liquid* UF_6 will first flash to the solid and gas phases, and the entire inventory may then be transported downwind.

Within the GDPs, UF_6 gas flows through pipes to and from various processing units. After processing, the liquid UF_6 is stored in 14-ton cylinders. These cylinders are then cooled so that the UF_6 solidifies inside the cylinder.

Energy Systems engineers have identified three major source scenarios to be investigated with the new HGSYSTEM/UF_6 model. These scenarios are presented, in order of priority, in Sects. 3.1-3.3. "Worst-case" ambient atmospheric conditions are chosen for these scenarios. For near-ground-level sources, the worst-case impacts will be associated with light winds, stable conditions, and high water-vapor contents (i.e., high temperatures and relative humidities).

3.1 SCENARIO 1: RUPTURE OF A PIPE OR VALVE ON A 14-TON LIQUID STORAGE CYLINDER

The UF_6 in the 14-ton cylinder is assumed to be in the liquid phase. The ground-based tank is pressurized and is above 64°C. A pipe or valve with about a 5-cm diam is ruptured at a height about 1 m above the ground. The UF_6 approaches the orifice as a liquid and flashes to a two-phase (gas-plus-solid) jet as it escapes the orifice. The solid UF_6 is assumed to be suspended as small particles in the gas jet. Because it takes several minutes to empty the tank, the release must be treated as transient (i.e., the source emission rate varies with time over a period of several minutes). The jet can escape from the ruptured pipe or valve at any angle. Generally, hazardous gas modelers recommend a worst-case jet angle that is horizontal or parallel to the ground since dilution is minimized and the plume centerline remains near the ground.

3.2 SCENARIO 2: COMPLETE RUPTURE OF A 14-TON LIQUID STORAGE CYLINDER

This scenario involves the same tank as the first scenario. However, in this case, the 14-ton tank is completely ruptured or split open instantaneously, resulting in the creation of an initial volume of flashed UF_6 gas and suspended UF_6 particles.

3.3 SCENARIO 3: RUPTURE OF A PIPE WITHIN A PROCESSING BUILDING

As mentioned previously, gaseous UF_6 flows through thousands of meters of pipelines within the GDP processing buildings. In this scenario, a 5-cm-diam, pressurized, high-temperature pipeline is assumed to rupture. The resulting transient gas jet will persist until the pipeline empties, with the mass of the release determined by the positioning of check valves along the pipe (for our tests, a 1-ton release is assumed). The jet will be transported and diffused within the building, and if sufficient water vapor is present in the building, the products (UO_2F_2 and $HF{\cdot}H_2O$) will be exhausted from the building by a vent system. Consequently, for calculating environmental impacts outside of the GDP boundaries, the source scenario consists of a dilute UO_2F_2 and $HF{\cdot}H_2O$ jet from a building vent. The mass release rate will likely be transient, depending on the release characteristics of the pipe rupture and the rate at which the ventilation occurs.

4. OVERVIEW OF COMPONENTS OF HGSYSTEM/UF_6

This chapter provides a brief overview of the HGSYSTEM/UF_6 model. The model is described in detail in Chaps. 5, 6, and 7. HGSYSTEM/UF_6 is a hybrid model that combines the dispersion and HF-thermodynamics aspects of HGSYSTEM (developed by Shell over the past 10 years) with the UF_6 chemistry and thermodynamic aspects of PLM89A (developed by Energy Systems during the same time). Some new modules have been added that relate to plume lift-off, meteorological scaling, dry and wet deposition, averaging times, canyon effects, and dispersion on building roofs. During the course of our HGSYSTEM/UF_6 project, Shell has continued to develop certain parts of HGSYSTEM, and we have coordinated our development efforts with them.

The HGSYSTEM/UF_6 model consists of several modules that are applied to various stages of the plume or puff. The following modules can be chosen by the user:

- ***AEROPLUME/UF_6*** - This module treats elevated two-phase momentum jets of UF_6 solid and vapor and HF vapor. It is intended for application to plumes from the moment they are emitted from a pressurized tank or pipe rupture to the time when they either (1) strongly interact with the ground or (2) become passive (i.e., density approaches ambient air density, excess momentum disappears, and chemical reactions end). Although AEROPLUME/UF_6 can treat jets at any initial angle, the user should select initial angles that will result in the plume hitting the ground at only a slight angle. The UF_6 chemistry and thermodynamics algorithms used in this module also are used in the HEGADAS/UF_6 and HEGABOX/UF_6 modules.

- ***HEGADAS/UF_6*** - This module treats continuous, ground-based, dense gas plumes. It is applied to scenarios (1) with area source emissions or (2) in which the AEROPLUME/UF_6 module predicts that the plume strongly interacts with the ground. HEGADAS/UF_6 has steady-state (-S) and transient (-T) versions. Generally, finite duration releases of 1 or 2 minutes or less should be treated by the transient version. HEGADAS/UF_6 uses the same UF_6 chemistry and thermodynamics modules found in AEROPLUME/UF_6 and in HEGABOX/UF_6.

- ***HEGABOX/UF_6*** - This module treats instantaneous, ground-based dense gas puffs. It "transitions" to HEGADAS-T/UF_6 after the gravity-slumping phase ends and uses the same UF_6 algorithms as the previous two modules.

- ***PGPLUME*** - This module represents the final passive phase of an elevated plume. No chemistry or thermodynamics are treated in PGPLUME. AEROPLUME/UF_6 will eventually "transition" to PGPLUME if the plume remains elevated.

In addition to these modifications to HGSYSTEM that are specific to UF_6, several more general improvements were made that can be used in applications to any type of emissions. Chapters 5, 6, and 7 provide details on these topics:

- Removal of gases and particles by dry and wet deposition.
- Lift-off of plumes initially on the ground as their buoyancy changes from negative to positive due to the heat inputs from chemical reactions.
- Parameterization of boundary layer meteorological variables using state-of-the-art algorithms.
- Accounting for variations in concentration with averaging time and for concentration fluctuations.
- Effects of buildings on constricting lateral plume spread.
- Predictions of concentrations on building roofs and sides due to emissions from vents.

5. FORMULATION OF UF_6 CHEMISTRY AND THERMODYNAMICS MODULES

This chapter provides a detailed description of the chemistry and the thermodynamics modules included in the HGSYSTEM/UF_6 model. These two modules are developed to be generic, so they can be used in combination with different modules in HGSYSTEM to form a comprehensive modeling system for UF_6 releases.

5.1 MODEL APPROACH

Under ambient pressures and temperature conditions, UF_6 may be released as a gas or a mixture of gas and solid. Releases from pressurized storage vessels may be in the liquid phase, in which case the UF_6 plume will flash to a mixture of gas and solid. In time, the UF_6 solid will sublimate. A chemical reaction between UF_6 vapor and water vapor will occur as ambient water vapor is entrained into the plume, resulting in the production of HF vapor and UO_2F_2 solid. Polymerization and depolymerization of HF and production of the $HF{\cdot}H_2O$ compound will also take place. The $HF{\cdot}H_2O$ compound is assumed to remain in the vapor phase, since sensitivity tests have demonstrated that the concentrations of $HF{\cdot}H_2O$ liquid are less than 1% of the concentrations of $HF{\cdot}H_2O$ vapor. A schematic diagram for these processes is shown in Fig. 5-1. The chemical reactions involved can be described by the following formulas, where *g* and *s* refer to gas and solid, respectively.

$$UF_6(g) + 2H_2O(g) \rightarrow UO_2F_2(s) + 4HF(g)\ . \qquad (5\text{-}1a)$$

$$2(HF) = (HF)_2 \quad (gas)\ . \qquad (5\text{-}1b)$$

$$6(HF) = (HF)_6 \quad (gas)\ . \qquad (5\text{-}1c)$$

$$8(HF) = (HF)_8 \quad (gas)\ . \qquad (5\text{-}1d)$$

$$HF(g) + H_2O(g) = (HF{\cdot}H_2O) \quad (gas)\ . \qquad (5\text{-}1e)$$

The plume mixture is assumed to be composed of the following species:

Vapor: UF_6, HF, $(HF)_2$, $(HF)_6$, $(HF)_8$, H_2O, $HF{\cdot}H_2O$, dry air

Solid: UF_6, UO_2F_2 (5-2)

The molecular weights of the above species are as follows:

Air	H_2O	UF_6	UO_2F_2	HF	$(HF)_n$
28.966	18.016	352.025	308.025	20.008	20.008n

(5-3)

Molecular weights of UF_6 and UO_2F_2 may change with ^{235}U content. The values listed above are the default values assumed in the code. The user has the option of changing these values.

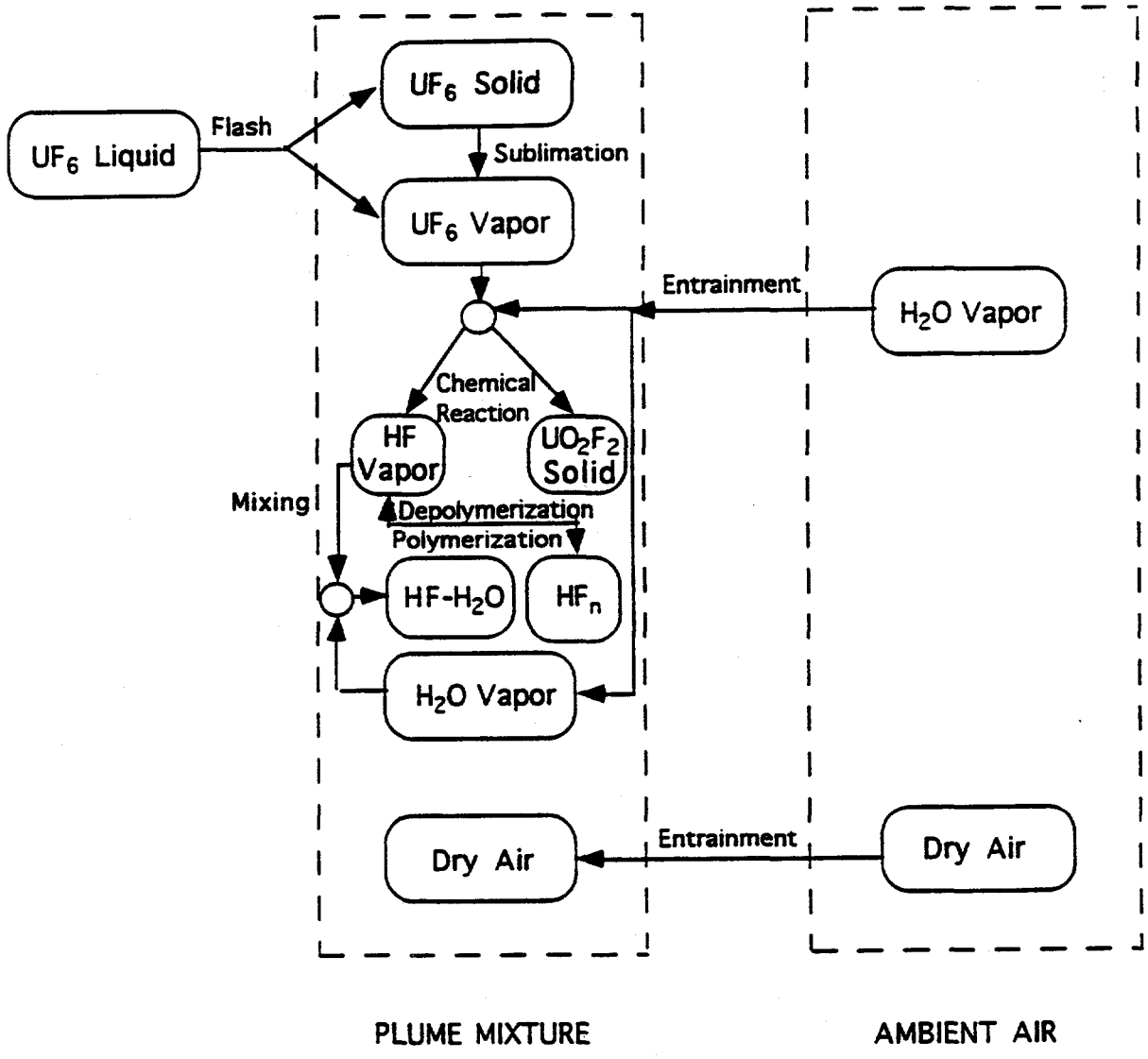

Fig. 5-1. Schematic diagram of processes involved in UF_6 releases.

For UF_6, the triple point occurs at a temperature of 65°C and a pressure of 1.5 atmosphere. At one atmosphere, UF_6 has a sublimation temperature of 56°C. In its gas phase, UF_6 closely approximates an ideal gas (DeWitt, 1960).

As the UF_6 plume disperses downwind, the total amount of UF_6 is gradually reduced and the total amount of the products, HF and UO_2F_2, is increased. A proper description of the plume development requires calculations of temporal and spatial distributions of concentrations of all involved species. For pure HF releases, on the other hand, the total amount of HF does not change as the plume disperses because there are no destruction or generation mechanisms. Thus, the chemistry and thermodynamics processes for UF_6 releases are different from that for pure HF releases since, in the former case, HF is produced and UF_6 is consumed according to the chemical reaction shown in Eq. (5-1a). The UF_6 chemical and thermodynamics modules are difficult to derive by simply modifying the existing HF thermodynamics module in the original HGSYSTEM model. It is logical to develop a new formulation so that UF_6 releases can be properly modeled.

The UF_6 dispersion process is assumed to be divided into five stages with respect to mechanisms that dominate the changes in enthalpy, as shown in Fig. 5-2. The first stage is related to the UF_6 release scenario. Although many potential releases are pure vapor or partially reacted UF_6, liquid releases are likely to result in the most severe consequences. If liquid UF_6 is released from a pressurized container, it will change from liquid to a combination of vapor and solid as the pressure drops to ambient pressure. The molar fraction f_v of vapor UF_6 is defined as the ratio of the molar amount of UF_6 vapor to the total amount of UF_6. For a liquid UF_6 release, f_v jumps from zero to a value between zero and one ($0 < f_v < 1$). The enthalpy change in this stage is dominated by the flashing process. Except for pure UF_6 vapor releases, the plume immediately downwind of the release is generally composed of both gas and solid.

After UF_6 flashes, the plume enters stage two in which moist ambient air is entrained into the plume. During this stage, the solid UF_6 is subliming into vapor. Water vapor in the entrained air reacts with UF_6 vapor, releasing heat and generating HF gas and UO_2F_2 solid. HF may polymerize (depending on its concentration) and absorb heat until the mixture reaches thermal equilibrium. Sublimation of the UF_6 solid causes the UF_6 vapor fraction to increase. This sublimation process, which absorbs heat and thus reduces the plume temperature, has a dominant effect on the plume enthalpy. Furthermore, the plume density decreases due to the sublimation of the UF_6 solid and the entrainment of the ambient air. The plume may descend to the ground if its density is much greater than that of the ambient air.

In the third stage, the sublimation process has ended and the vapor fraction of UF_6 is now 100%. However, the UF_6 chemical reaction with water vapor is still active, releasing heat that raises the plume mixture temperature. This reaction process dominates the change in the plume enthalpy. At the same time, the entrainment process brings in ambient air. The plume temperature may reach the maximum near the point where the UF_6 vapor has been completely used up in the chemical reaction. The plume mixture density may be less than that of air, and the plume may rise due to its positive buoyancy.

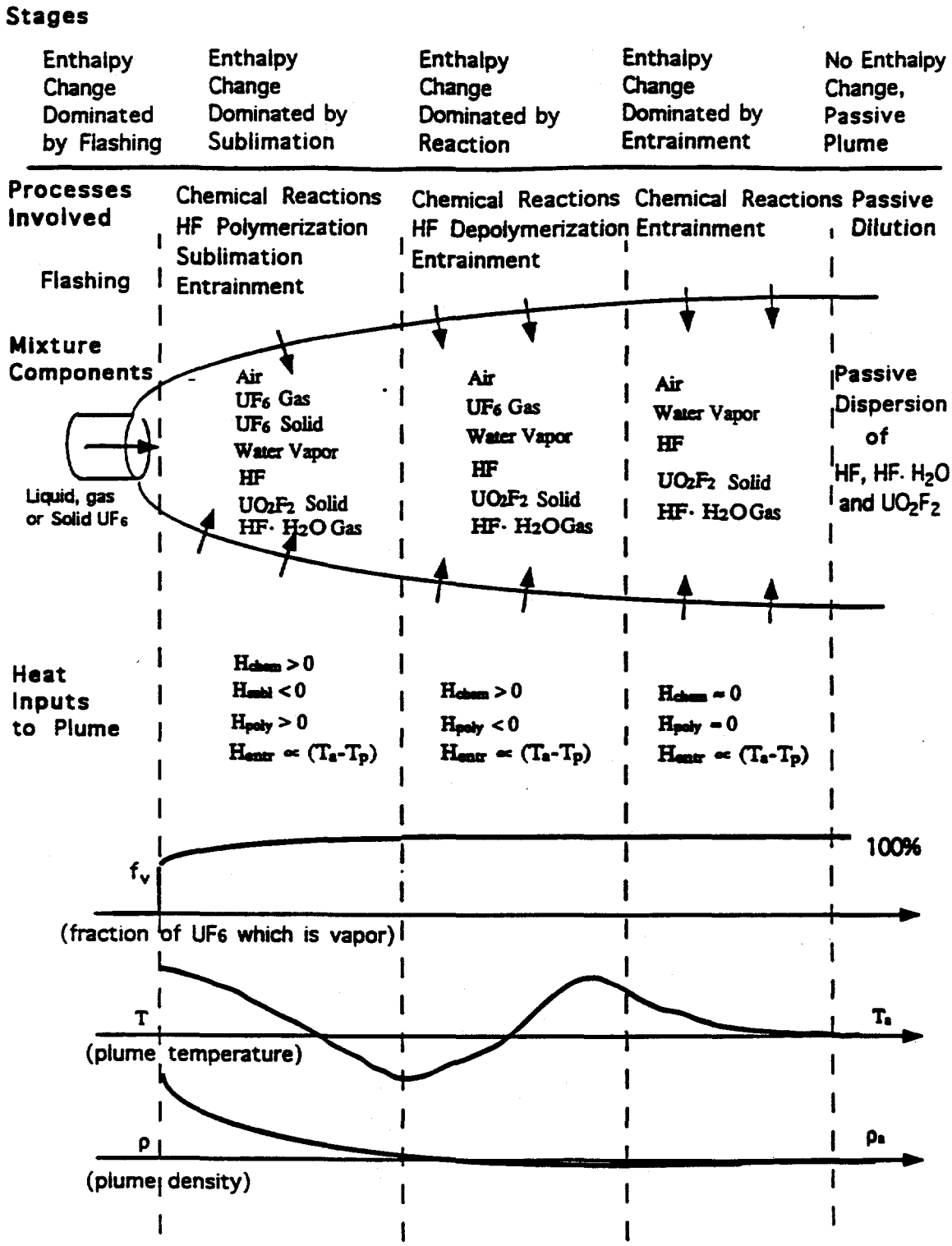

Fig. 5-2. Schematic diagram of UF_6 plume and the evolution of its properties showing the five stages as determined by their influence on enthalpy changes.

The fourth stage begins after all the UF_6 is consumed in its chemical reaction with water vapor. In this stage, as the plume entrains ambient air, the plume temperature and density gradually approach those of the ambient air. Except for a small amount of heat generated from the mixing of HF and H_2O, no heat is generated or destroyed in this stage.

The fifth and last stage occurs when the plume density reaches that of the ambient air and the plume becomes neutrally buoyant. Dilution of the plume is dominated by atmospheric turbulence.

In summary, the UF_6 dispersion process can be characterized by five stages according to the mechanisms that dominate the changes in temperature:

- Flash
- Sublimation
- Chemical reaction
- Entrainment
- Passive dispersion

To model these complicated processes, some assumptions are necessary in order to simplify the problem.

Although an algorithm post-processor has been added that calculates the deposition of gases and particles in the plume, it is assumed that the effects of the deposition on dispersion, chemical reactions, and thermodynamics can be neglected. All the UF_6 that is released (including solid UF_6) is assumed to eventually react with water vapor. This assumption ensures that conservative estimates of the amounts of UO_2F_2 and HF in the plume will be made. The effects of the deposition of solid UF_6 and UO_2F_2 on plume thermodynamics and chemistry may be accounted for in the future if more information on particle size becomes available.

Since the chemical reaction of UF_6 vapor with water vapor proceeds at an extremely high rate (Armstrong et al., 1991), the UF_6 hydration process is assumed to be an instantaneous, irreversible reaction that dominates other associated chemical reactions. Water vapor entrained into the plume is assumed to first react with UF_6, at a finite reaction rate due to incomplete mixing (see Sect 5.4). Any remaining water vapor then mixes and reacts with HF, a product of the UF_6 hydration process, and reaches an equilibrium. As proposed by Schotte (1988) and implemented in the HGSYSTEM model, we assume that the HF and water vapor mixture thermodynamics can be treated by an instantaneous equilibrium model.

The UF_6 modeling system is divided into three interrelated subprocesses: plume dispersion, UF_6 chemistry, and UF_6/HF thermodynamics. The dispersion subsystem calculates the plume geometry and the air entrainment rate as the plume travels downwind. The chemistry subsystem uses the air entrainment rate provided by the dispersion subsystem to calculate the composition of the plume based on the mixing-limited chemical reaction rate (see Sect. 5.4). The thermodynamics subsystem calculates the plume equilibrium temperature and density based on the new plume composition. The plume temperature and density then affect the dispersion subsystem.

A schematic diagram of the interaction of these three subprocesses is given in Fig. 5-3. The numerical method and the formulation and implementation of these three modules are described in more detail in the following sections.

5.2 SOLUTION METHODOLOGY AND SPLITTING ALGORITHM

The release of UF_6 is a complex problem due to interactions among the plume dispersion, chemical reaction, and thermodynamics processes. A process-splitting numerical scheme is used to (1) efficiently use the existing dispersion module in the HGSYSTEM model and (2) combine that module with the UF_6 chemistry and the thermodynamics modules described in Sects. 5.4 and 5.5. This scheme is adapted from the operator-splitting scheme, in which several mathematical operators in the governing differential equations are treated separately within each integration step. This method, described below, increases computational efficiency while still maintaining numerical accuracy and stability.

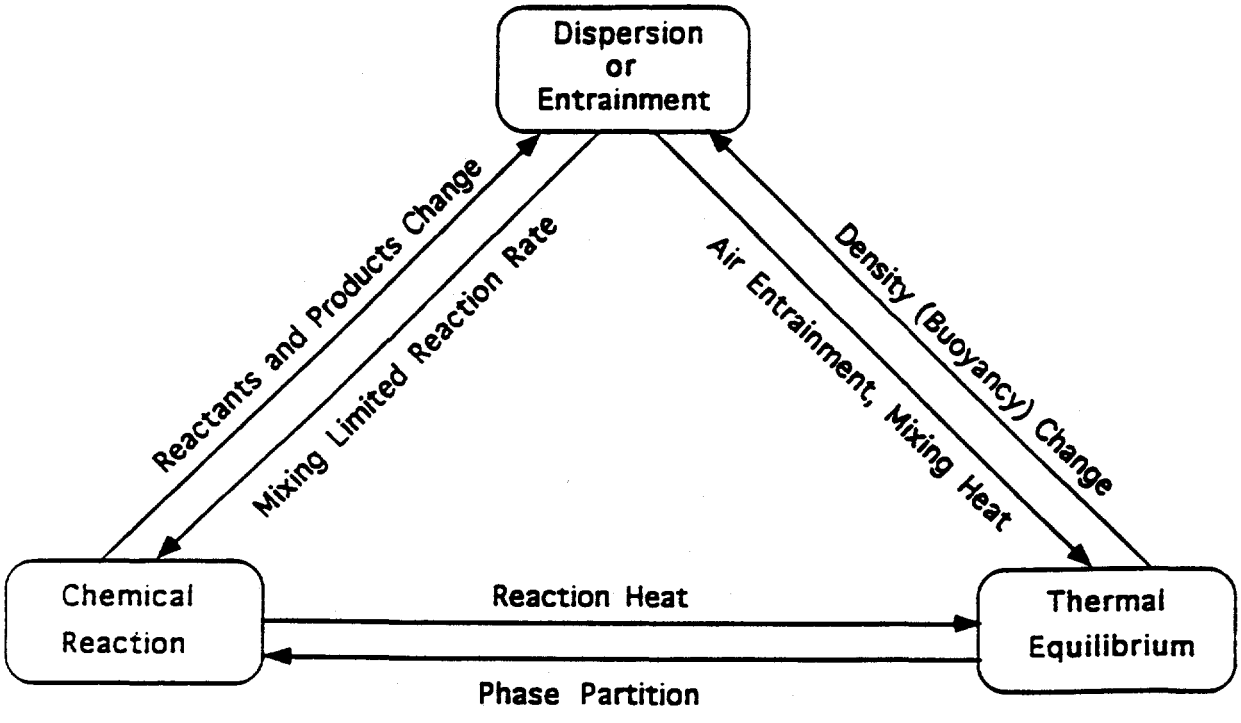

Fig. 5-3. Interaction of three subprocesses important in modeling a UF_6 plume.

If a dependent variable y changes in time due to three interrelated processes, the governing equation can be expressed as

$$\frac{dy}{dt} = f_1(y,t) + f_2(y,t) + f_3(y,t) \ , \tag{5-4}$$

where each function f_i corresponds to one process i such as transport, chemical reaction, or mixing. Instead of integrating Eq. (5-4) in one step, integration is accomplished numerically by three fractional steps.

$$\frac{y^{n+a} - y^n}{\Delta t} = f_1\left(y^n, t^n\right) \ . \tag{5-5a}$$

$$\frac{y^{n+b} - y^{n+a}}{\Delta t} = f_2\left(y^{n+a}, t^{n+a}\right) \ . \tag{5-5b}$$

$$\frac{y^{n+1} - y^{n+b}}{\Delta t} = f_3\left(y^{n+b}, t^{n+b}\right) \ . \tag{5-5c}$$

This splitting algorithm is based on the assumption that, within each step Δt, each of the three individual processes can be efficiently solved. This technique has been widely used in computational fluid dynamics (e.g., Chorin, 1973).

As described previously, the whole system in the new HGSYSTEM/UF_6 model is divided into three processes: dispersion (see Sect. 5.3), chemistry (see Sect. 5.4), and thermodynamics (see Sect. 5.5). These three processes are solved sequentially in each integration step. For example, for the AEROPLUME model in HGSYSTEM, the SPRINT package solves the 14 equations that govern plume dispersion (see Sect. 5.3). The UF6CHEM module solves the finite UF_6 chemical reaction equation. The UF6THRM module solves equations associated with the thermodynamic equilibrium for the UF_6/HF system. The flow chart for the implementation of these three modules is shown in Fig. 5-4. The flow chart is generic and applies to any model of HGSYSTEM. In models without flashing, the flashing block in Fig. 5-4 should be removed. Since the new model is modular in design, future upgrades to include other chemical reactions and other physical processes can be accomplished relatively easily. Furthermore, model debugging is more efficient due to its modularity.

5.3 DISPERSION AND ENTRAINMENT RATE MODULE

HGSYSTEM contains several models that treat the dispersion of different types of releases. In the following, the AEROPLUME module is used as an example to show the interaction of the three numerical steps (see Fig. 5.4) and the incorporation of chemistry and thermodynamics into HGSYSTEM.

AEROPLUME is intended to simulate the dispersion of jet releases of any orientation, as long as the plume does not strike the ground at an angle close to vertical. Jet development is assumed to pass through three sequential stages after release: airborne, touchdown, and slumped. McFarlane et al. (1990) and Post (1994c) give a detailed description of AEROPLUME. The following paragraphs briefly describe basic governing equations and relevant output variables. The notation used in these equations is consistent with that used by Post (1994b). The following 14 equations [Eqs. (5-6) through (5-19)] for plume dispersion are solved in the AEROPLUME module.

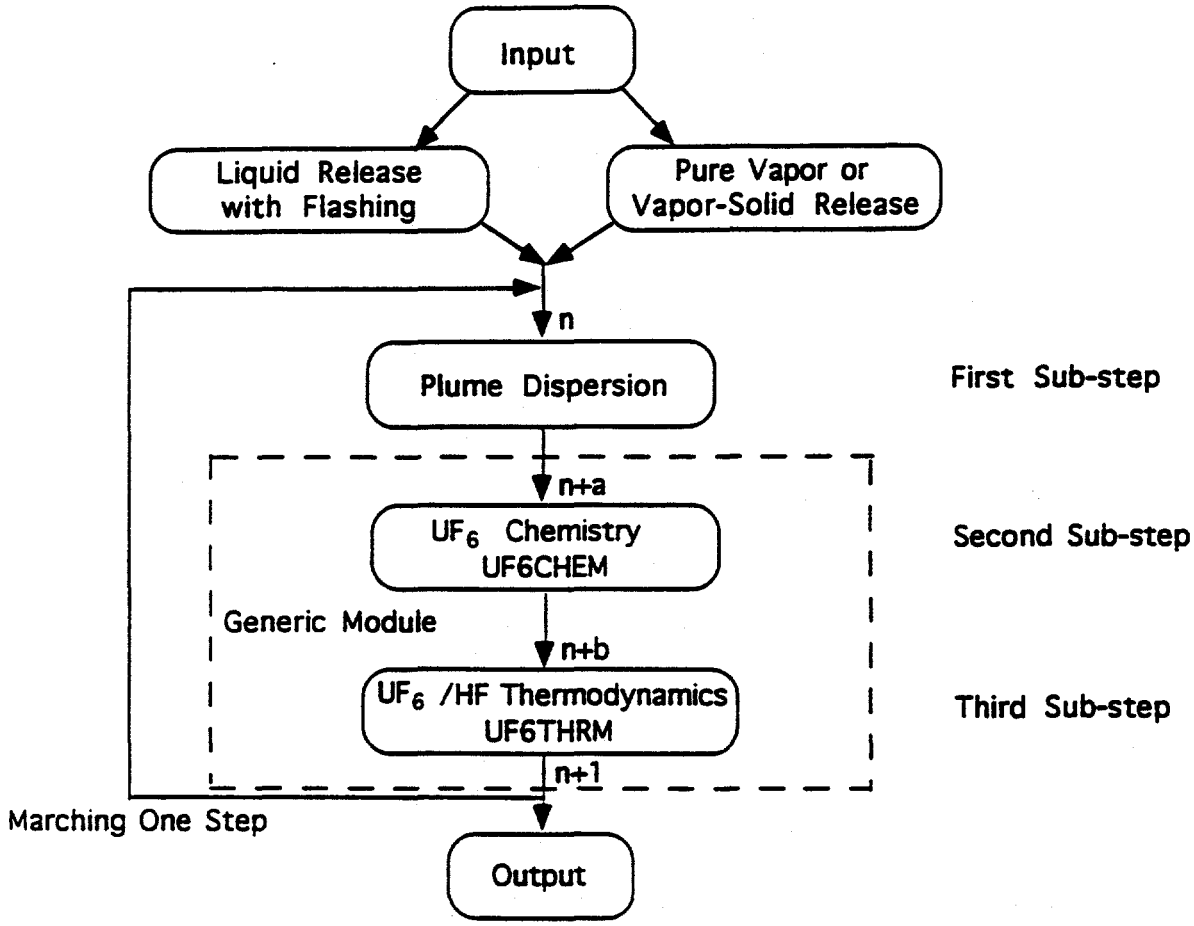

Fig. 5-4. Flow chart of the process-splitting algorithm used in HGSYSTEM/UF_6 model.

The mass flow rate along the plume centerline can be defined as

$$\dot{m} = A(D,Z,\varphi)\,\rho\,U \quad , \tag{5-6}$$

where the plume cross-sectional area A is a function of plume diameter D, plume height Z, plume centerline inclination angle φ, and plume state (airborne, touchdown, or slumped). The plume density ρ is calculated by the chemistry and thermodynamics modules at every time step. U is the plume velocity along the plume trajectory.

We can also define the horizontal and vertical excess momentum and the excess energy of the plume, as shown in Eqs. (5-7) through (5-9), respectively.

$$\dot{P}_x = \dot{m}\left[U\cos(\varphi) - U_{atm}\right] \quad , \tag{5-7}$$

$$\dot{P}_z = \dot{m}\,U\sin(\varphi) \quad , \tag{5-8}$$

$$\dot{E} = \dot{m}\left[H + U^2/2 - H_{atm} - U_{atm}^2/2\right] \quad , \tag{5-9}$$

where U_{atm} and H_{atm} are the wind speed and specific enthalpy, respectively, of the ambient air at plume height Z.

The changes in the ambient pressure, P_{atm}, ambient temperature, T_{atm}, and ambient wind speed, U_{atm}, along the plume trajectory, s, are defined in the following three equations.

$$\frac{dP_{atm}}{ds} = -\rho_{atm} g \sin(\varphi) \quad , \tag{5-10}$$

$$\frac{dT_{atm}}{ds} = \frac{dT_{atm}}{dZ}\sin(\varphi) \quad , \tag{5-11}$$

$$\frac{dU_{atm}}{ds} = \frac{dU_{atm}}{dZ}\sin(\varphi) \quad . \tag{5-12}$$

where the symbol ρ_{atm} is the ambient air density

The conservation laws for the variables defined in Eqs. (5-6) through (5-9) are as follows:

$$\frac{d\dot{m}}{ds} = Entr \quad . \tag{5-13}$$

$$\frac{d\dot{E}}{ds} = -\dot{m}\left[\frac{dH_{atm}}{dZ} + U_{atm}\frac{dU_{atm}}{dZ} + g\right]\sin(\varphi) \quad . \tag{5-14}$$

$$\frac{d\dot{P}_x}{ds} = - Shear - Drag_x - Impact_x \quad . \tag{5-15}$$

$$\frac{d\dot{P}_z}{ds} = - Buoy - Foot - Drag_z - Impact_z \quad . \tag{5-16}$$

In Eqs. (5-13) through (5-16),
Entr = entrainment,
Shear = shear force associated with vertical wind shear,
$Drag_x$ = horizontal drag force,
$Drag_z$ = vertical drag force,
$Impact_x$ = horizontal impact force due to the plume impinging the ground,
$Impact_z$ = vertical impact force due to the plume impinging the ground,
Buoy = buoyancy force,
Foot = gravity-slumping pressure force.

A more detailed description regarding the parameterizations of the above terms is presented in Post (1994c, Sect. 5.B).

Finally, there are the following three geometric relations:

$$\frac{dX}{ds} = \cos(\varphi) \quad , \tag{5-17}$$

$$\frac{dZ}{ds} = \sin(\varphi) \quad , \tag{5-18}$$

$$\frac{dt}{ds} = \frac{1}{U} \quad , \tag{5-19}$$

where
X = horizontal downwind distance,
Z = height,
t = time.

Given enough information, such as the initial plume density and temperature, the following 14 plume variables can be calculated by solving Eqs. (5-6) through (5-19) using the SPRINT package in AEROPLUME. Other variables such as the entrainment rate of ambient air, *Entr* (in kg/m/s), also can be determined from this set of variables at any downwind distance.

- Specific enthalpy — H (J/kg)
- Plume velocity — U (m/s)
- Cross-sectional diameter — D (m)
- Centerline inclination — φ

- Ambient velocity — U_{atm} (m/s)
- Ambient pressure — P_{atm} (Pa)
- Ambient temperature — T_{atm} (K or °C)
- Total mass flow rate — $\dot{m}$ (kg/s)
- Excess energy flux — $\dot{E}$ (J/s)
- Excess x momentum flux — $\dot{P}_x$ (kg.m/s^2)
- Excess z momentum flux — $\dot{P}_z$ (kg.m/s^2)
- Plume downwind displacement — X (m)
- Plume centroid height — Z (m)
- Elapsed time — t (s)

Note that Eq. (5-14) does not account for heat sinks or sources due to chemical reaction, phase change, etc. For any control volume (see Fig. 5-5), the complete energy conservation equation can be written as

$$d\left[\dot{m}\left(H + U^2/2 + gZ\right)\right] = d\dot{m}\left(H_{atm} + U_{atm}^2/2 + gZ_{atm}\right) + d\dot{R}_{UF6} + d\dot{R}_{TH} \quad . \quad (5\text{-}20)$$

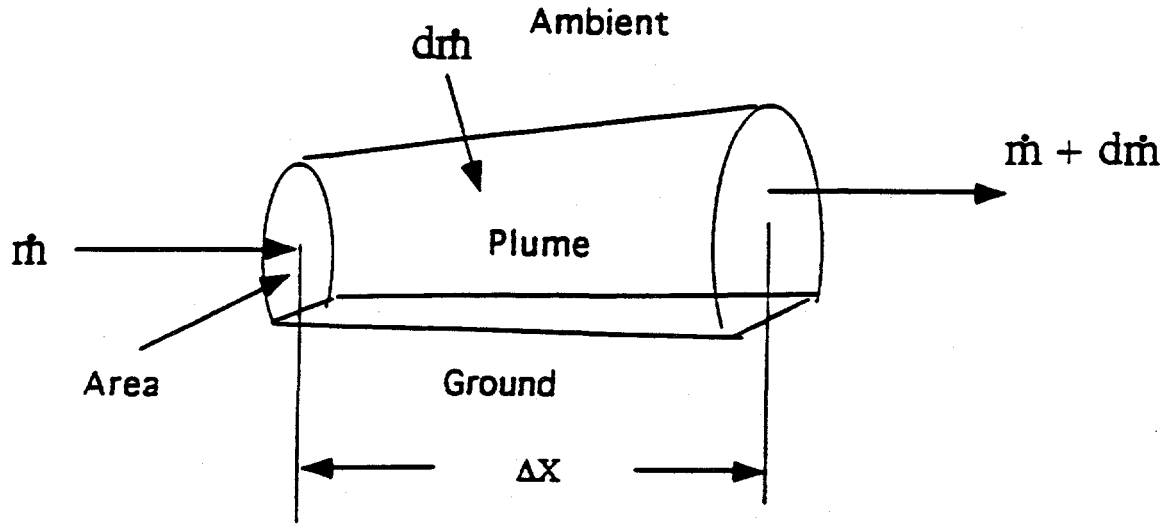

Fig. 5-5. Schematic diagram of a computational control volume in the plume.

According to Eq. (5-20), the change of energy flux for the control volume is due to the following:

- Energy brought into the plume by the entrainment of ambient air.
- Heat release due to the exothermic reaction of UF_6 with H_2O as denoted by $d\dot{R}_{UF6}$.
- Heat release/absorption due to other thermodynamic effects such as the mixing of HF with H_2O, the sublimation of UF_6, and the heat transfer through the ground surface, etc., as denoted by $d\dot{R}_{TH}$.

If we assume $Z = Z_{atm}$ (i.e., the entrained air has the same potential energy as the plume), the energy equation can be rewritten as

$$\frac{d}{ds}\left[\dot{m}\left(H + U^2/2 - H_{atm} - U_{atm}^2/2\right)\right] = -\dot{m}\left(\frac{dH_{atm}}{dZ} + U_{atm}\frac{dU_{atm}}{dZ} + g\right)\sin\phi + \frac{d\dot{R}_{UF6}}{ds} + \frac{d\dot{R}_{TH}}{ds} \quad , \quad (5\text{-}21)$$

which is the same as Eq. (5-14) if the last two terms on the right side are removed. This similarity is expected because Eq. (5-14) is valid only for dispersion in the absence of chemical reactions and complex thermodynamic processes. The last two terms in Eq. (5-21) are to be calculated in the chemistry and thermodynamics modules and are included in the enthalpy balance equation in the thermodynamics module.

Note that the plume density is not one of the unknowns solved by the SPRINT package. This variable is calculated in the chemistry and thermodynamics modules.

5.4 UF_6 CHEMISTRY MODULE

Both dry air and water vapor are entrained into the plume during the dispersion process (Sect. 5.5). The entrained water vapor, combined with the remaining water vapor in the plume, is assumed to first react with the UF_6 vapor rather than with the HF vapor. This assumption is justified by the extremely fast UF_6 reaction rate. If any condensed water vapor (fog, rain, snow) is in the ambient air, it is assumed not to react with the UF_6 (Barber, 1994) and not to affect the plume thermodynamics. The remaining water vapor that has not reacted with UF_6 will then participate in the formation of $HF{\cdot}H_2O$. Prior to making calculations of thermodynamic equilibrium, the chemistry module (UF6CHEM) calculates the molar flow rates (in kmole/s) of various chemical species after the UF_6 reaction with water vapor. Note that the total mass flux (in kg/s) of the plume has already been calculated in the plume dispersion module. To simplify the problem, secondary reactions such as the formation of hydrated UO_2F_2, $UO_2F_2{\cdot}H_2O$ are neglected (Leitnaker, 1989). The reaction between UF_6 vapor and water vapor is assumed to be dominant.

The rate of water vapor entrained into the plume, F_1 (in kmole/s,) is given by

$$F_1 = Entr\ \Delta s\ y/M_{ma} \quad , \tag{5-22}$$

where

Entr = entrainment rate calculated from the dispersion module,
Δs = integration step (in meters) along the plume centerline,
M_{ma} = equivalent molecular weight of the moist air,
y = molar fraction of water vapor in the ambient air.

Note that

$$y = \frac{P_v}{P} r_H \quad , \tag{5-23}$$

where

P_v = saturation pressure,
P = ambient pressure,
r_H = relative humidity in fractions ($0 \le r_H \le 1$).

For temperatures from 0°C to 50°C, the vapor pressure of water can be calculated (in millibars, with T in °C), from McFarlane et al. (1990):

$$P_v = a_o + T\left[a_1 + T\left(a_2 + T\left\{a_3 + T\left[a_4 + T\left(a_5 + T\,a_6\right)\right]\right\}\right)\right] \tag{5-24}$$

where,

$a_0 = 6.1078$,
$a_1 = 4.4365 \times 10^{-1}$,
$a_2 = 1.4289 \times 10^{-2}$,
$a_3 = 2.6506 \times 10^{-4}$,
$a_4 = 3.0312 \times 10^{-6}$,
$a_5 = 2.0341 \times 10^{-8}$,
$a_6 = 6.1368 \times 10^{-11}$.

The rate of entrainment of dry air into the plume, F_2 (in kmole/s), during the same integration step is thus,

$$F_2 = Entr\ \Delta s\ (1 - y)/M_{ma} \quad . \tag{5-25}$$

The molar flow rates (in kmole/s) of water vapor and dry air are then, respectively,

$$M_w^{n+a} = M_w^n + F_1^n \quad , \tag{5-26}$$

$$M_a^{n+a} = M_a^n + F_2^n \quad , \tag{5-27}$$

where the superscripts n and $n + a$ refer to the dispersion and chemistry processes, respectively (see Fig. 5-4).

Then, total molar flow rate (in kmole/s) of the plume is

$$M_{tot}^{n+a} = M_{tot}^{n} + F_1^n + F_2^n \quad . \tag{5-28}$$

Note that M_{tot} is normalized, or assumed to be unity, in the HF thermodynamic module of the original HGSYSTEM. However, in the present section, dimensional physical quantities are used throughout the formulation.

The literature indicates that the hydrolysis of UF_6 proceeds rapidly. This rapid reaction is limited by the rate at which water vapor is entrained from the ambient air into the plume and its subsequent mixing rate with UF_6 molecules (Varma, 1982). In a turbulent plume, the ambient air and moisture are entrained by large eddies at the edges of the plume. Moisture contained in these large eddies is not immediately mixed with plume reactants at a molecular level. Since chemical reactions require mixing on the molecular scale, the initial chemical reaction between the plume components and the atmospheric moisture is limited to the contact surface regions between eddies. As large eddies break down into smaller and smaller eddies, the reaction gradually proceeds to completion. Consequently, the effective reaction rate is significantly smaller than the rate obtained if all entrained moisture were to immediately and thoroughly mix with the plume. Since the mixing of entrained air with UF_6 vapor in the plume is not complete, the effective reaction rate is smaller than that for a well-mixed reactor. Varma (1982) formulated a finite reaction rate equation, which was implemented in the PLM89A model by Bloom et al. (1989). The finite reaction rate (in kmoles/s) due to incomplete mixing can be represented by the equation

$$\dot{R} = \frac{q\, M_w^a\, M_{UF_6}^a}{\Lambda \left[2\, M_{UF_6}^a + M_w^a\right]} \quad , \tag{5-29}$$

where

q = the square root of the turbulent kinetic energy (m/s),
Λ = turbulence macroscale (m),

$M_{UF_6}^a$ = molar flow rate (kmoles/s) of UF_6 vapor in the plume prior to the UF_6 chemical reaction,
M_w^a = molar flow rate (kmoles/s) of water vapor in the plume prior to the UF_6 chemical reaction.

Effective reaction rate $\dot{R}$ is finite because the mixing of the ambient air into the plume is through turbulent eddies that limit the direct contact of reactants in the entrained air and in the plume, as illustrated in Fig. 5-6a. Many velocity scales could be used to describe the turbulent eddies in the plume. Varma (1982) assumed that q is proportional to the entrainment velocity and found, from data for nonreacting jets, that cross-sectional averaged turbulence level q was on the order of 3.6 V_E, where V_E is the entrainment velocity. Consequently, q = 3.6 V_E is asssumed in Eq. (5-29). The reader is referred to Sect. 7.1 regarding the parameterization of V_E in more detail.

The macroscale of turbulence, Λ, depends on the mechanisms by which the turbulence is generated. AEROPLUME deals with jet releases, where the turbulence field controlling the entrainment of air into the plume is generated by the shear instability between the plume and the ambient wind, and the density difference between the plume and the air. For both mechanisms, the radius of the largest turbulent eddy is half of the plume radius (Fig. 5-6b). This is consistent with Varma's (1982) result based on his examination of standard data for jets and shear layers. For the HEGABOX and HEGADAS modules, the turbulence scale in ground-based slumping puffs or plumes is dominated by the vortex ring at the spreading front (see Figs. 5-6c and 5-6d). In these cases, turbulence scale Λ can be assumed to be one-half of the plume height. The reader is referred to Sect. 7.1 regarding the parameterization of Λ in more detail

The rate equations that govern the consumption and production of reactants and products are listed below:

$$U \frac{d M^{v}_{UF6}}{d s} = - \dot{R} \quad . \tag{5-30}$$

$$U \frac{d M_{w}}{d s} = - 2 \dot{R} \quad . \tag{5-31}$$

$$U \frac{d M_{HF}}{d s} = 4 \dot{R} \quad . \tag{5-32}$$

$$U \frac{d M_{UO2F2}}{d s} = \dot{R} \quad . \tag{5-33}$$

These rate equations can be solved by a simple first-order forward finite difference scheme:

$$M^{v,n+b}_{UF6} = M^{v,n+a}_{UF6} - \dot{R} \, \Delta s / U \quad , \tag{5-34}$$

where the superscripts $n + a$ and $n + b$ refer to the chemistry and thermodynamics processes, respectively (see Fig. 5-4), and the superscript v refers to vapor phase.

The rate of heat released due to the exothermic chemical reaction is given by

$$\Delta H^{CHEM,n}_{UF6} = (2\dot{R}\Delta s / U) \cdot 25199 \cdot 1.055/0.454 \; (kJ/s) \quad , \tag{5-35}$$

where 1.055 is the conversion factor from Btu to kJ and 0.454 is the conversion factor from lb to kg. The value of the heat of reaction (25,199 Btu/lb-mole of water vapor) is from Bloom et al. (1989). This heat release is included in the enthalpy balance equation in the thermodynamics module, UF6THRM, described in Sect. 5.5.

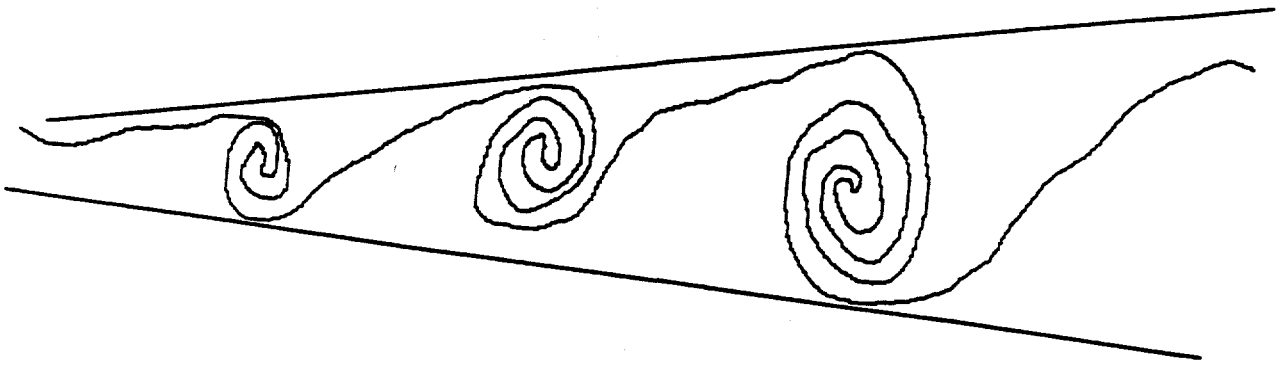

Fig. 5-6a. Mixing pattern in a shear layer.

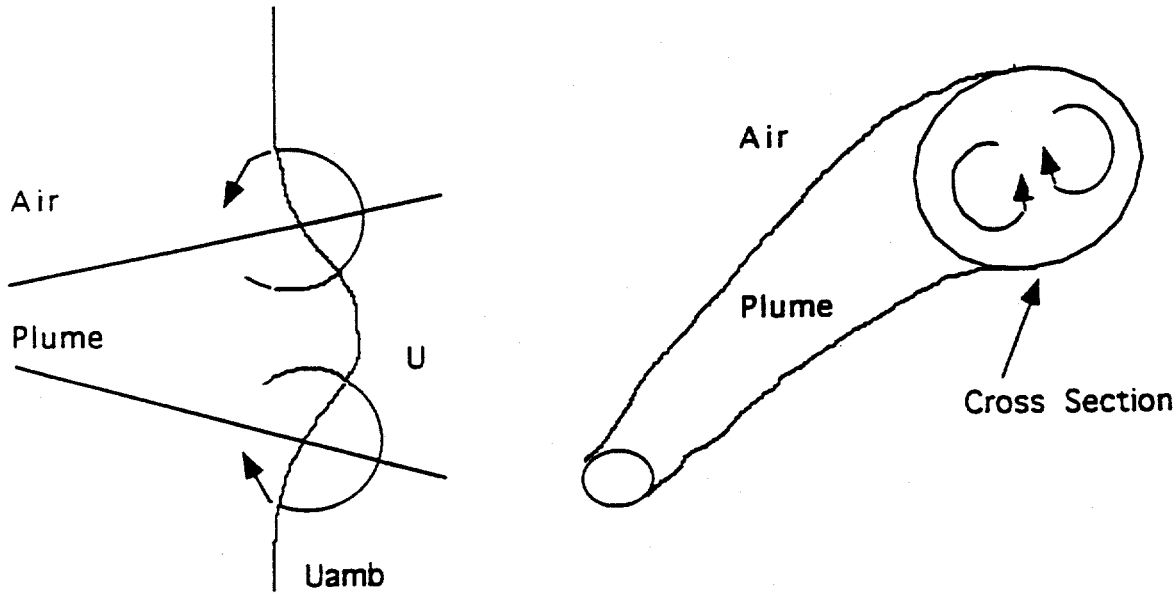

Fig. 5-6b. Large-scale turbulent eddies in jets.

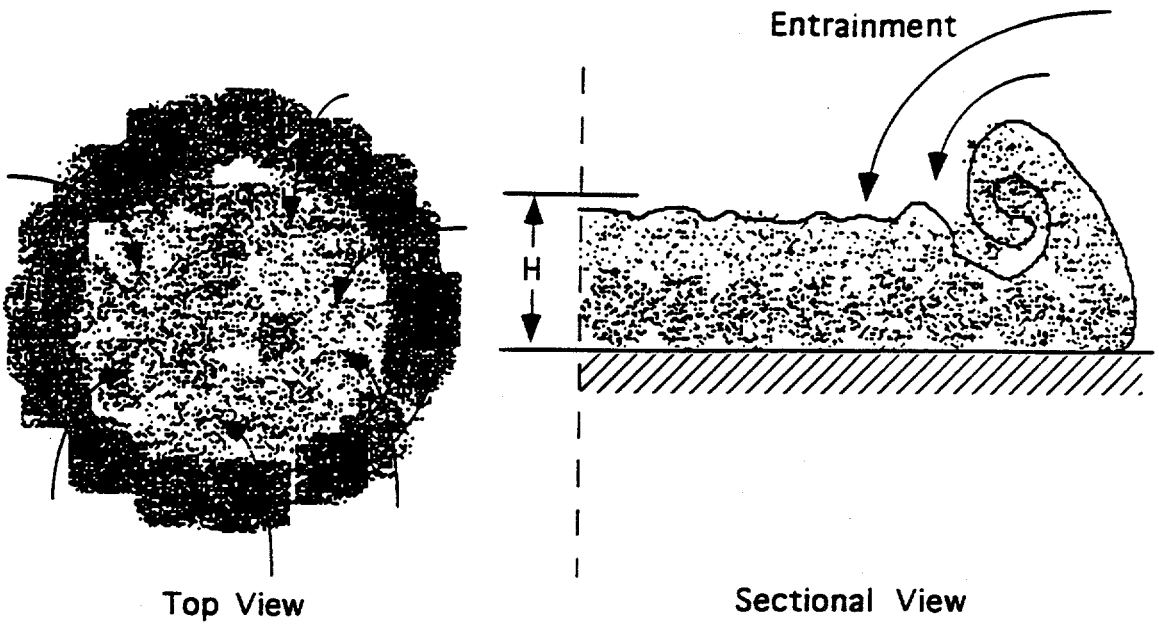

Fig. 5-6c. Frontal ring in a spreading cloud.*

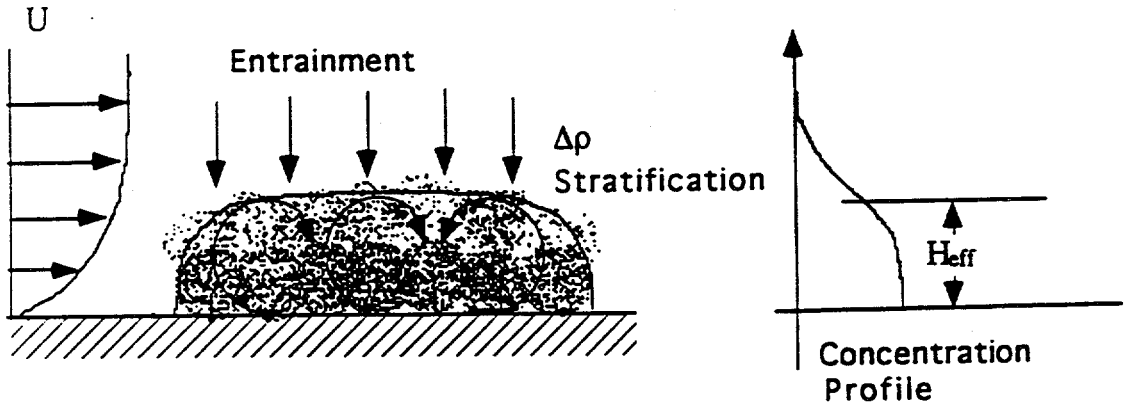

Fig. 5-6d. Top entrainment for plumes described in HEGADAS model.*

*H and H_{eff} are defined in Sect. 7.1 and Appendix A

Finally, the UF6CHEM chemistry module also calculates the molar flow rates (in kmole/s) of various species (all phases) that contribute to the thermodynamic equilibrium. For example, the molar flow rate of the total UF_6 after chemical reaction is given by

$$M_{UF6}^{n+b} = M_{UF6}^{v,n+b} + \left(1 - f_v^n\right) M_{UF6}^{n+a} \quad , \tag{5-36a}$$

where f_v^n is the fraction of UF_6 that is vapor.

The molar flow rate of dry air remains the same following the UF_6 chemical reaction:

$$M_a^{n+b} = M_a^{n+a} \quad . \tag{5-36b}$$

The total molar flow rate for all species following the UF_6 chemical reaction is the sum of the molar flow rates of all species:

$$M_{tot}^{n+b} = M_{UF6}^{n+b} + M_{UO2F2}^{n+b} + M_a^{n+b} + M_w^{n+b} + M_{HF}^{n+b} \quad . \tag{5-36c}$$

The total enthalpy flow rate (in kJ/s) can be obtained by the following expression:

$$H_{tot}^{n+b} = 0.001\ H^{n+a}\ \dot{m} + \Delta H_{UF6}^{CHEM,n} + \Delta H_e^n \quad , \tag{5-36d}$$

where

H^{n+a} (in J/kg) is the specific enthalpy of the plume prior to the UF_6 chemical reaction as described in Sect. 5.3 (0.001 is the conversion factor from J to kJ). Its value is obtained from the plume dispersion module, where the heat associated with the entrained air has been accounted for in Eq. (5-14).

ΔH_e^n (kJ/s) is the vertical heat flux from the ground to the plume during one integration step. Its computation can be found in McFarlane et al. (1990, Chap. 5, App. 3).

Molar flow rates computed by Eqs. (5-34a) and (5-36) are used to determine the thermodynamic equilibrium state of the mixture. Other state variables, such as plume temperature and density, are derived in the thermodynamics module, UF6THRM, to be described in Sect. 5.5.

5.5 THERMODYNAMICS MODULE

5.5.1 Solution Algorithm for the Thermodynamics Module

The thermodynamics module, UF6THRM, calculates the equilibrium state of the system consisting of HF, water vapor, UF_6, dry air, and UO_2F_2. As currently implemented, this module is applied following the application of the UF6CHEM module. The formulation of

UF6THRM is developed based on Schotte's algorithm (1988) and its implementation in HEGADAS for HF and water vapor mixture thermodynamics. The UF6THRM module contains HF-related processes such as the formation of HF-polymers, depolymerization of HF-polymers (endothermic), and exothermic reaction of HF with water vapor to form $HF{\cdot}H_2O$. UF6THERM also contains thermodynamic contributions from UF_6 sublimation, heat transfer through the substrate, and UF_6 heat of reaction.

The description of the module below closely follows the technical manual for HGSYSTEM (Post, 1994a), and similar notation is used. Appendix A contains a complete listing of the symbols that are used.

The state of the thermodynamic system for a UF_6 plume is determined by molar flow rates M_{HF}, M_w, M_{UF6}, M_a, M_{UO2F2}, and M_{tot} and by total enthalpy flow rate H_{tot}. These variables have been calculated in UF6CHEM and do not change during the thermodynamic equilibrium calculation. The solution for the equilibrium state is reached as described in the following.

To fully describe the thermodynamic equilibrium state, the following twelve unknowns must be determined:

(1) molar fraction of HF-monomer y_{11} in the vapor mixture,
(2) molar fraction of HF-dimer y_{12} in the vapor mixture,
(3) molar fraction of HF-hexamer y_{16} in the vapor mixture,
(4) molar fraction if HF-octamer y_{18} in the vapor mixture,
(5) molar fraction of $HF{\cdot}H_2O$ y_c in the vapor mixture,
(6) molar fraction of water vapor y_w in the vapor mixture,
(7) molar fraction of UF_6 vapor y_{UF6} in the vapor mixture,
(8) molar fraction of dry air y_a in the vapor mixture
(9) molar flow rate of vapor M_{vap} (kmole/s),
(10) molar fraction of UF_6 vapor in total UF_6, f_v,
(11) molar flow rate of solid M_{sol} (kmole/s), and
(12) mixture temperature T (K).

To obtain a solution to these twelve unknown variables, twelve independent governing equations must be derived. These equations in turn can be reduced to a set of three equations for three basic unknowns:

(1) the fugacity of the HF monomer, $f_1 = y_{11}\Phi_1 P$;
(2) mixture temperature, T;
(3) molar fraction of UF_6 vapor in the total UF_6, fv;

where $\Phi \sim 1$, and the total vapor pressure $P \sim 1$ atm.

The other ten unknowns can be expressed as functions of these three basic variables. The governing equations for the original twelve thermodynamic state variables are listed below and are marked with additional Roman numerals at the left side of each equation. Furthermore, the steps by which the twelve equations are reduced to three are also indicated.

- *Step 1.* Express $y_{11}, y_{12}, y_{16}, y_{18}$, and y_c/y_w, as functions of f_1, and T.

The equilibrium equations for the HF dimer, the HF hexamer, the HF octamer, and the $HF{\cdot}H_2O$ compound must be satisfied (Schotte, 1988):

I
$$y_{12}(f_1,T) = K_2(T) f_1^2/(\Phi_1 P) \quad , \tag{5-37}$$

II
$$y_{16}(f_1,T) = K_6(T) f_1^6/(\Phi_1 P) \quad , \tag{5-38}$$

III
$$y_{18}(f_1,T) = K_8(T) f_1^8/(\Phi_1 P) \quad , \tag{5-39}$$

$$y_c(f_1,T) = K_c(T)\, f_1 P_{wt}/(\Phi_1 P) \quad , \tag{5-40}$$

where fugacity $f_1 = y_{11}\Phi_1 P$, fugacity coefficient $\Phi_1 \sim 1$, total vapor pressure $P \sim 1$ atmosphere, $K_2(T)$, $K_6(T)$, $K_8(T)$, and $K_c(T)$ are equilibrium constants associated with the formation of $(HF)_2$, $(HF)_6$, $(HF)_8$, and $HF{\cdot}H_2O$, respectively, and are defined as functions of temperature (in K) by Schotte (1988).

$$K_2 = \exp[(53458.697/T - 200.76387)/R] \ (atm^{-1}) \ , \tag{5-41a}$$
$$K_6 = \exp[(175448.07/T - 579.77837)/R] \ (atm^{-5}) \ , \tag{5-41b}$$
$$K_8 = \exp[(209734.20/T - 694.02013)/R] \ (atm^{-7}) \ , \tag{5-41c}$$

where the gas constant R is 8.3143 J/K/mole

In Eq. (5-40), f_w is the fugacity of water vapor,

$$f_w = y_w \phi_1 P \quad . \tag{5-42}$$

From Eqs. (5-40) and (5-42), we obtain

IV
$$y_c(f_1,T)/y_w(f_1,T) = K_c(T)\, f_1 \quad , \tag{5-43}$$

where,

$$K_c(T) = \exp[(26220.445/T - 94.989486)/R] \quad (atm^{-1}) \quad . \tag{5-44}$$

- ***Step 2.*** **Express the molar flow rates of vapor M_{vap} and solid M_{sol} and fraction of water vapor y_w as functions of three basic unknowns and the variables derived above.**

The molar flow rate of the solid phase consists of the UO_2F_2 that was generated and the UF_6 that has not sublimated.

V
$$M_{sol} = M_{UO2F2} + (1 - f_v) M_{UF6} \quad . \tag{5-45}$$

The molar flow rate of the vapor phase is

VI
$$M_{vap} = M_{tot} - M_{sol} \quad . \tag{5-46}$$

In the absence of liquid HF fog, the partial vapor pressure of water (including the $HF{\cdot}H_2O$ complex) satisfies

$$y_w + y_c = \frac{M_w}{M_{vap}} \quad . \tag{5-47}$$

The molar fraction of water vapor y_w in the vapor mixture can be obtained from the relation

VII
$$y_w = \frac{M_w / M_{vap}}{1 + y_c / y_w} \quad . \tag{5-48}$$

Based on Eqs. (5-43) and (5-48), the molar fraction of $HF{\cdot}H_2O$ in the vapor mixture, y_c, can be calculated.

- ***Step 3.*** **Derive y_a and y_{UF6} based on the conservation of dry air and UF_6 vapor.**

From the definitions of the molar fractions, y_a and y_{UF6},

VIII
$$y_a = \frac{M_a}{M_{vap}} \quad , \tag{5-49}$$

IX

$$y_{UF6} = \frac{P_{UF6}^{Sat}}{P} \qquad if \quad M_{UF6}^{s} > 0 \ ,$$

$$y_{UF6} = \frac{f_v \, M_{UF6}}{M_{vap}} \qquad if \quad M_{UF6}^{s} = 0 \ , \tag{5-50}$$

where P_{UF6}^{Sat} is the saturation vapor pressure of UF_6. At temperature T_F in °F (Williams, 1985a), P_{UF6}^{Sat} (in psia) can be calculated from the equation:

$$\ln\left(P_{UF6}^{Sat}\right) = 10.443 + 9.64233 \times 10^{-3} T_F - 3907.41/(T_F + 298.149) \ . \tag{5-51}$$

Thus far, the number of unknowns has been reduced from twelve to three. As a final step, the three equations are listed for the three basic unknowns, f_l, T, and f_v.

- ***Step 4.*** **Formulate a set of equations for the three basic unknowns. These three final equations are solved by the proprietary nonlinear algebraic equation solver NAESOL (Nonlinear Algebraic Equation Solver), developed by Shell Research.**

The sum of the molar fractions of all components in the vapor mixture must equal 1:

X

$$y_{11} + y_{12} + y_{16} + y_{18} + y_c + y_w + y_{UF6} + y_a = 1 \ . \tag{5-52}$$

The molar flow rate of HF is conserved (i.e., the molar flow rate prior to the thermodynamic equilibrium is equal to the molar flow rate afterward).

XI

$$M_{HF} = \left(y_{11} + 2y_{12} + 6y_{16} + 8y_{18} + y_c\right) M_{vap} \ . \tag{5-53}$$

Finally, the enthalpy balance equation states that

XII

$$H_{tot} = H_{HF} + H_w + H_a + H_{UF6} + H_{UO2F2} \ , \tag{5-54}$$

where H_{TOT} is obtained from the chemistry module (see Eq. 5-36d), and should equal the sum of the enthalpies (in kJ/s) of all species in the plume mixture. These enthalpies are computed from Eqs. (5-55) through (5-60).

The enthalpy of HF is

$$H_{HF} = M_{HF}\left[H^{\Delta HF} + c_p^{HFV}\,(T - T^*)\right] \quad , \tag{5-55}$$

where

$$H^{\Delta HF} = \frac{y_{12}\Delta H_2 + y_{16}\Delta H_6 + y_{18}\Delta H_8 + y_c\Delta H_c}{y_{11} + 2y_{12} + 6y_{16} + 8y_{18} + y_c} \tag{5-56}$$

is the enthalpy departure of the HF vapor from the ideal monomeric gas at temperature T, c_p^{HFV} is the specific heat of the HF vapor, T^* is the reference temperature (25° C).

Similarly, the enthalpy of the water vapor is

$$H_w = M_w\, c_p^{wv}\,(T - T^*) \quad , \tag{5-57}$$

where c_p^{wv} is the specific heat of the vapor water.

The enthalpy of UF_6 is the sum of the enthalpies of vapor UF_6 and solid UF_6:

$$H_{UF6} = f_v\, M_{UF6}\, H^v_{UF6}(T) + (1 - f_v)\, M_{UF6}\, H^s_{UF6}(T) \quad . \tag{5-58}$$

The enthalpies of dry air and UO_2F_2 can be calculated from the relations

$$H_a = M_a\, c_p^a\,(T - T^*) \quad , \tag{5-59}$$

$$H_{UO2F2} = M_{UO2F2}\, c_{UO2F2}(T - T^*) \quad , \tag{5-60}$$

where c_p^a and c_{UO2F2} are the specific heats of dry air and UO_2F_2 solid, and $H^v_{UF6}(T)$ and $H^s_{UF6}(T)$ are the specific enthalpies of UF_6 vapor and solid, respectively.

The coefficients and correlations used in Eqs. (5-57) through (5-60) are obtained from Bloom et al. (1989) for UF_6 and UO_2F_2 and from HGSYSTEM (Witlox, 1993a) for HF, water, and dry air.

5.5.2 Thermodynamic Properties

The thermodynamic properties discussed so far in this section are summarized below.

ΔH_α = enthalpy of association of HF species α (cal/mole);
α = 2 (dimer, ΔH_2 = -12775), 6 (hexamer, ΔH_6 = 41927),
8 (octamer, ΔH_8 = -50121), or c ($HF{\cdot}H_2O$, ΔH_c = -6266).

c_p^α = specific heat at constant pressure of species α (cal/mole/°C);
α = a (dry air; c_p^a = 6.96), w (water, c_p^w = 8.05), HFV (gaseous HF, c_p^{HFV} = 6.96).

H^s_{UF6} = specific enthalpy of UF_6 solid (Btu/lb)

$$= 50.4460 - 5.70531 x\, 10^{-2}\, T_a + 1.27509 x\, 10^{-4}\, T_a^2 - 9645.63/T_a \ .$$

H^ℓ_{UF6} = specific enthalpy of UF_6 liquid (Btu/lb)

$$= 30.6133 + 5.10057\ x\ 10^{-2}\ T_a + 5.13165\ x\ 10^{-5}\ T_a^2 - 6139.34/T_a \ .$$

H^v_{UF6} = specific enthalpy of UF_6 vapor (Btu/lb)

$$= 43.2614 + 9.21307 x\, 10^{-2}\, T_a + 6.26265 x\, 10^{-6}\, T_a^2 + 2951.71/T_a \ .$$

where
T_a = absolute temperature (°R): T_a = T(°F) + 459.67.

c_{UO2F2} = specific heat of UO_2F_2 (Btu/lb-F) = 0.0821 (Bloom et al.,1989).

5.5.3 Mixture Density

The volume flow rate $\dot{V}$ (in m^3/s) of the mixture is obtained by applying the ideal gas law assuming that the contribution of solids to the total volume is negligible:

$$\dot{V} = \frac{[R\ (T + 273.15)]\ M_{vap}}{P} \ , \qquad (5\text{-}61)$$

where R = 0.082 (atm m^3/K/kmole) is the gas constant. The density of the mixture is the ratio of the total mass flow rate (kg/s) to the total volume flow rate (m^3/s).

$$\rho = \frac{\dot{m}}{\dot{V}} \ . \qquad (5\text{-}62)$$

The plume density ρ and temperature T calculated in the thermodynamics module are communicated back to the dispersion module for the next integration step.

6. GENERAL TECHNICAL IMPROVEMENTS TO HGSYSTEM

Several technical improvements were added to HGSYSTEM that are general in the sense that they apply to all types of chemical releases and are not specifically linked to UF_6. These new algorithms have been included in Version 3.0 of the HGSYSTEM code released by Shell. Sections 6.1 through 6.5 provide technical discussions of the following five topics. Their implementation in the code is further discussed in Sect. 7.1.

- Removal by dry and wet deposition
- Plume lift-off
- Meteorological pre-processor
- Concentration fluctuations and averaging time
- Buildings and terrain obstacles

6.1 REMOVAL BY DRY AND WET DEPOSITION

6.1.1 Overview of Removal Processes

The UF_6 plume will consist of a mixture of gases, solid particles, and aerosols. Larger particles and aerosols will fall to the ground due to gravitational settling. Smaller particles, aerosols, and gases will deposit on the surface due to a process called dry deposition, which is caused by a combination of phenomena such as chemical reactions and physical interception by the ground and vegetation. In the presence of rain, fog, or snow, the pollutant may be removed from the plume and deposited on the ground either by absorption or collection by the water drops or snowflakes. A comprehensive schematic diagram illustrating these processes is given in Fig. 6-1. Thorough reviews of dry deposition and wet scavenging are given by Sehmel (1984) and Slinn (1984), respectively.

Models for hazardous gas dispersion (e.g., SLAB, DEGADIS, or HGSYSTEM) generally do not account for dry or wet deposition because at distances within a few hundred meters of the source, these processes are significant only for large particles (diam D_p > 1000 μm). Most research on dry and wet deposition has been connected with larger space and timescales (e.g., acid deposition over the northeastern United States over several days). In addition, there has been concern about deposition of toxic substances, such as dioxin, that are produced at solid waste incinerators. Consequently, comprehensive wet and dry deposition modules have been built into the EPA's Regional Acid Deposition Model (RADM) and Industrial Source Complex-Version 2 (ISC-2) model.

Original research on wet and dry deposition in the 1950s was spurred by concern of the U.S. Atomic Energy Commission with fallout from nuclear weapons tests and with deposition from fuel production and reprocessing facilities (Sehmel, 1984; Slinn, 1984]. Results of this work formed the basis for models currently in use.

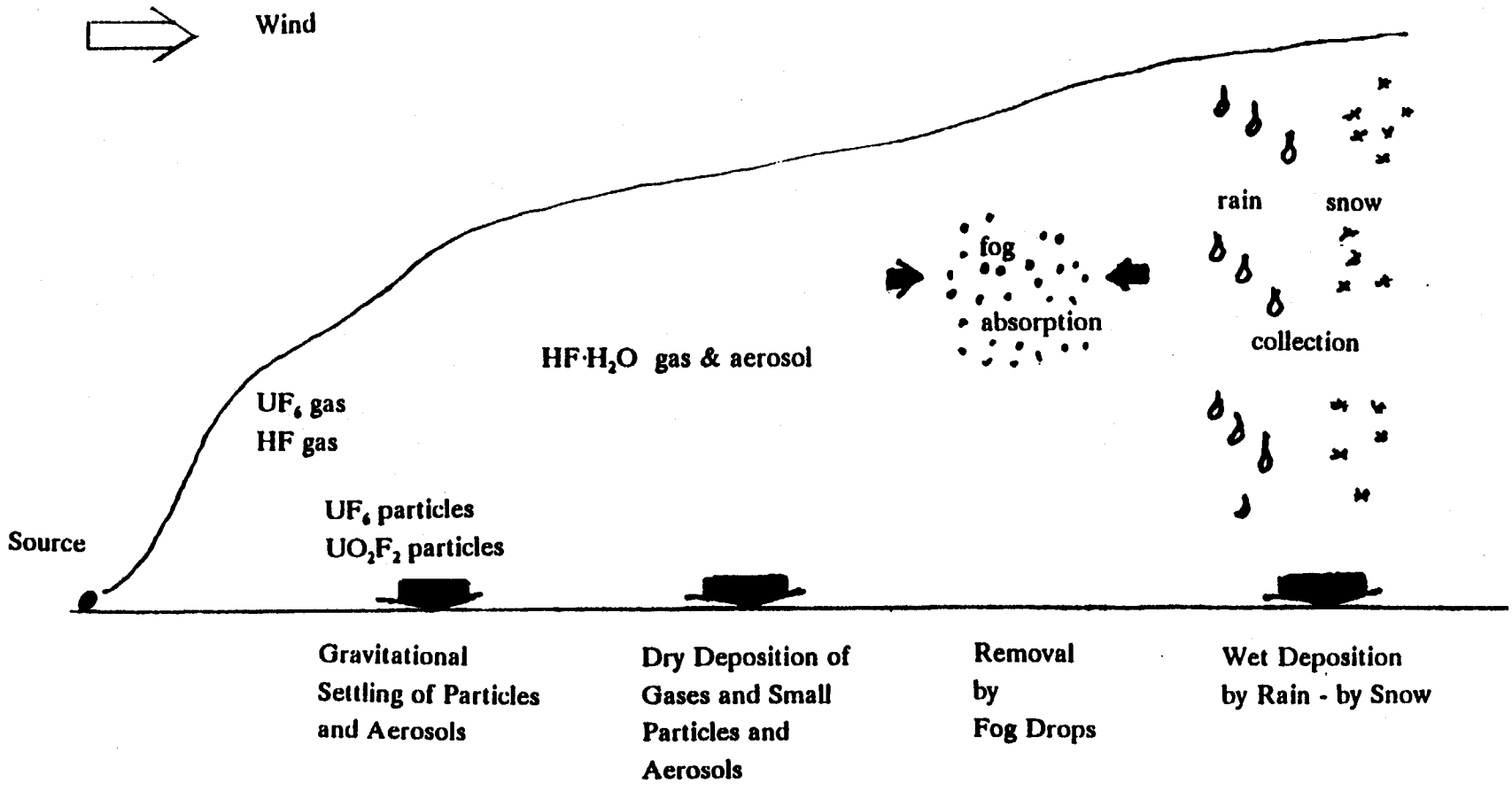

Fig. 6-1. Schematic diagram of processes leading to removal of plume material by deposition to the ground.

6.1.2 Desired Level of Complexity in Deposition Algorithms in HGSYSTEM/UF_6 Model

Energy Systems' PLM89A model (Bloom et al., 1989) contains some simplified dry and wet deposition formulas for the UF_6 plume. These formulas have been reviewed and some have been added for gravitational settling and wet removal. Deposition is recognized to be a minor component of the conservation equation for most chemicals in the plume; accounting for all the various details of the removal processes is not necessary. Furthermore, simplified default methods are suggested since large uncertainties are in the required input information, such as the size spectrum for particles formed after the flashing UF_6 liquid release. If future field experiments suggest certain details must be included, revised formulas can be developed.

Dry deposition formulas are applied as a post-processor in HGSYSTEM/UF_6, given the ground-level distribution of calculated concentrations. Presently, it is assumed there is no feedback between dry deposition and the plume chemistry and thermodynamics.

6.1.3 Removal by Gravitational Settling and Dry Deposition

Gravitational settling of large particles or aerosols

Large particles or aerosols with diameter D_p greater than about 50 μm (1 μm = 10^{-6} m), will have a gravitational settling speed v_s greater than 10 cm/s. In that case, removal will be dominated by simple gravitational settling. Stoke's law can be used with a slip correction factor:

$$v_s = \frac{(\rho_p - \rho_{air})\, g\, D_p^2\, c_2}{18\, \mu}\, S_{CF} \quad , \tag{6-1}$$

where

ρ_p = particle density (g/m^3),
ρ_{air} = air density (g/m^3),
g = acceleration of gravity (9.81 m/s^2),
D_p = particle diameter (μm),
μ = 1.81 x 10^{-2} g/m·s = air viscosity,
c_2 = 1 × 10^{-12} m^2/μm^2 = conversion factor,
S_{CF} = the slip correction factor for larger particles.

$$S_{CF} = 1 + \frac{0.13\left(1.257 + 0.4\, e^{-8.5\, D_p}\right)}{D_p} \quad , \tag{6-2}$$

where D_p must have the units μm in this expression.

The implication is that a plume of large particles with a given diameter D_p will fall away from the gaseous part of the plume with a speed of v_s, as illustrated in Fig. 6-2. The vertical distance "fallen" by the particle plume, relative to the remainder of the gas plume at downwind distance x, is given by $v_s x/u$. This is called the "tilted plume" model in the literature. The tilted plume has the same shape as the remainder of the gas plume but is displaced downward due to the settling of particles.

The large particles (i.e., UF_6 particles) are modeled in HGSYSTEM/UF_6 by two steps:

1. Assume that the large particles can be divided into a few size classes, where each size class is characterized by diameter D_p and concentration $C(D_p)$. The particle plume is assumed to ***not*** affect the remainder of the plume.

2. The local particle deposition flux to the ground is given by

$$F_{D_p} = v_s\, C(D_p, x, y, 0) \quad , \tag{6-3}$$

where $C(D_p, x, y, 0)$ refers to the ground level concentration of that size-class of particles at position (x, y) of the tilted plume.

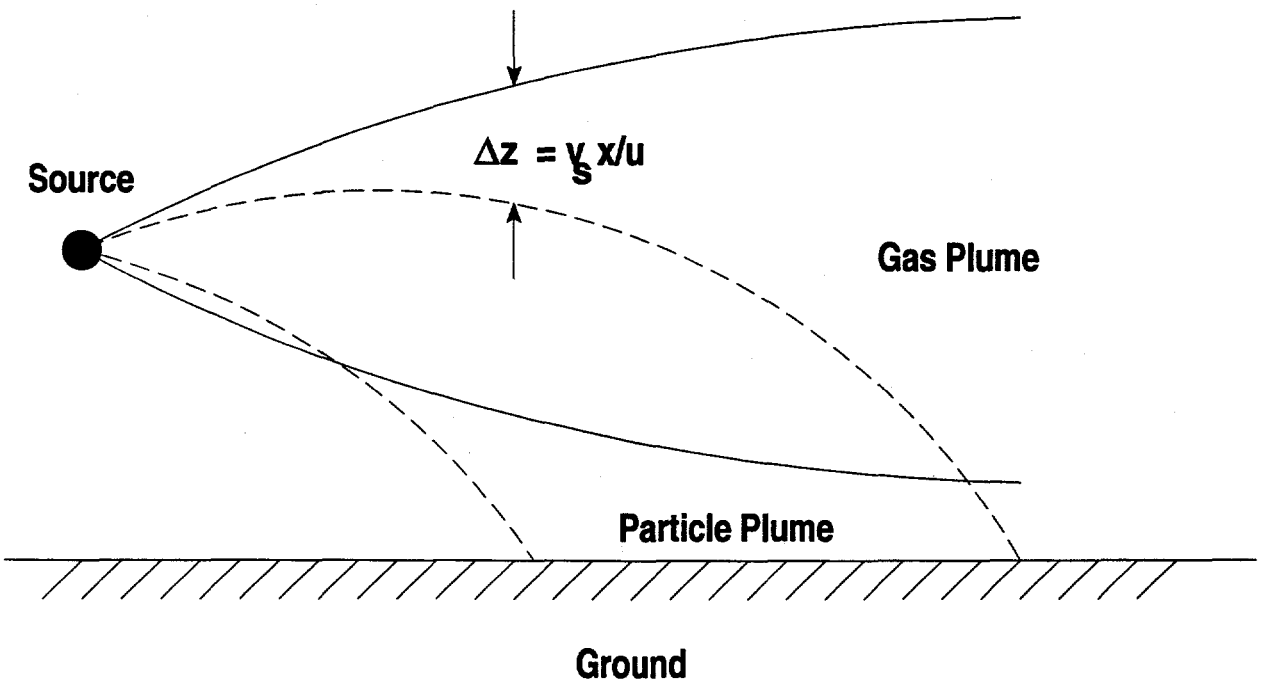

Fig. 6-2. Illustration of how a large particle plume will fall away from the rest of the gas plume.

Dry deposition of small particles and gases

Aside from the large UF_6 particles, the remaining components of the plume (UF_6 gas, UO_2F_2 particles, HF gas, and $HF{\cdot}H_2O$) do not have appreciable settling velocities. UO_2F_2 particles are observed by Bayne and Bostick (1985) to have very small diameters (about 1 μm). The current version of the model assumes the $HF{\cdot}H_2O$ compound is in the gas phase. But even if this compound were in the liquid phase, the $HF{\cdot}H_2O$ aerosol drops would have diameters typical of natural fogs (about 1 to 10 μm). Consequently, standard dry deposition formulas can be used to calculate the deposition of UO_2F_2 and $HF{\cdot}H_2O$ to the ground surface. Mass removal due to dry deposition is assumed to be insignificant when compared with the total mass flux in the plume because (1) we are primarily interested in distances within a few hundred meters of the source and (2) it is desirable in the plume thermodynamics algorithms that no mass be removed from the plume.

The dry deposition formula used is based on that in the EPA's revised ISC-2 model and is similar to one used in the PLM89A model by Bloom et al. (1989). Currently, most state-of-the-art deposition models use the resistance analog, where the deposition velocity is assumed to be inversely proportional to the sum of a set of resistances, i.e,

$$v_d = \frac{1}{r_a + r_s + r_t} + v_s \quad , \tag{6-4}$$

where

v_s = gravitational settling speed, which is non-zero for particles (see Eqs.[6-1] and [6-2]) and zero for gases,
r_a = aerodynamic resistance (s/m),
r_s = surface or laminar layer resistance (s/m),
r_t = transfer resistance dependent on surface characteristics (s/m).

Aerodynamic resistance r_a is the same for gases and for small particles:

$$r_a = \frac{1}{0.4\, u_*} \left(\ln \frac{z_d}{z_o} - \psi_H \left(\frac{z_d}{L} \right) \right) \quad , \tag{6-5}$$

where

u_* = friction velocity,
L = Monin-Obukhov length
z_d = reference height (assumed to equal 10 m),

and

the function ψ_H is given by Eqs. (6-6a), (6-6b), (6-6c).

$$\Psi_H\left(\frac{z}{L}\right) = -5\ z/L \qquad 0 < z/L \ . \tag{6-6a}$$

$$\Psi_H\left(\frac{z}{L}\right) = 0 \qquad z/L = 0 \ . \tag{6-6b}$$

$$\Psi_H\left(\frac{z}{L}\right) = 2\ \ell n\left(\frac{1 + (1 - 16\ z/L)^{1/2}}{2}\right) \qquad z/L < 0 \ . \tag{6-6c}$$

The HGSYSTEM/UF_6 model automatically will provide values of u_* and L based on observations of wind speed and stability and estimates of stability class based on surface roughness, length, and estimated value of L. As a default, the following parameterizations can be made:

$$u_* = u(10\ m)/15 \ . \tag{6-7}$$

$$L = \begin{cases} -20\ m & Class\ A \\ -50\ m & Class\ B \\ -100\ m & Class\ C \\ \infty & Class\ D \\ 50\ m & Class\ E \\ 20\ m & Class\ F \end{cases} \tag{6-8}$$

Surface, or laminar layer resistance, r_s is dependent on the molecular diffusivity of gases or the Brownian diffusivity of particles and can be estimated from the formula:

$$r_s = \left[Sc^n + \frac{St}{(1 + St^2)}\right]^{-1} u_*^{-1} \ , \tag{6-9}$$

where

Sc = Schmidt number,
St = Stokes number,
n = -0.5 for $z_o < 0.1$ m,
n = -0.7 for $z_o > 0.1$ m. (6-10)

The Schmidt number is given by:

$$Sc = \nu/D_B \qquad for\ particles \ , \tag{6-11a}$$

$$Sc = \nu/D \qquad for\ gases \ , \tag{6-11b}$$

where

ν = molecular viscosity of air ($\nu = \mu/\rho = 0.15$ cm^2/s),
D_B = Brownian diffusivity of the particles in air,
D = molecular diffusivity of the pollutant gas in air.

For many gases, *Sc* is on the order of unity. For particles, Brownian diffusivity D_B is a strong function of particle size, ranging from $D_B \sim 10^{-7}$ cm^2/s for $D_p \sim 1$ μm to $D_B \sim 0.1$ cm^2/s for $D_p \sim 10^{-4}$ μm. To calculate D_B (in cm^2/s) for particles, the model uses the formula

$$D_B = 0.81 \times 10^{-9} \frac{T S_{CF}}{D_p} \quad , \tag{6-12}$$

where

T = air temperature (K),
S_{CF} = slip correction factor [see Eq. (6-2)],
D_p = particle size (μm).

The Stokes number is non-zero only for particles and is given by

$$St = \left(\frac{v_s}{g}\right)\left(\frac{u_*^2}{\nu}\right) \quad . \tag{6-13}$$

It is evident that r_s is important only for gases or very small particles (diameter of 10^{-3} μm or less) and can be ignored for particles with sizes about 1 μm or greater.

Transfer resistance r_t, the subject of extensive research, is generally parameterized by Eqs. (6-14a, b). For particles,

$$r_t = r_a r_s v_s \quad , \tag{6-14a}$$

and for gases,

$$r_t = \frac{1}{\frac{LAI}{r_f} + \frac{LAI}{r_{cut}} + \frac{1}{r_g}} \quad , \tag{6-14b}$$

where

LAI = leaf area index (area of leaves over a unit area of ground surface),
r_f = stomate resistance,
r_{cut} = cuticle resistance,
r_g = resistance to transfer across the nonvegetated ground or water surface.

The first two terms are significant only when vegetation is actively growing and the pollutant is sufficiently reactive to be absorbed by the vegetation. The last term is significant only if the pollutant is reactive with the surface. For nonreactive gases, surface transfer resistance r_t is infinity, and the deposition velocity is therefore zero (see Eq. [6-4]).

Terms r_f, r_{cut}, and r_g are well known only for gases involved in acid deposition processes, such as SO_2, NO_2, HNO_3, PAN, and O_3. For these gases, Pleim et al. (1984) suggest r_t is about 10 s/cm, with variations of plus or minus a factor-of-three depending on the particular gas. Little is known about these terms for UF_6, HF, and HF-H_2O. Bloom et al. (1989) cite Varma (1982) to justify their choice of 0.02 s/cm for r_t. With such a low value, r_t is not the dominant term for determining the dry deposition velocity in Eq. (6-4). In other words, pollutants in the UF_6 + HF plume are so reactive with other substances that their deposition rate is not limited by the surface transfer term.

As a default, set r_t = 0.02 s/cm in the HGSYSTEM/UF_6 model. If future field and laboratory studies permit r_f, r_{cut}, and r_g to be estimated, that new information can be used to update r_t by means of Eq. (6-14b).

6.1.4 Removal of Particles and Gases by Precipitation and Clouds (Wet Deposition)

Particles and gases can be removed from the plume by rain, snow, clouds, or fog by two mechanisms:

- In-cloud scavenging by small cloud or fog water drops.
- Below-cloud scavenging as large precipitation drops or snowflakes fall through a polluted plume.

In-cloud scavenging, is important only for reactive gases and particles since the water drops are assumed to be ***not*** moving through the pollutant cloud; therefore, the only way the gases or particles can mix with the drops is by an absorption process. As Slinn (1984) explains, if the pollutant and drops are exposed to each other for a long time, the concentration of chemicals such as SO_2 and NO_2 in the liquid reach an equilibrium determined by Henry's law. This process is clearly different from the second mechanism, when the liquid drops fall through the pollutant cloud in a relatively short time (a few seconds, at most), and the primary removal mechanism is via capture of pollutant particles or aerosols by the droplets.

Both in-cloud and below-cloud scavenging mechanisms are parameterized in models using scavenging scale Λ with units s^{-1}, which is approximately proportional to the precipitation rate P with units mm/hr. Local concentration C is assumed to decrease exponentially with time.

$$C(t) = C(0)\, e^{-\Lambda t} \quad , \tag{6-15}$$

where t is the time the plume has been exposed to the liquid water drops.

The precipitation-induced flux of material to the ground F_{wet} is given by

$$F_{wet} = \int_0^{z_w} \Lambda\, C(z)\, dz \quad , \tag{6-16}$$

where z_w is the depth of the wetted plume layer.

Bloom et al. (1989) include a wet removal time factor in their PLM89A model and assume it equals 10^{-3} s^{-1} for HF, ClF_3, and ClO_2; $2 \times 10^{-3} s^{-1}$ for UF_6 and UO_2F_2; and zero for HCl, F_2, and inert substances. Ramsdell et al. (1993) use the following parameterizations for Λ for iodine gas and aerosol compounds as a function of precipitation rate in their RATCHET model:

For rain: $$\Lambda = 4 \times 10^{-4} \, Pr^{3/4} \quad , \tag{6-17a}$$

For snow: $$\Lambda = 6 \times 10^{-5} \, Pr \quad , \tag{6-17b}$$

where precipitation rate Pr is in mm/hr.

The rates in the following table are suggested:

	Pr (mm/hr liquid equivalent)		
	Light	**Moderate**	**Heavy**
Rain	0.1	3	5
Snow	0.03	1.5	3.3

As an example, Eq. (6-17a) gives $\Lambda \approx 10^{-3} s^{-1}$ or about $(15 \text{ min})^{-1}$ for moderate rain. This means that most of the pollutant would be removed after being subjected to 15 min of moderate rain.

The Λ values in the PLM89A and RATCHET models are consistent. A default value of $(1000 \text{ s})^{-1}$ is suggested for use in the HGSYSTEM/UF_6 code if the precipitation rate is not known. Equations (6-17a) and (6-17b) can be used if the precipitation rate is known. In the future, as experimental data become available, revised Λ values can be prescribed for specific chemicals such as HF-H_2O. When Λ and $C(z)$ are known, Eq. (6-16) is used to calculate the wet flux to the ground.

Because travel times to receptors of interest would be about 10 to 100 s for expected UF_6 accidental releases, it is possible to neglect the reduction in total mass flux due to wet deposition of chemicals in the plume. Plume chemistry and thermodynamics calculations are not assumed to be affected by wet removal at these times and distances. For larger travel times of 1000 s or more and for distances of a few kilometers, the wet removal may be significant and may affect the plume thermodynamics. The present version of HGSYSTEM neglects the in-cloud scavenging by fog drops since that term is insignificant for travel times of 10 to 100 s.

6.2 PLUME LIFT-OFF MODULE

A buoyant plume blowing along the ground may "lift off" the ground if buoyancy forces exceed turbulent forces within the ambient boundary layer. The few previous analyses of this problem all dealt with plumes that tend to conserve their initial buoyancy flux (Briggs, 1973; Meroney, 1979; Poreh and Cermak, 1986; Hall and Waters, 1986; Slawson et al. 1990).

$$F_o = w_o R_o^2 g(\rho_a - \rho_o)/\rho_a ,$$

where

$_o$ = initial plume,
$_a$ = ambient environment,
w = plume vertical velocity,
R = plume radius,
g = acceleration,
ρ = density.

However, a UF_6 plume, as well as its subsequent products, does not conserve its initial buoyancy flux. In fact, relative plume density $(\rho_a - \rho)/\rho_a$ may change from positive to negative, depending on the influence of the following:

- Molecular weights of the gases that exist
- Enhanced effective density due to small particles carried by the plume
- Addition of heat due to exothermic reactions and condensation of liquids
- Removal of heat due to endothermic reactions, depolymerization, and evaporation of liquids

For example, consider a simple system where pure UF_6 is released at ambient temperature and then reacts with ambient water vapor. The plume will first be very dense $[(\rho_a - \rho)/\rho_a < 0]$ but may eventually become buoyant $[(\rho_a - \rho)/\rho_a > 0]$. All during this process, the plume will be growing in the vertical (depth H) and the horizontal (width W) and will be characterized by a local buoyancy flux:

$$F = (V/\pi)\, g(\rho_a - \rho)/\rho_a \quad , \tag{6-18}$$

where V is the plume volume flux in m^3/s. For a plume of dimensions H and W that is traveling at speed u, the volume flux V equals uHW. Figure 6-3 shows the typical time series of these variables. Also shown is the time series for the Briggs (1973) lift-off parameter L_p, which is defined by the following expression:

$$L_p = \frac{gH(\rho_a - \rho)/\rho_a}{u_*^2} \quad , \tag{6-19}$$

where u_* is the friction velocity (approximately given by $u_* \approx u(10\text{ m})/15$). Parameter L_p is proportional to the ratio of internal plume turbulent energy due to buoyancy forces to ambient atmospheric turbulent energy.

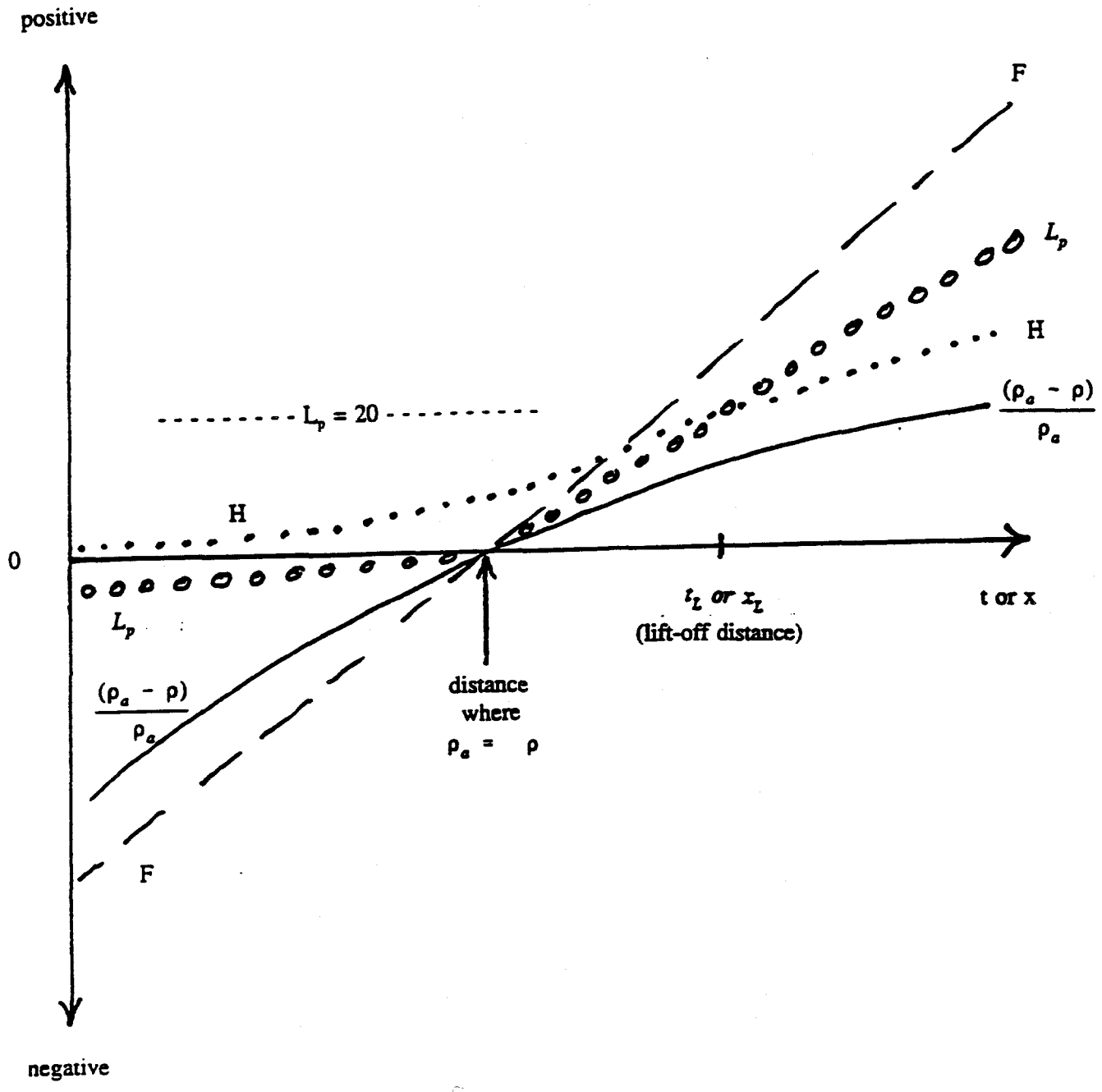

Fig. 6-3. Typical time series of $(\rho_a - \rho)/\rho_a$, buoyancy force F, plume depth H, and lift-off parameter L_p for a UF_6 plume.

Observations of plume lift-off in laboratory studies by researchers mentioned previously suggest that the ground-based plume will lift off the ground when $L_p \approx 20$; this number has an uncertainty of about a factor-of-two. Prior to that point, the plume may stretch vertically without lifting completely off the ground. Note that the criterion in Eq. (6-19) implies that, once a plume is buoyant [$(\rho_a - \rho) > 0$], a wind speed always exists that will give $L > 20$. If we assume that $u_* = u/15$, we can use Eq. (6-19) to calculate that lift-off will occur when

$$u < 3.4\left(gH(\rho_a - \rho)/\rho_a\right)^{1/2} \quad . \tag{6-20}$$

For example, if $H = 10$ m and $(\rho_a - \rho)/\rho_a = 0.01$, then lift-off will occur if $u < 3.4$ m/s. If $H = 1$ m and $(\rho_a - \rho)/\rho_a = 0.001$, then lift-off will occur only if $u < 0.34$ m/s.

Briggs and others employ the criterion of Eq. (6-19), along with assumptions for the growth of volume flux V with time, to derive formulas for calculating the distance at which $L_p = 20$ for plumes where buoyancy flux F is conserved. These formulas are ***not*** given here because F is not conserved in a UF_6 plume. The default procedure for calculating plume lift-off in HGSYSTEM is the following:

1. Once the plume is on the ground, either because it initially was released at the ground or it sank to the ground due to the excess density of UF_6, it will remain on the ground (i.e., plume base at the ground) as long as the ***local*** $L_p < 20$. Note that H and ρ are the local plume depth and density as calculated by the AEROPLUME or HEGADAS algorithms in HGSYSTEM/UF_6.

2. Once the plume depth and buoyancy increase so that $L_p = 20$, the plume centerline (or point of maximum concentration) is allowed to begin lifting off the ground at the rate determined by the buoyant plume vertical equation of motion in AEROPLUME or by the Briggs "two-thirds law" in HEGADAS.

After plume lift-off is triggered in HEGADAS, the code carries out its calculations as if the plume were still touching the ground, but the code "remembers" that lift-off is to be accounted for later. In a post-processor, the rise of the plume centerline is calculated by using the differential form of the plume rise formulas suggested by Briggs (1975) and Weil (1988):

$$\Delta z = \left(\frac{3\, l_b}{2\, \beta^2}\right)^{1/3} \frac{2}{3}\, x^{-1/3}\, \Delta x \quad , \tag{6-21}$$

where Δx is the integration step size, and Δz is the amount of plume rise within a downwind distance increment Δx. Buoyancy length scale ℓ_b is defined by

$$\ell_b = \frac{H^2\, g\, \Delta\rho}{u^2\, \rho_a} \quad . \tag{6-22}$$

In the lift-off algorithm applied to HEGADAS,

z = height that refers to the "bottom" of the HEGADAS plume, since that model assumes maximum concentration occurs at the bottom of the plume;
x = downwind distance from the point where L_p first equals 20;
β = 0.6, an empirical constant;
u = the ambient wind speed (taken to be measured at 10 m).

Note that l_b, defined in Eq. (6-21), is based on plume parameters at the point when L_p first equals 20 and is treated as a conserved quantity in subsequent calculations.

The so-called break-up formula is used to determine final buoyant plume rise. The plume will stop rising when the plume vertical velocity becomes less than ambient turbulent velocity. The following criterion is used:

$$\frac{\frac{dz}{dt}}{1.1\ u_*} = \frac{\textit{plume vertical velocity}}{\textit{ambient}\ \sigma_w} \sim 1 \quad . \tag{6-23}$$

This criterion is satisfied when $x = \ell_b\ (u/u_*)^3$. It can be shown that $x \approx 100H$ for HEGADAS, if $L_p = 20$ and H equals the plume depth at the point of lift-off.

6.3 METEOROLOGICAL PRE-PROCESSOR

6.3.1 Background

The original HGSYSTEM model (McFarlane et al., 1990) had a brief and limited meteorological processor. A few basic meteorological parameters (wind speed, stability class, surface roughness, relative humidity, temperature) were input to the model. The model used a simple power law formula to calculate the Monin-Obukhov length L as a function of surface roughness and stability class and then used standard Monin-Obukhov similarity formulas to calculate the variation of wind speed with height.

Crosswind passive dispersion parameters σ_y and σ_z in the HGSYSTEM model are functions of stability class, downwind distance, surface roughness, and averaging time. The along-wind passive dispersion parameter is, in addition, a function of vertical wind shear.

The methods in the original HGSYSTEM model are standard, robust procedures that have been used by modelers for more than 40 years. Similar procedures are used in the PLM89A model (Bloom et al., 1989). However, as recommended by Sykes and Lewellen (1992), advanced procedures now exist for calculating boundary layer turbulence and dispersion that can be incorporated in the HGSYSTEM/UF_6 model. These advanced procedures can be divided into three categories: (1) meteorological surface flux formulas, (2) meteorological profile formulas, and (3) dispersion algorithms.

Hanna et al. (1982) described simple formulas for each category of the new algorithms. For example, observations of wind speed and cloudiness could be used to estimate surface fluxes of heat and momentum. These flux estimates could then be used to generate vertical profiles of wind speed and turbulence. Finally, dispersion σ_y and σ_z could be calculated based on this knowledge of turbulent energy and timescales. These new formulas have been incorporated in the new version of HGSYSTEM.

6.3.2 Approach to Development of Revised Meteorological Pre-processor for HGSYSTEM/UF_6

Hanna and Chang (1992; 1993) discussed state-of-the-art formulas for surface fluxes, vertical profiles, and turbulent dispersion for their SIGPRO meteorological pre-processor and HPDM dispersion model. These are closely related to formulas suggested by Sykes and Lewellen (1992) and to algorithms in recent models developed by Weil (1992) and Carruthers et al. (1992).

If one were to adapt the entire set of formulas in SIGPRO and HPDM, major changes would be required to the passive dispersion algorithms in HGSYSTEM. Because the HGSYSTEM dispersion algorithms produce σ_y and σ_z estimates that are not much different than those in HPDM, retaining HGSYSTEM dispersion algorithms is preferable currently. In the future, revising those passive dispersion algorithms may be appropriate.

As a first step, the SIGPRO and HPDM meteorological surface flux and profile pre-processors are adapted for use in HGSYSTEM. With this approach, no major revisions to HGSYSTEM were needed because that model did not include a major meteorological pre-processor algorithm. The codes from SIGPRO and HPDM have been directly used in the new HGSYSTEM/UF_6 model.

6.3.3 Description of Revised Meteorological Pre-processor

Two articles by Hanna and Chang (1992; 1993) detail the SIGPRO and HPDM meteorological pre-processor, so the derivations are not repeated here. For example, Hanna and Chang (1993, Sect. 3) list the assumptions and formulas for surface heat flux Q_H, friction velocity u_*, Monin-Obukhov length L, mixing depth h, vertical profiles of wind speed u, turbulence components σ_v and σ_w, and temperature T. The following input parameters are required:

z_o	surface roughness
α	surface moisture availability
L_{min}	minimum stable Monin-Obukhov length
u	wind speed at some reference height, z_{ref}
ν	solar elevation angle
N	cloud cover

The references give tables of z_o, α, and L_{min} as a function of land-use type. The reference height for the wind speed observation is usually about 10 m. The solar elevation angle, which is used for calculating solar energy flux, is known from astronomical tables. For example, the ISC-2 model contains methods for determining v from a knowledge of latitude, longitude, and time of day. Cloud cover N, which ranges from 0.0 to 1.0, is observed routinely at National Weather Service stations.

To be consistent with EPA and NRC regulatory models, this revised method is designed to permit estimation of the Pasquill-Gifford-Turner stability class. The new HGSYSTEM/UF$_6$ meteorological processors use the Golder (1972) nomogram (see Fig. 6-4), in which stability class is given as a function of z_o (in the range from 0.1 cm to 50 cm) and $1/L$ (ranging from -0.13 m^{-1} to 0.09 m^{-1}). The HGSYSTEM model employs this nomogram in reverse, calculating L as a function of z_o and stability class. Depending on the requirements of the regulatory agency or project sponsors, the meteorological processor can be applied using a range of types of input parameters.

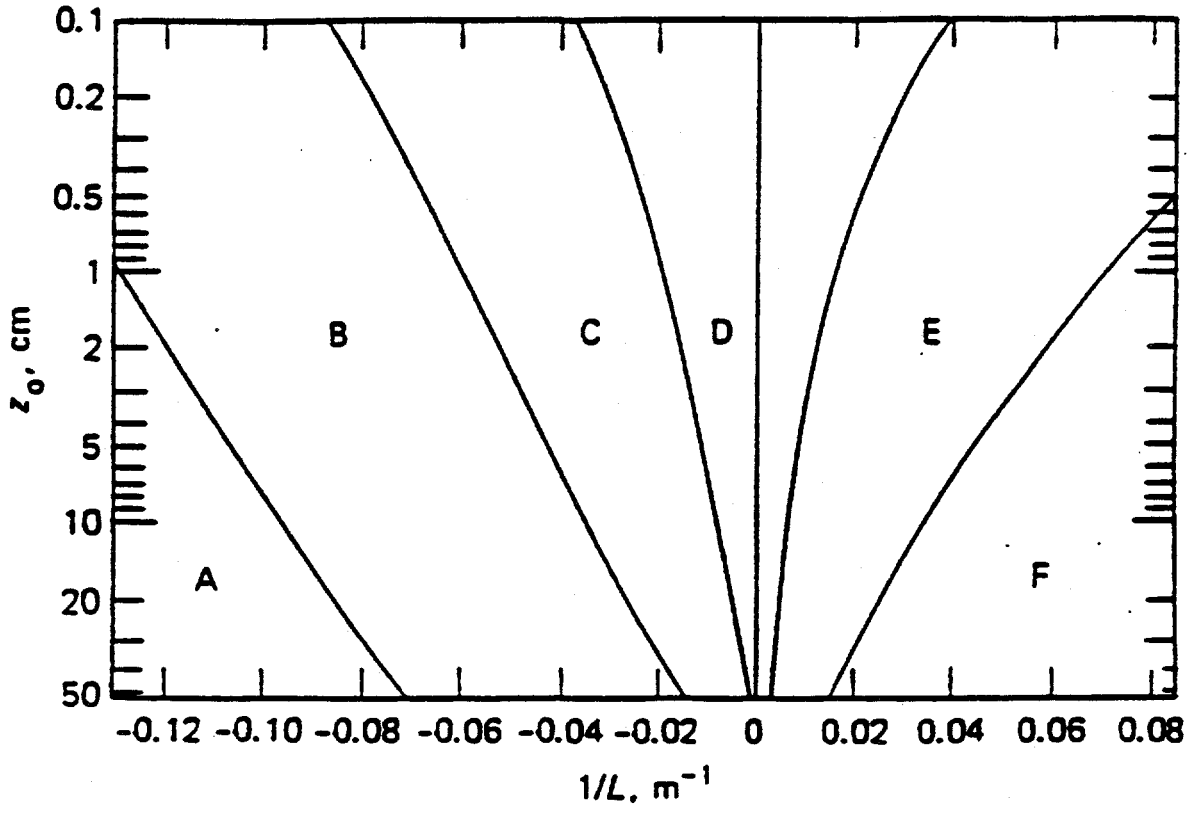

Fig. 6-4. Curves showing Pasquill-Gifford-Turner turbulence types as a function of the Monin-Obukhov length and the aerodynamic roughness length. *NOTE:* Conditions are as follows: A - extremely unstable; B - moderately unstable; C - slightly unstable; D - neutral (applicable to heavy overcast day or night); E - slightly stable; F - moderately stable. *Source:* D. Golder, "Relations Among Stability Parameters in the Surface Layer," *Bound. Layer Meteorol.*, 3, 56, 1972.

6.4 ALGORITHMS FOR CONCENTRATION FLUCTUATIONS AND VARIATIONS WITH AVERAGING TIME

Effects of concentration fluctuations and averaging time are discussed in Sects. 6.4.1 and 6.4.2 for two types of receptor definitions: a receptor on the plume centerline and a receptor at a fixed geometric position. Since HGSYSTEM is intended for application to the first type, the model has been modified following the suggested formulas in Sect. 6.4.1.

6.4.1 Predictions of Plume Centerline Concentrations at a Given Downwind Distance as a Function of Averaging Time T_a

Hazardous gas models such as HGSYSTEM can predict the crosswind concentration distribution at distance x from the source for a certain averaging time T_a. Basic model predictions of dense gas modules are appropriate for averaging times of about 2 min, which corresponds to field data on which the dense gas algorithms are based. Generally, predictions of passive gas models refer to an averaging time of about 10 or 20 min—the time for passive gas field data used in deriving the Pasquill-Gifford-Turner σ_y and σ_z curves. Also, the HGSYSTEM prediction is for an ensemble average, which is the average of millions of independent realizations of that particular experiment for those specific initial and boundary conditions and other input parameters. Those millions of individual realizations would themselves have a distribution about the ensemble average.

Model predictions of the ensemble average plume centerline concentration $C_{cl}(x, T_a)$ are not keyed to any specific geographic point—the only restriction is that the downwind distance must be x. But because natural plumes meander or swing back and forth, the ensemble average centerline concentration will drop as averaging time increases; the position of the centerline may also shift as T_a varies. Effects of averaging time on plumes are thoroughly discussed in the report by Wilson and Simms (1985).

Consider an ensemble of concentration observations under certain initial and boundary conditions: variation of the distribution of C_{cl} with T_a at a fixed x would be as shown in Fig. 6-5. Box plots indicate key points on the distribution function at each T_a. The dashed line passes through the mean, or median, of the distributions. If model predictions are corrected for averaging time T_a, corrected ensemble average concentrations should fall along this dashed line. As T_a approaches zero, i.e., an instantaneous snapshot of the plume, concentration C_{cl} should approach a value representative of the instantaneous plume.

Some models such as TRACE are designed to be conservative: to predict concentrations C_{cl} higher than the mean. These models' descriptions do not specify the quantitative percentile (e.g., the 99th) of the distribution being aimed for. However, if a model were designed (1) to predict the 99th percentile at each T_a, concentration predictions would follow the dotted line, or (2) to give the maximum at a given T_a for a given total sampling time (60 min in this case), concentration predictions would follow the dashed-dotted line (see Fig 6-5). In the latter case, the percentile associated with the single maximum concentration would increase as T_a decreases since the total number of concentration values equals 60 min/T_a.

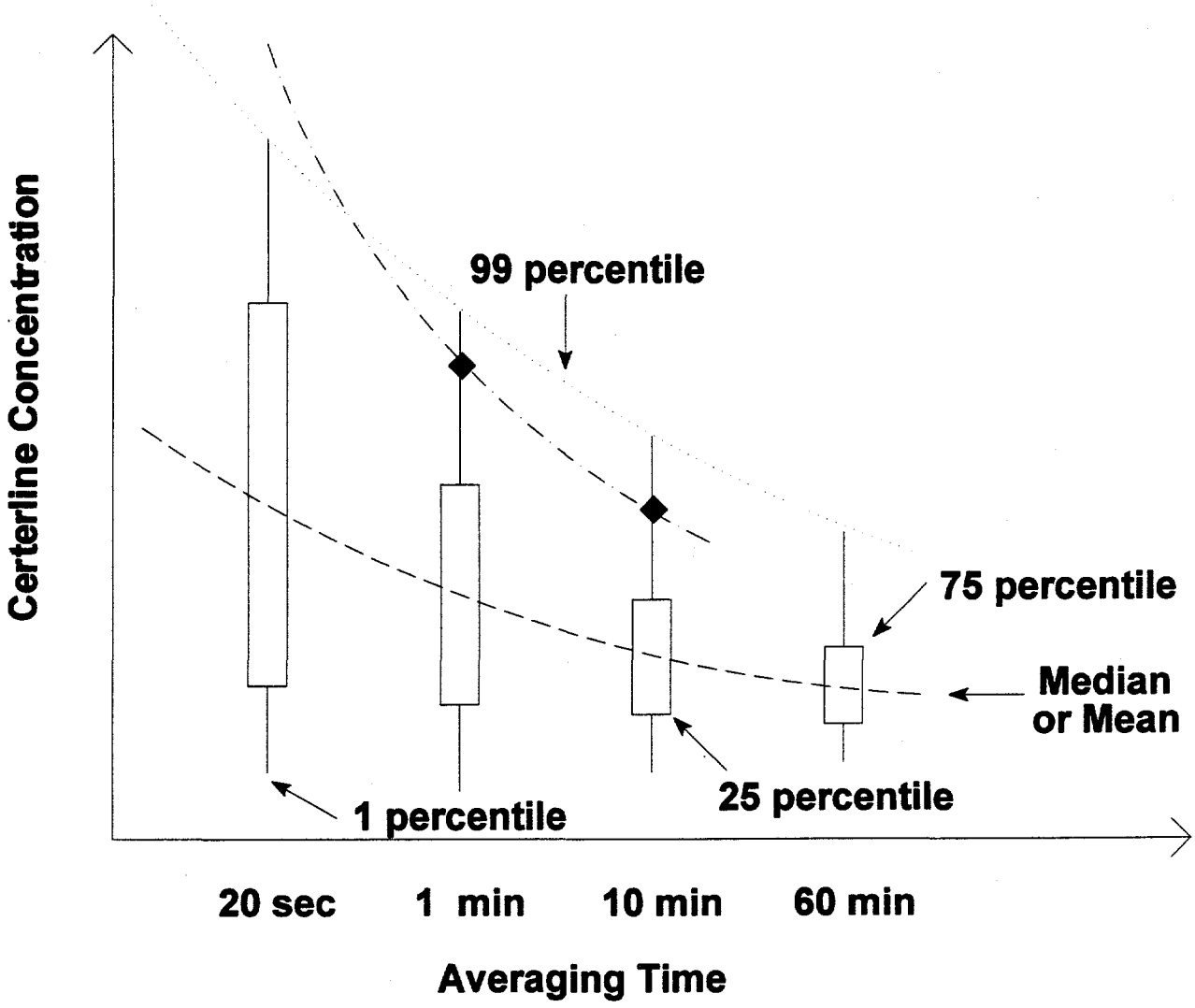

Fig. 6-5. Typical distributions of centerline concentration C_{cl}, at a given x, for various averaging times T_a. NOTE: The *dashed* line goes through the means at each T_a; the *dotted* line goes through the 99th percentile of each distribution; and the *dashed-dotted* line goes through the maximum at that T_a, if the sampling time is assumed to be 60 min.

Parameterizations

Most hazardous gas models that correct for averaging time are attempting to follow the dashed line in Fig. 6-5, even though they do not specify these conditions. Most models accomplish this correction by applying a $T_a^{1/5}$ power law to the lateral dispersion coefficient σ_y, due to ambient turbulence.

$$\sigma_y\,(T_{a2}) / \sigma_y(T_{a1}) = (T_{a2} / T_{a1})^{1/5} \tag{6-24}$$

To prevent σ_y from dropping below its known value for instantaneous conditions, which would inevitably happen with Eq. (6-24) as $T_{a2} \to 0$, a "minimum T_{a2}" criterion is usually applied. This is the T_{a2} that would result in σ_y being equal to the following values given by Slade (1968) for instantaneous plumes or puffs:

Unstable: $$\sigma_{yI} = 0.14\ x^{0.92}\ . \tag{6-25}$$

Neutral: $$\sigma_{yI} = 0.06\ x^{0.92}\ . \tag{6-26}$$

Very stable: $$\sigma_{yI} = 0.02\ x^{0.89}\ . \tag{6-27}$$

For neutral conditions, this criterion is satisfied at T_{a2} equal to about 20 s, where it is assumed that σ_y for continuous plumes is given by the Briggs-EPA formulas. However, this minimum T_{a2} is dependent on what is assumed for distance x and for representative averaging time for the Briggs-EPA formulas. Furthermore, Eqs. (6-25) through (6-27) themselves are based on limited data and would have significant uncertainties—perhaps ±50%.

The existing formulas in HGSYSTEM for accounting for averaging time are used as a default parameterization, with the following assumptions:

- The σ_y Briggs-EPA formulas for continuous plumes are valid for an averaging time of 10 min.
- The "minimum T_a" criterion is 20 s.
- Eq. (6-24) is valid for σ_y corrections for T_a.

The HEGADAS model assumes the lateral distribution in a dense gas plume is made up of a dense gas core of width W and Gaussian edges with standard deviation σ_y. The averaging time correction is then applied only to Gaussian edges. We depart from this approach by assuming the averaging time correlation applies to the entire plume width:

$$C_{ct}(T_{a1}) / C_{ct}(T_{a2}) = (T_{a2} / T_{a1})^{1/5}\ . \tag{6-28}$$

If the centerline concentration is of interest at a given averaging time at a given percentile as the distribution (see dotted line on Fig. 6-5), an assumption is needed for the form of the distribution. For in-plume fluctuations, a log-normal distribution is applicable (Hanna, 1984):

$$P(\ell nC) = \int_{-\infty}^{\ell nC} p(\ell nC')\, d(\ell nC') \quad , \tag{6-29}$$

$$p(\ell nC') = \frac{1}{\sqrt{2\pi}\ \sigma_{\ell nC'}}\ e^{-(\ell nC' - \overline{\ell nC'})^2 / 2\sigma^2_{\ell nC'}} \quad , \tag{6-30}$$

where

P = cumulative distribution function (ranges from 0.0 to 1.0),

p = the probability distribution function.

At small averaging times (T_a ~ 20 s or less), atmospheric data show

$$\sigma_{\ell nC} / |\overline{\ell nC}| \approx 1.0 \quad . \tag{6-31}$$

We assume this relation is valid and that $\sigma_{\ell nC}$ decreases as averaging time increases according to the following approximation to Taylor's formula:

$$\frac{\sigma^2_{\ell nC}\,(T_a)}{\sigma^2_{\ell nC}\,(20\ s)} = \frac{1}{1 + T_a / 2T_I} \qquad (T_a > 20\ s) \quad , \tag{6-32}$$

where

T_I = integral scale for turbulent fluctuations in concentration.

For plumes in the atmospheric boundary layer, a default assumption would be

$$\textbf{Default} \qquad T_I \approx 300\ s \quad . \tag{6-33}$$

With this value of T_I, Eqs. (6-31) and (6-32) give

$$\sigma_{\ell nC}(1\ hr) = 0.4\ \sigma_{\ell nC}\,(20\ s) \quad .$$

The above formulas have been implemented in HGSYSTEM.

6.4.2 Predictions of Concentrations at a Given Receptor Position as a Function of Averaging Time T_a

Discussions in Sect. 6.4.1 were concerned with predicted concentrations on the plume centerline or axis, which can shift position with time. For that type of model application, the analyst is concerned only with the maximum plume impact independent of location. The HGSYSTEM model takes this approach. Another type of model application would be concerned with the plume impact at a given receptor position as defined by, for example, a monitoring site or a critical subset of the surrounding population, such as a school or hospital. The HGSYSTEM model currently does not treat this type of receptor. Nevertheless, the equations are derived below because they possibly can be used in future modifications.

Consider an ensemble of concentration observations from a given monitoring site. Data are taken from many independent field studies, all with nearly the same ambient conditions: release rate, wind speed and direction, stability. These observations would show a variation of distribution functions with averaging time as suggested in Fig. 6-6. In the table below, note the three major differences between Figs. 6-5 and 6-6. In the case of Fig. 6-6, these differences are because the plume can meander away from the receptor, leading to the possibility of $C = 0$ observations at that receptor. Conversely, by definition, C_{cl} is always greater than zero in Fig. 6-5, which is appropriate for HGSYSTEM.

Fig. 6-5 Centerline C	Figure 6-6 Fixed Receptor C
Median C decreases as T_a increases	Median C is constant with T_a
C has no zeros	C has many zeros
σ_c is relatively small	σ_c is relatively large

Often, the variation of C_{max} with T_a is calculated from data at fixed receptors. A time series $C(t)$ is searched to identify the various $C_{max}(T_a)$; for example, this was done using the field data from the Burro, Coyote, and Desert Tortoise experiments. The resulting C_{max} values would follow the dot-dashed curve in Fig. 6-6, where the total length of the time series is 60 min, which is sampling time T_s. The percentile of C_{max} for each T_a is given by

$$Percentile/100 = 1 - (T_a/60\ \text{min}) \quad . \tag{6-34}$$

Note the variation of C_{max} with T_a is greater than the variation of fixed percentile C with T_a. From a theoretical viewpoint, C is preferable, but from a practical viewpoint, researchers usually work with C_{max}. Clearly, it is important to at least recognize the difference.

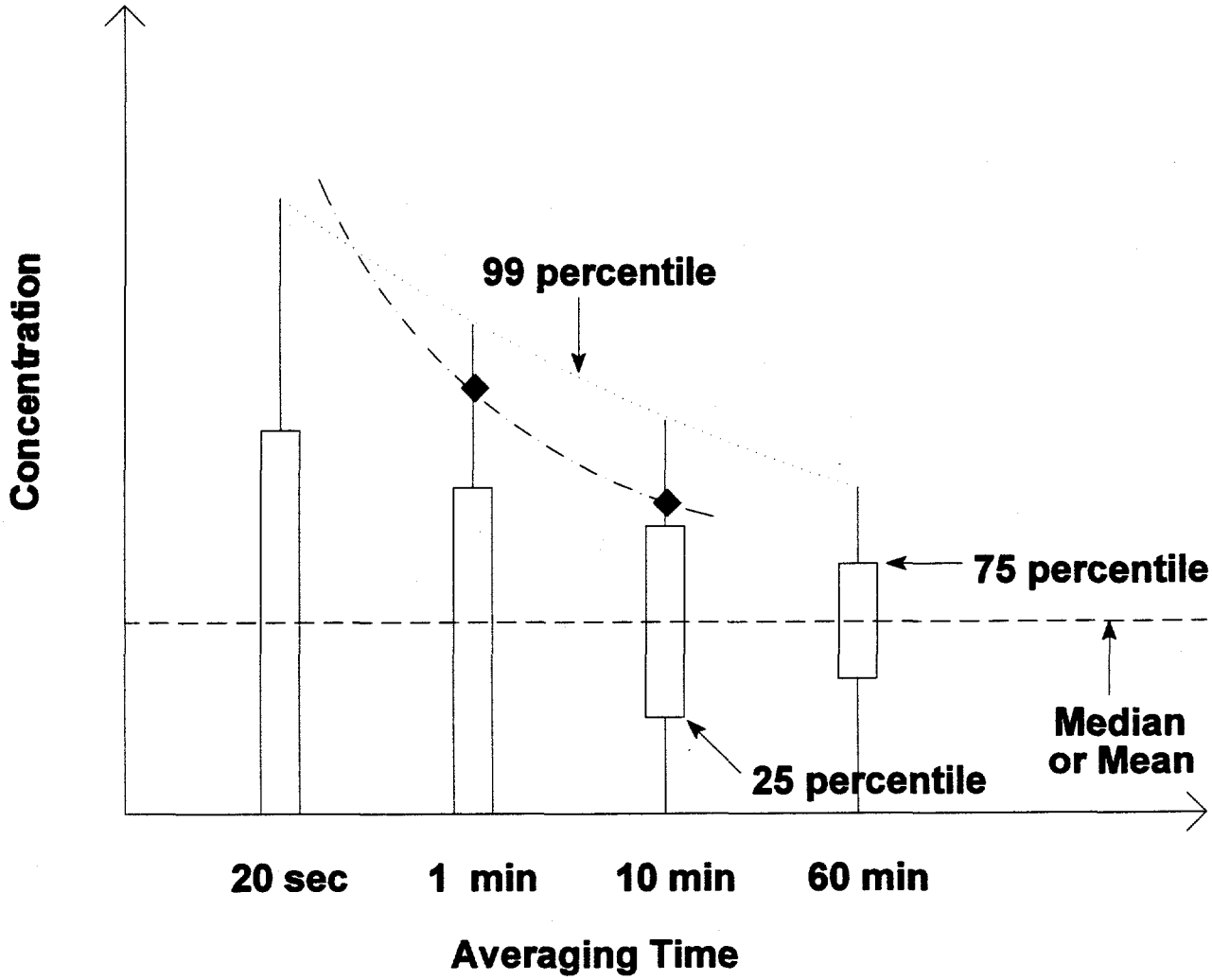

Fig. 6-6. Typical distributions of concentration observed at a given monitor location for various averaging times T_a. NOTE: The *dashed* line goes through the means at each T_a; the *dotted* line goes through the 99th percentile of each distribution; the *dashed-dotted* line goes through the maximum at that T_a, if sampling time is assumed to be 60 min.

The distribution function for data in Fig. 6-6 must account for the possibility of many zeros. The exponential cumulative distribution function has been recommended by Hanna (1984):

$$P(C) = 1 - I \exp(-IC/\overline{C}) \quad , \tag{6-35}$$

$$\sigma_c/\overline{C} = ((2/I) - 1)^{1/2} \quad , \tag{6-36}$$

where I is the so-called intermittency, or fraction of nonzero observations in the total record ($I = 1.0$ if the plume is always impacting the receptor). A typical value of I in the atmosphere is about 0.2, giving $\sigma_c/\overline{C} = 3$. In the absence of other information, a default value of $I = 0.2$ can be used for very small averaging times T_a:

$$\left.\begin{aligned} P(C) &= 1 - 0.2 \exp\left(-0.2C/\overline{C}\right) \\ \sigma_c/\overline{C} &= [(2/I) - 1]^{1/2} = 3 \end{aligned}\right\} \; as \; T_a \to 0 \quad . \tag{6-37}$$

As averaging time increases to 60 min, Eq. (6-31) can be used to calculate $\sigma_c^2(T_a)/\sigma_c^2(0)$, if again we assume the integral timescale is 300 s and $\sigma_c/\overline{C} = 3$ at $T_a \to 0$. I can be calculated by inverting Eq. (6-36):

$$I = 2/\left[1 + (\sigma_c/C)^2\right] \quad . \tag{6-38}$$

The sequence to be followed is given below.

Step 1: Calculate $\dfrac{\sigma_c^2(T_a)}{\sigma_c^2(0)} = \dfrac{1}{1 + T_a/600\ s}$.

Step 2: Calculate $I(T_a) = \dfrac{2}{\left[1 + (\sigma_c/\overline{C})^2\right]}$.

Step 3: Calculate $P(C) = 1 - I \exp(-IC/\overline{C})$.

We assume $\overline{C}$ is known, and $\sigma_c/\overline{C}(T_a \to 0) = 3$; therefore $I(T_a \to 0) = 0.2$. ***Note:*** These formulas should ***not*** be used at $T_a > 3600$ s since intermittency I would be calculated to exceed 1.0, which is impossible; use $I = 1.0$ and $\sigma_c/\overline{C} = 1.0$ at $T_a > 3600$ s.

As mentioned previously, formulas in Sect. 6.4.2 for the fixed receptor position are not implemented in HGSYSTEM since the model is used to calculate concentrations for receptors on the plume centerline. Future modifications might make use of Sect. 6.4.2.

6.5 EFFECTS OF BUILDINGS AND TERRAIN OBSTACLES

6.5.1 Introduction

Releases of UF_6 are likely to occur in the vicinity of buildings and may be influenced by nearby terrain obstacles. These obstacles may alter the boundary layer wind flow patterns, so the trajectory and rate of dilution of the UF_6 plume may be altered. In the past, hazardous gas models ignored the influence of buildings and other obstacles because the model developers believed these obstacles generally led to enhanced dilution and lower concentrations. However, we believe it is best to include methods for accounting for the effects of obstacles for these reasons:

- Buildings at GDPs are large, with relatively narrow "canyons" between them. A UF_6 plume would be constrained by the walls of the buildings.
- UF_6 releases could occur from storage tanks and pipes within buildings, with emissions to the outside through exhaust vents on the roofs of the buildings.
- Releases from short stacks could be mixed to the ground in the wakes of buildings, leading to increased ground level concentrations.

Simplified algorithms have been added to the HGSYSTEM/UF_6 code to account for these three phenomena. Later, other algorithms can be added to account for the myriad of other possible scenarios involving the effects of buildings and terrain obstacles.

6.5.2 Background

Algorithms described in Sects. 6.5.3 through 6.5.6 are based on results of a review of the effects of structures on toxic vapor dispersion (Schulman, Hanna, and Britter, 1990). Their document drew heavily from previous reviews (Britter, 1989; Brighton, 1989) of the effects of structures on passive and dense gas plumes. U.S. Air Force research reviewed literature on the effects of structures on toxic vapor dispersion to assess the feasibility of producing a viable quantitative model and to determine whether building effects were significant relative to overall model uncertainty. The literature survey followed a framework defined by the source and receptor locations relative to the structure:

Source location?	Upwind of structure On structure Downwind of structure
Receptor location?	On face of structure In wake or cavity of structure Downwind of wake of structure

The literature also was stratified into dense and passive gases and into puff and continuous plume sources. The research attempted to answer these questions:

- Do sufficient data and mathematical models exist for developing quantitative models for effects of structures that can be used as subroutines in existing toxic vapor dispersion models?
- Are the expected changes in concentrations due to effects of structures significant relative to overall model uncertainties?
- Do models and data exist for trapping of toxic clouds inside large open structures?
- What is the relative accuracy of the subroutines for various source scenarios and structure geometries?
- At what level of structure complexity do the models become inaccurate?

Results of the review showed that sufficient information existed to develop models for a few of the source-receptor combinations listed above. In those cases, simplified formulas were suggested; these are given in the following section. In other cases, no information existed to permit even simple models to be suggested, and further wind-tunnel or field studies would have to be done to fill in the matrix. Fortunately, experimental data and empirical formulas have been developed for the three topics of interest in the current study:

- Lateral confinement in building canyons
- Concentration patterns on building faces due to vent releases
- Downwash into building wakes

Most of the literature dealt with neutral or passive gases. Dense gases have not been studied as much, although dense gases are recognized to tend to spread more laterally and less vertically.

6.5.3 Plume Confinement by Canyons

Consider the scenario in which the hazardous gas source is near or within a canyon between large buildings (Fig. 6-7). The building height is H_B and the canyon width is W_C. Laboratory experiments by Konig (1987) and Marotzke (1988) suggest maximum concentrations are increased by as much as a factor-of-three due to the confinement by the canyon. This effect can be decreased if the plume height grows so that leakage occurs above the buildings. The simple model described below is used in the new HGSYSTEM model.

If the source is between the buildings or if the source is upwind of the buildings and $\sigma_y < W_C/2$ when the plume enters the canyon and if $H/H_B < 1$, then σ_y is not allowed to exceed the limit

$$\sigma_y \text{ (maximum)} = W_C/\sqrt{12} \quad . \tag{6-39}$$

This value of σ_y corresponds to a uniform lateral distribution across W_C. Note that σ_y, as used here, is assumed to apply to the total plume width, not just to the plume edge.

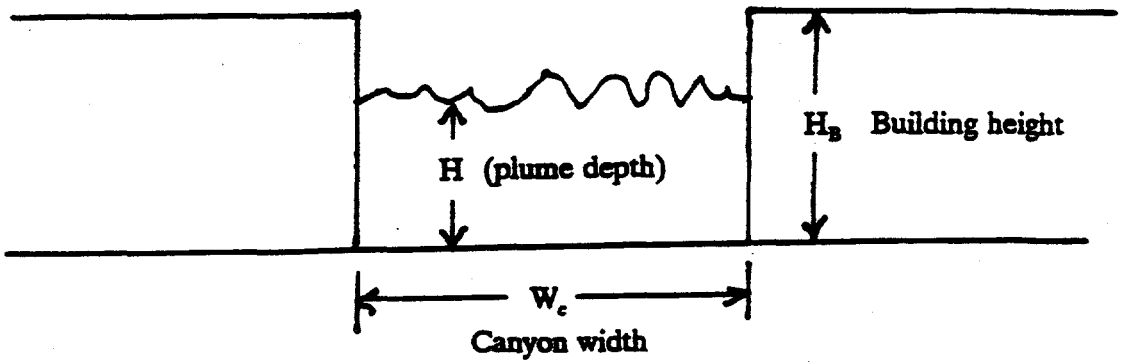

a) Cross-section in the vertical and lateral dimensions

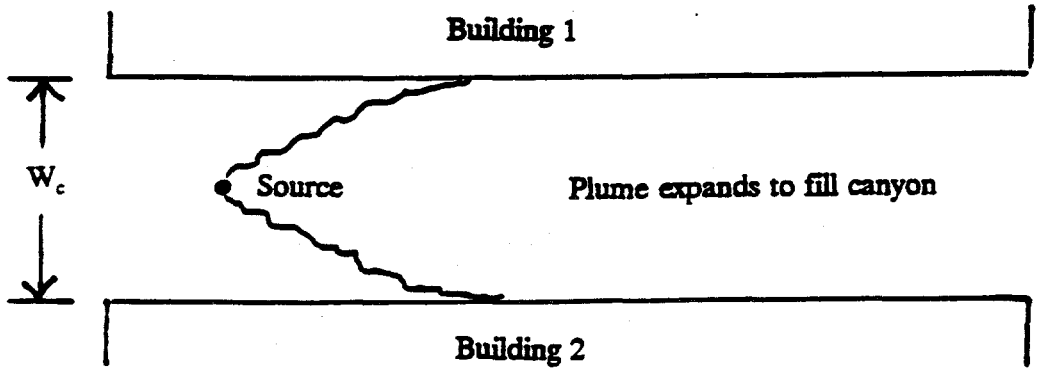

b) View looking down

Fig. 6-7. Hazardous gas release in a canyon between buildings.

If $H/H_B > 1$, then only the lower part of the plume is confined by the canyon, and the upper part of the plume is free to disperse laterally as if the canyon were not there. In this case, the following interpolation formula is used:

$$\text{Effective } \sigma_y \text{ (maximum)} =$$

$$(H_B/H)\left(W_C/\sqrt{12}\right) + \left[(H - H_B)/H\right]\left[\sigma_y \text{ (without canyon effect)}\right] \quad , \tag{6-40}$$

where σ_y (without canyon effect) refers to the lateral dispersion as usually calculated by the model in the absence of obstacles. When the plume reaches the end of the canyon, lateral diffusion resumes, and a virtual source procedure is applied to calculate concentrations further downwind.

6.5.4 Concentrations on Building Faces due to Releases from Vents

If UF_6 is released accidentally within a building, it will be exhausted by vents that typically take the form of very short stacks on the roof of the building. The concentration in the plume in the exhaust vent will have been reduced by dilution through the volume of the building, and most chemical reactions will have taken place (i.e., the plume will consist of small UF_6 and UO_2F_2 particles and $HF{\cdot}H_2O$ gas and aerosol). Because there will be little buoyancy to the plumes being vented, the gas can be modeled as if it were neutral or passive.

Many wind-tunnel studies have been made of distributions of dimensionless concentration on the faces of buildings of various shapes due to releases from vents on various positions on the buildings.

$$K = \frac{CuA}{Q} \quad , \tag{6-41}$$

A is a representative area of the building. The source and receptors are assumed to be on the same or adjacent faces. Meroney (1982) and Wilson and Britter (1982) provide reviews of some of that work. When definitions in Fig. 6-8 are used, maximum concentrations on the building at distance r from the source are given by these formulas:

- For $r/A^{1/2} < 1.73$ and source and receptor on upper two-thirds of building,

$$C = 9\ Q/u_H r^2 \quad , \tag{6-42}$$

- For $r/A^{1/2} < 1.73$ and source and receptor on lower one-third of building,

$$C = 30\ Q/u_H r^2 \quad , \tag{6-43}$$

where u_H is wind speed at the height of the building in the flow upwind of the building, and A is building area, assumed to equal $H_B W_B$. As distance r (shortest distance along the surface between the source and receptor) decreases, concentration does not increase indefinitely but is capped by the concentration in the vent exhaust [$C_{max} = Q$/(volume flux from vent)].

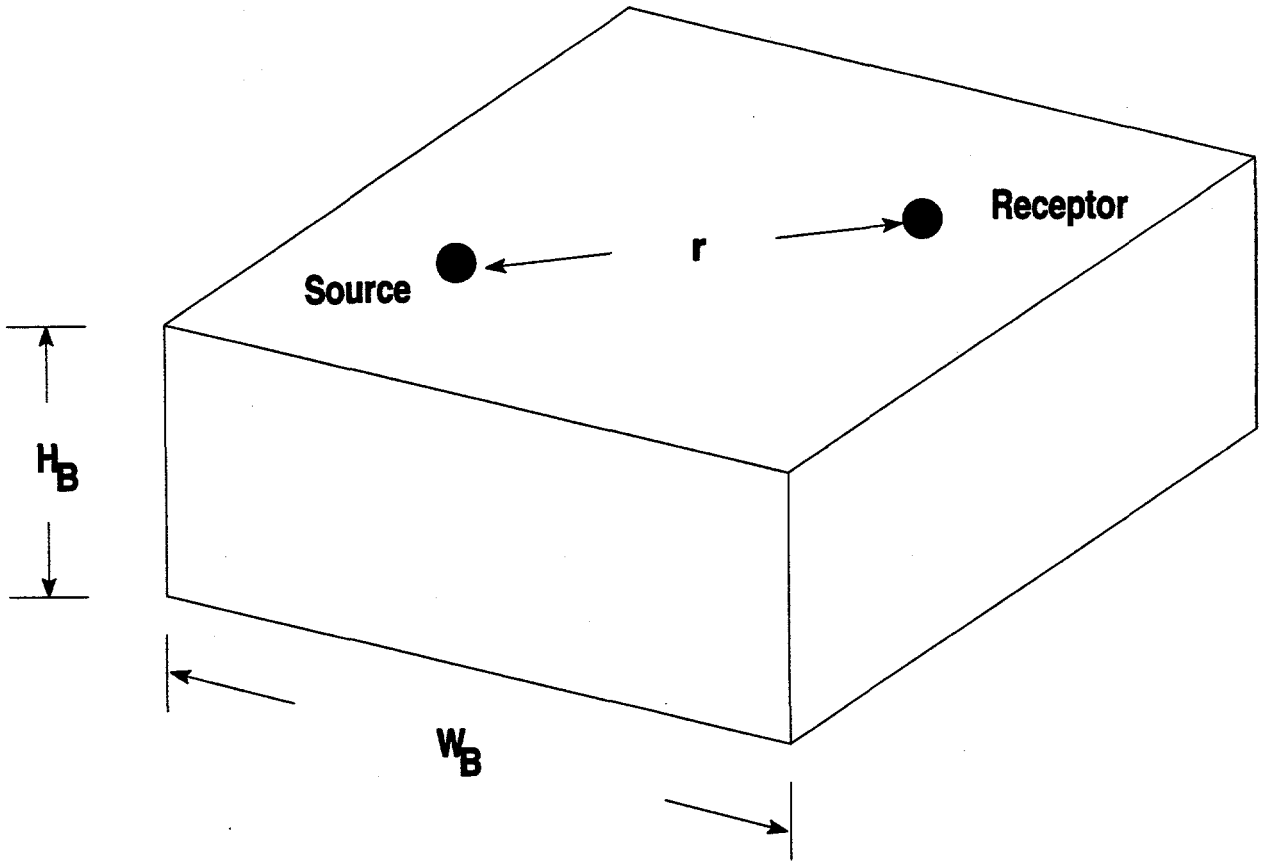

Fig. 6-8. Definitions of parameters for calculating concentrations on building faces due to emissions from vents.

Note that if a significant air flow from the vent exists, the vent plume may be transported up and away from the roof. In that case, the concentrations given by Eqs. (6-42) and (6-43) would be conservative. These formulas do not consider the lateral or vertical extent of the plumes from the vents. Equations (6-42) and (6-43) are most useful for estimating maximum concentrations with the condition that the plume is being blown directly from the source vent to the receptor position on the building face.

The restriction that $r/A^{1/2} < 1.73$ in Eqs. (6-42) and (6-43) is applied so that concentrations smoothly transition to the formula in the next section for the near wake, that is,

$C = 3Q/u_H A$.

6.5.5 Concentrations on the Building Downwind Face (the Near-Wake) due to Releases from Sources on the Building

This algorithm is concerned with a continuation of the vent scenario covered in Sect. 6.5.4. Again, source emissions are assumed to be neutral or passive, and we are now concerned with the concentration in the near-wake or the recirculating cavity. This is a turbulent well-mixed zone that extends about two to five building dimensions downwind, and concentrations are assumed to be uniform across this zone. Wilson and Britter (1982) found the concentrations in the near wake are given by

$$C = \frac{3Q}{u_B A} \qquad (r/A^{1/2} \geq 1.73) \ , \tag{6-44}$$

where $A = W_B H_B$ for block-shaped buildings and $A = H_B^{4/3} W_B^{2/3}$ for wide buildings. Figure 6-9 provides a schematic depiction of this scenario. Note that the condition $r/A^{1/2} \geq 1.73$ is applied to Eq. (6-44), where r is the distance from the source to the receptor.

6.5.6 Other Effects of Buildings

All three building effects covered in Sects. 6.5.3—6.5.5 are handled easily through simple empirical formulas and tend to increase concentration impacts. In the future, other types of effects can be included in the model as new information comes from wind-tunnel and field experiments. Some building effects have been ignored here because they tend to significantly

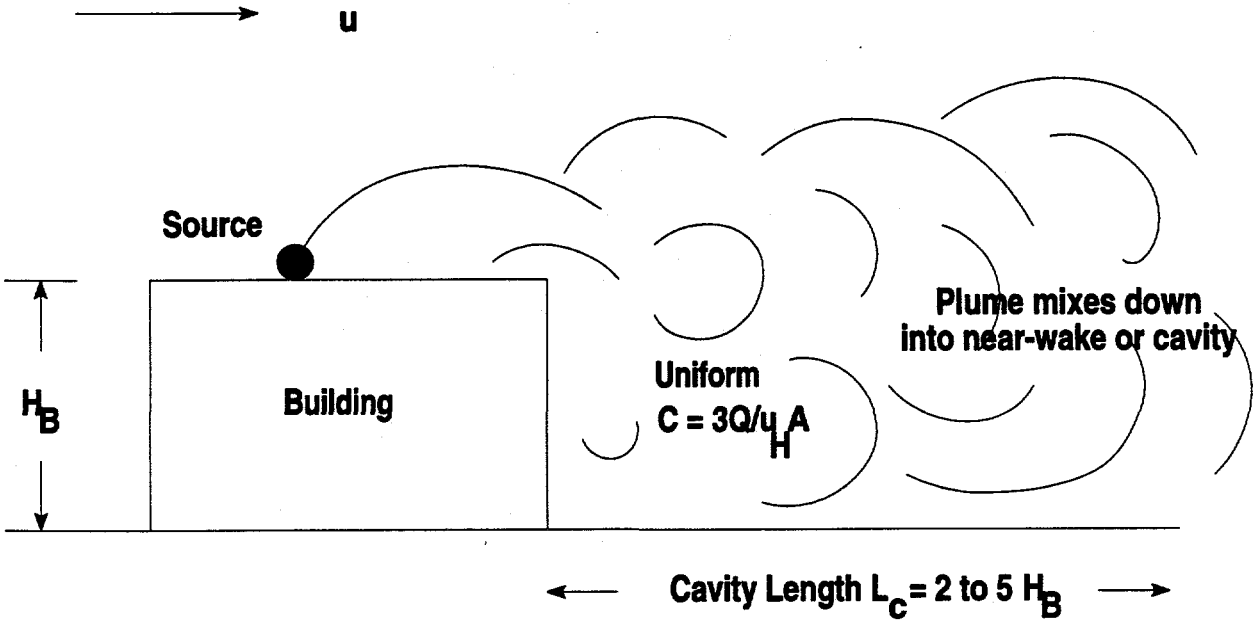

Fig. 6-9. Schematic diagram of passive plume mixing into near-wake.

decrease concentrations below the "flat-terrain" solution. For example, if a source is upwind of a building, fence, or other obstacle, increased turbulence due to the obstacle will tend to dilute the hazardous gas plume). Fences have been investigated because of their potential for mitigating the plume, and enhanced dilutions of a factor-of-three or more have been observed. Also, shallow dense gas plumes approaching taller obstacles have been seen to be caught in the horseshoe vortices formed around the obstacle and therefore were transported laterally away from the obstacle.

Generally, chemical reactions have been assumed to be insignificant in the simple models in previous sections. If chemical reactions were included, the entrainment rate of ambient air would have to be estimated so that the reactions of UF_6 and HF with water vapor could be included. Unfortunately, these entrainment rates are not well known for plumes under the influence of obstacles. Future wind-tunnel studies should emphasize observations of entrainment into plumes being influenced by obstacles. We suggest that the model could next include the EPA's downwash algorithm for the *far* wake as implemented in their ISC model. This algorithm applies to the scenario when there is a stack of significant height (h_s equal to about 1 to 2 H_B) near the building and ground-level concentrations are to be calculated at a distance of about 10 H_B or greater from the stack (see Fig. 6-10). The algorithm allows for enhancement of σ_y and σ_z, depending on the ratio h_s/H_B. This algorithm is not implemented in the HGSYSTEM/UF_6 model at the present time because (1) most UF_6 sources are at the ground or at vents on the roofs of buildings and (2) maximum impacts would occur in the near wake during the scenarios described in Sects. 6.5.4 and 6.5.5.

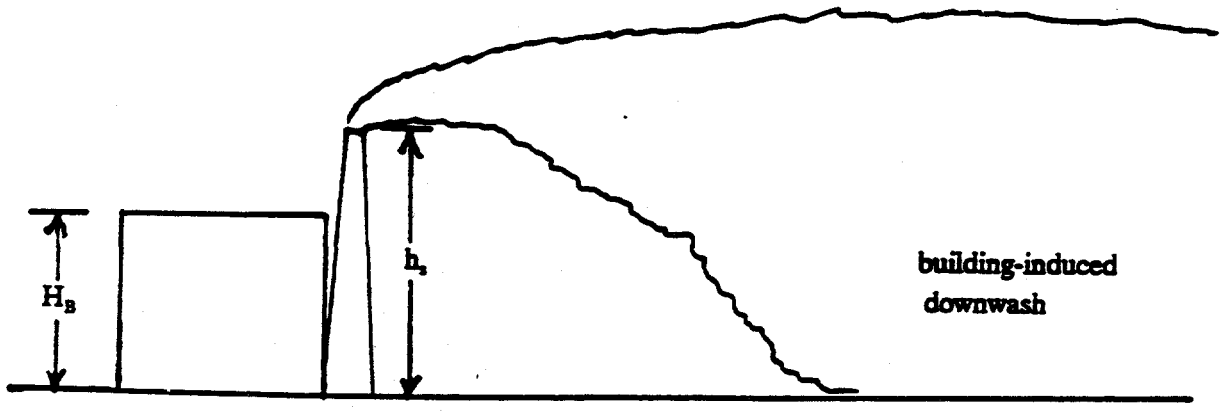

Fig. 6-10. Scenario of dispersion in the far-wake, for which the ISC model downwash algorithm is applicable.

7. DETAILED DESCRIPTION OF HGSYSTEM/UF_6 MODULES

This chapter details the implementation in HGSYSTEM of the new modules discussed in Chaps. 5 and 6. The topics in Chap. 5 relate only to UF_6, while the topics in Chap. 6 are of general interest. HGSYSTEM consists of a suite of modules. Six of these can perform dispersion calculations: AEROPLUME, HFPLUME, PGPLUME, HEGADAS-S, HEGADAS-T and HEGABOX. The following table summarizes the intended application for each module.

Module	Application
AEROPLUME	Elevated pressurized plume (jet) dispersion
HFPLUME	Elevated pressurized plume (jet) dispersion for HF only
PGPLUME	Passive far-field plume dispersion
HEGADAS-S	Steady-state ground-level dispersion of heavy gas
HEGADAS-T	Transient ground-level dispersion of heavy gas
HEGABOX	Instantaneous ground-level dispersion of heavy gas

AEROPLUME treats any nonreacting two-phase aerosol. HFPLUME treats only HF and accounts for the presence of HF aerosols. HEGADAS-S, HEGADAS-T, and HEGABOX treat both nonreacting aerosols and HF. There is no treatment of chemistry or thermodynamics in PGPLUME.

HGSYSTEM has been under active development over the past ten years, as discussed in Chap. 2. During a meeting on November 16, 1993, representatives from Energy Systems, EARTH TECH, API Air Modeling Task Force, and Shell Research UK agreed that HGSYSTEM Version 2.2 (the latest version at that time) would be used as the basis for the UF_6 modeling system. EARTH TECH and Shell agreed to coordinate their model-development efforts so that a single code and user guide would be prepared, with both groups as co-authors. All code changes described below were eventually migrated to Version 3.0 of HGSYSTEM (Post, 1994c; 1994d) released in 1995

After HGSYSTEM was selected as the host model, the groups determined that the UF_6 chemistry and thermodynamics modules required the most work because they involved fundamental changes to the code to accommodate the chemical reactions of UF_6 with water vapor and the associated thermodynamics. The original HGSYSTEM already contained state-of-the-art treatments of the transport, entrainment, and diffusion of dense gas plumes and puffs. Most of the general changes (see Chap. 6) were planned to be implemented as post- or pre-processors that would be independent from the existing calculations in the host model, described in more detail in Sect. 7.1. The following sections describe methods of incorporating the new modules within the original HGSYSTEM and also describe the new model input and output requirements.

7.1 OVERVIEW OF GENERAL IMPLEMENTATION PROCEDURES FOR NEW MODULES

It was first considered that the HFPLUME module should be modified to serve as a base model for pressurized releases of UF_6 because (1) HF is one of the products of the chemical reaction of UF_6 with water vapor and (2) HFPLUME already contained a state-of-the-art model for HF. However, it was decided that the addition of UF_6 to HFPLUME would be difficult because the 17 equations governing the plume dispersion and thermodynamics are solved simultaneously by Shell's proprietary SPRINT solver package.

Dr. Lourens Post (1994a), the Shell HGSYSTEM model developer, suggested an alternative approach—that AEROPLUME be used as the starting point since it is more modular in structure than HFPLUME. This approach was ultimately adopted in the research program. AEROPLUME equations that govern the dispersion process are solved separately from equations that govern the thermodynamics equilibrium of the system. This modularity allows the user to readily adapt the code to treat different chemicals. In the case of reacting chemicals, both the thermodynamics and the chemistry parts of the code must be revised, while the dispersion part of the code remains unchanged. The dispersion part is separated from the thermodynamics part in the AEROPLUME, HEGADAS, and HEGABOX codes.

The original HGSYSTEM has some differences regarding the treatment of HF in different modules:

- For area sources and instantaneous releases, the HEGADAS and HEGABOX modules consistently treat generic aerosols and HF.
- For jet releases, the AEROPLUME module treats only generic aerosols (not HF), while the HFPLUME module treats only HF.
- The HF thermodynamics algorithms in HFPLUME, HEGADAS, and HEGABOX are all based on Schotte's article (1987), while the HF thermodynamics implementation in HFPLUME is slightly different from that in HEGADAS and HEGABOX.

These inconsistencies are due partly to the time sequence in which module upgrades have been made. For consistency and ease of future upgrades, we have added the same set of UF_6-specific routines in all modules (AEROPLUME, HEGADAS, and HEGABOX). The AEROPLUME/UF_6 module can be considered as a replacement to what would have been referred to as HFPLUME/UF_6.

Originally, it was thought that the existing HF routines in HEGADAS and HEGABOX could be modified to account for the UF_6 chemistry and thermodynamics. However, later we determined that, rather than modifying the existing HF routines, a new set of UF_6 routines should be coded which was not only consistent with Schotte's (1987) original algorithm for HF but also included UF_6. Modifications to the original code were not practical because too many changes were involved. Furthermore, because the original HF routines were equilibrium solutions that did not treat time-dependent chemical reactions, developing a new routine would have been necessary to account for the mass transfer-limited chemical reactions of UF_6 with H_2O.

In general, the UF_6 versions of AEROPLUME, HEGADAS, and HEGABOX have three subsystems that can be distinguished in the code: plume dispersion, chemistry, and thermodynamics. The dispersion subsystem is used to describe plume geometry and air entrainment as the plume travels downwind. This module involves integration of several differential equations from one downwind distance to the next. The chemistry subsystem uses the air entrainment rate provided by the dispersion subsystem to calculate new mass flow rates for all species after applying a set of mass transfer-limited chemical reactions. The thermodynamics subsystem, based on new mass flow rates for all species, calculates the equilibrium temperature and associated density of the mixture. The new plume density is then used by the dispersion subsystem for the next integration step, thus repeating the procedure just described. The dispersion subsystem calculates air entrainment over one step, the chemistry subsystem updates plume composition over that step based on the prescribed air entrainment; the thermodynamics subsystem calculates plume temperature and density based on the new plume composition. Plume properties averaged over the integration step are used when calling the chemistry and thermodynamics subsystems at the end of each integration step.

Time rates of change for the species participating in the chemical reactions are calculated by using a simple first-order finite difference scheme (see Chap. 5). Because the finite reaction rate for the chemical reaction is a nonlinear function of the molar flow rates of UF_6 and water vapor, an iteration scheme is set up in the chemistry subsystem to ensure convergence. This scheme involves dividing the external integration step into equally spaced smaller internal steps. The finite difference scheme for the chemical reactions is applied to one such internal step at a time rather than applied just once over the entire external step. Plume composition and finite reaction rate also are updated after every smaller internal step. The process is iterated, with the size of the internal step halved during each subsequent iteration, until the ***average*** (the mean over all internal steps) finite reaction rates between two successive iterations satisfy a convergence criterion. Tests demonstrate the scheme is computationally efficient and convergence typically can be achieved after only a few iterations. The average finite reaction rate over all internal steps for the last iteration is used in subsequent calculations of the heat of chemical reactions.

The finite reaction rate depends on the square root, q, of the turbulence kinetic energy and turbulence length scale, Λ, within the plume. As described in Chap. 5 and shown in Fig. 5-6, q is parameterized as $3.6V_e$, where V_e is the entrainment velocity, and Λ is parameterized as follows:

- AEROPLUME: $\Lambda = 0.5r$, where r is the plume radius.
- HEGADAS: $\Lambda = 0.5H_{eff}$, where H_{eff} is the effective plume height (discussed later).
- HEGABOX: $\Lambda = 0.5H$, where H is the cloud height.

Because the entrainment velocity V_e is not specifically calculated and given by any of the above three modules, algorithms for V_e have been derived from the Shell documentation for HGSYSTEM (Post, 1994c). These are presented in Eqs. (7-1), (7-2), and (7-3).

- ***In AEROPLUME,***

$$V_e = \frac{E}{\rho_{atm}\,\Gamma} \quad , \tag{7-1}$$

where

E = total air entrainment rate per unit downwind distance in kg/s/m,
ρ_{atm} = density of the ambient air,
Γ = exposed circumference of the plume cross-section.

- ***In HEGADAS,***

$$V_e = \frac{E}{2\,\rho_{atm}\,(B_{eff} + H_{eff})} \quad , \tag{7-2}$$

where

E = total air entrainment rate per unit downwind distance in kg/s/m,
H_{eff} = effective plume height,
B_{eff} = effective half-width (discussed later).
The exposed circumference of the plume cross section equals $2(H_{eff} + B_{eff})$.

- ***In HEGABOX,***

$$V_e = \frac{E}{\rho_{atm}\,(\,\pi\,R^2 + 2\,\pi\,R\,H\,)} \quad , \tag{7-3}$$

where

E = total air entrainment rate in kg/s,
R = cloud radius,
H = cloud height, and
the terms within the parentheses represent the exposed area of the cloud.

The preceding paragraphs are related to the implementation of UF_6 chemistry and thermodynamics algorithms. Other generic enhancements have been made to HGSYSTEM that are not specific to UF_6 (see Chap. 6). Most of these enhancements were implemented as pre- or post-processor modules that can be easily added or removed from the model. Their presence does not influence fundamental dispersion, chemistry, and thermodynamics calculations in the code. Summaries of the characteristics of these algorithms are given in the remainder of this section.

- *Removal by Dry and Wet Deposition* (See Sect. 6.1)

  Algorithms have been added to calculate dry and wet deposition. The dry and wet deposition flux is assumed to be small compared with the total flux of material in the plume, which is assumed to remain unchanged. The local gas or particle deposition flux to the ground is assumed to be the product of the ground-level concentration and deposition velocity. Dry deposition velocity v_d is held constant for any model run and does not vary with space. Conversely, wet deposition velocity v_w varies with downwind distance because it involves an integration over the depth of the plume as the plume grows vertically with downwind distance. Effects of deposition are implemented as a post-processor module and do not affect the original calculations of the HGSYSTEM model.

- *Plume Lift-Off* (See Sect. 6.2)

  AEROPLUME and HEGADAS codes have been revised to account for the possibility that the plume may "lift off" the ground if it becomes less dense than the air. Because AEROPLUME includes calculation of the plume trajectory, the effect of plume lift-off must be "integrated" into the code. This approach is different from the one used in HEGADAS, in which basic similarity profiles assume the maximum concentration always occurs at the ground. In HEGADAS, plume trajectory is calculated independently using the "two-thirds law" (Briggs, 1975; Weil, 1988) applied to the HEGADAS results at a given downwind distance. The treatment of plume lift-off does not influence basic HEGADAS calculations.

- *Meteorological Pre-processor* (See Sect. 6.3)

  A state-of-the-art meteorological pre-processor has been added. The original AEROPLUME, HEGADAS, and HEGABOX use empirical correlations to calculate the friction velocity, u_*, and the Monin-Obukhov length, L, based on the Pasquill-Gifford stability class and surface roughness. The user can decide to apply the new meteorological processor to estimate u_* and L based on ambient observations and site characteristics. The new pre-processor will be called only once during the initialization stage of the model (i.e., before any dispersion calculations are carried out). Once u_* and L are known, the meteorological pre-processor can be used to determine an equivalent Pasquill-Gifford stability class using Golder's (1972) nomogram. All subsequent plume calculations will be based on the newly obtained values of u_* and L.

- *Concentration Fluctuations and Averaging Time* (See Sect. 6.4)

  A general post-processor module has been included which corrects the ensemble-mean predicted concentrations for averaging time and that allows any percentile (e.g., the 95th percentile) of the expected concentration probability density function to be estimated.

- *Building Effects* (See Sect. 6.5)

  A post-processor module was developed to adjust the predicted concentrations to account for confinement due to building walls in case the source release occurs in the canyon between two buildings. In addition, a separate code was also developed to allow concentrations on building roofs and sides, due to releases from flush vents on the building, to be estimated.

The five algorithms just discussed are parameterized as correction factors, which are applied after the model has calculated concentrations at each downwind distance or time after release. Because these effects are included as post-processor modules, they do not influence the calculations of the primary HGSYSTEM modules. For example,

- If AEROPLUME predicts a 0.0010-kg/m^3 concentration of UF_6 at a given downwind distance, and if the presence of a building canyon would cause the concentration to increase to 0.0012 kg/m^3, a correction factor of 1.2 is associated with the canyon effect.

- If HEGADAS-T predicts a 0.0010-kg/m^3 centerline concentration of UF_6 at a given downwind distance, and the concentration fluctuation module predicts that the 99th percentile of the probability distribution function of that concentration is 0.0025 kg/m^3, then a correction factor of 2.5 is associated with the concentration fluctuation calculation. If two or more of these correction factors influence the concentrations, it is assumed that these processes are independent and their associated correction factors can be multiplied to obtain the final result.

7.2 INPUT REQUIREMENTS FOR NEW MODULES

A detailed description of input requirements for the original HGSYSTEM and other generic enhancements that are specific to UF_6 (see Sect. 6) are given in the user's manual (Post, 1994d). In order to run the UF_6 versions of HGSYSTEM modules, some deviations from the original input requirements are necessary. The reader is referred to Appendix C for the addendum to the HGSYSTEM user's manual so that UF_6 modules can be applied.

7.3 AEROPLUME/UF_6

The AEROPLUME (Post, 1993b) module of HGSYSTEM simulates the dispersion of a release from a pressurized tank or from a stack of a mixture of several nonreacting compounds, which can be in purely a vapor phase or in both vapor and liquid phases. The HFPLUME module is similar to the AEROPLUME module but treats only HF. AEROPLUME and HFPLUME have state-of-the-art treatments of physical processes associated with the airborne, touchdown, and slumped stages of the plume (jet) development. AEROPLUME replaces the PLUME module in the 1990 version of HGSYSTEM.

AEROPLUME is modular in design since the dispersion and thermodynamics subsystems are formulated separately. Connection between the two subsystems is accomplished by passing parameters and variables between the subsystems. The dispersion or jet entrainment subsystem of AEROPLUME calculates the position and geometry of the plume as it travels downwind and the associated entrainment of air. Predicted plume enthalpy and total mass flow rate (including the entrained air) are used to drive the thermodynamics subsystem. This subsystem, in turn, calculates plume density, temperature, and concentration. Plume density is then communicated back to the dispersion subsystem.

The distinction between the dispersion and thermodynamics subsystems is not as clear in HFPLUME as it is in AEROPLUME. Governing equations in both subsystems are combined in a single large system in HFPLUME. Consequently, modifying the existing thermodynamics subsystem in HFPLUME is difficult.

AEROPLUME is the only one of the six dispersion modules in HGSYSTEM that can also perform source term calculations. (Other HGSYSTEM modules, such as EVAP [McFarlane et al., 1990] and SPILL [Post, 1994b], can be used to calculate the source term but do not include any plume dispersion calculations.) The original AEROPLUME model contains a discharge module by which the maximum possible emission rate, $\dot{m}_{max}$, of a jet release can be estimated based on (1) storage pressure, storage temperature, and effective release diameter of the source aperture and (2) the physical properties of the pollutant. For a gas phase release, $\dot{m}_{max}$ is based on choked-flow formulas. For a two-phase release, the Fauske and Epstein (1988) formulas are used to calculate $\dot{m}_{max}$.

The original AEROPLUME has an internal check for what it calls plume lift-off, based on the plume geometry. The program recognizes that plume lift-off is imminent when the plume eccentricity E, which is the ratio of height to width, is greater than a certain value (e.g., 1.25). This criterion is based on the assumption that a high value of E is caused by high plume buoyancy. When E exceeds this critical value, the original AEROPLUME simply stops the execution.

Some enhancements and modifications to AEROPLUME have been made to account for UF_6. For example, the AEROPLUME/UF_6 code has disabled the generic reservoir and flash calculations in the original AEROPLUME code and replaced them by a simple flash module appropriate for UF_6. It is assumed that the source term of the UF_6 release is always specified in the input file. Furthermore, to completely separate plume dispersion algorithms from thermodynamics algorithms, all calls to the thermodynamics routine within a plume dispersion (or integration) step were disabled. This modularity of the code was accompanied by an increase in the integration resolution to maintain numerical stability. The value of SSTEP, the integration step size, has been greatly reduced (e.g., SSTEP = 0.001 m for $x < 0.5$ m and is gradually increased as x increases). In addition, a revised plume lift-off criterion has been implemented, primarily based on the plume density deficiency.

The plume lift-off criterion in AEROPLUME/UF_6 is implemented by continually calculating the Briggs plume lift-off parameter, L_p, defined in Sect. 6.2. When the plume is in the "touchdown" or "slumped" stage (i.e., its base contacts the ground), and when L_p is greater than 20, AEROPLUME/UF_6 assumes the plume returns to the "airborne" stage and

carries on the integration as if the ground does not exist. Once the Briggs lift-off parameter exceeds its critical value, AEROPLUME/UF_6 does not allow the plume to switch back to the "touchdown" or "slumped" mode. In other words, a second transition from AEROPLUME to HEGADAS is not allowed. The Shell version of the lift-off criterion was disabled in AEROPLUME/UF_6 to be consistent with the revised method to treat plume lift-off.

The dispersion module of AEROPLUME/UF_6 influences the thermodynamics and chemistry modules through the air entrainment rate, which is calculated from a set of empirically determined functions implemented in the subroutine ENTR. Because UF_6 plumes are initially very dense, users are cautioned that the plume trajectories may curve downward toward the ground. When the curvature of the plume trajectory at the point the plume reaches the ground is large, the local plume coordinate system is no longer valid; then the entrainment calculated by ENTR must be further modified based on geometrical constraints. The resulting modified entrainment is called the curvature-limited entrainment (Post, 1994c, Sect. 5.B.10).

To be consistent with the HF thermodynamics system implemented in the original HFPLUME, HEGADAS, and HEGABOX, the reference temperature is 25°C in AEROPLUME/UF_6, rather than 0°C in the original AEROPLUME.

7.4 PGPLUME

The PGPLUME module of HGSYSTEM is used to simulate the dispersion of passive (i.e., neutrally buoyant) plumes. PGPLUME is designed to be implemented as a far-field dispersion model after AEROPLUME has performed calculations near the source. By the time the plume reaches the PGPLUME stage, it is assumed that the effects associated with UF_6 chemical reactions and thermodynamics can be ignored.

For a UF_6 release, plume buoyancy possibly may switch back and forth from negative to positive due to the presence of dense gases and aerosols and to the heat of reaction associated with the chemical reactions of UF_6. Consequently, a concern exists that the transition from AEROPLUME/UF_6 to PGPLUME may occur too early, at a downwind distance where significant amounts of UF_6 still remain in the plume. However, sensitivity tests suggest this is not likely to be a problem since the transition from AEROPLUME to PGPLUME is made only when the following criteria are simultaneously met:

- Plume excess density must be sufficiently small.
- Excess velocity due to the jet must be sufficiently small.
- Total plume entrainment (sum of the passive, heavy-gas, jet, cross-flow, and gravity spreading components) is dominated by passive entrainment.
- The shape of the plume cross section is sufficiently close to a circle.

For a typical scenario in which UF_6 is released from a pressurized vessel through an orifice that is less than 10 m above the ground, the plume may descend toward the ground due to its high molecular weight and to the temperature decrease associated with the sublimation of solid UF_6. Once the plume is in contact with the ground, a transition to HEGADAS, rather

than to PGPLUME, is more likely to take place. Furthermore, even though heat released by the reaction may cause the plume temperature to rise and the plume density to approach ambient density, other criteria for the transition to PGPLUME may not be met. Therefore, if a transition to PGPLUME is made within HGSYSTEM/UF_6, it is assumed that most chemical reactions have already occurred and the plume is passive. Because the criteria mentioned above for the transition to PGPLUME are all specified in the input file of AEROPLUME, the user is able to change the transition criteria, thus delaying or even disabling the transition to PGPLUME.

In the scenario just discussed we assume UF_6 is released from an elevation that is sufficiently close to the ground so the plume quickly descends to, and interacts with, the ground. If UF_6 were released from vents or stacks on the roof of the building, a much higher release height would be appropriate. In the latter case, it can be assumed that by the time the plume is exhausted from the building by vents or stacks, most of the chemical reactions have already taken place and the plume is relatively dilute. Consequently, the plume can be directly modeled by a passive dispersion model, such as the building vent model described in Sect. 6.5 or the EPA's ISC model.

7.5 HEGADAS-S/UF_6

The HEGADAS-S module of HGSYSTEM is used to simulate steady-state, ground-level, area-source releases. The original HEGADAS-S treats releases of two-phase, nonreactive aerosols and two-phase HF. Witlox et al. (1990) and Witlox (1993c) provide detailed technical descriptions of the original model.

HEGADAS assumes the following similarity profiles for concentration and ambient wind speed:

$$c(x,y,z) = c_A(x) \exp\left[-\left(\frac{z}{S_z}\right)^{1+\alpha}\right] \quad |y| \le b \ , \tag{7-4}$$

$$c(x,y,z) = c_A(x) \exp\left[-\left(\frac{|y|-b}{S_y}\right)^2 -\left(\frac{z}{S_z}\right)^{1+\alpha}\right] \quad |y| > b \ , \tag{7-5}$$

$$u(z) = u_0 \left(\frac{z}{z_u}\right)^{\alpha} \ , \tag{7-6}$$

where

c_A = ground-level (peak) concentration,
b = half-width of the central core of the cloud,
S_z = vertical dispersion parameter,
S_y = lateral dispersion parameter,
α = wind-profile power-law exponent,
u_0 = reference wind speed,
z_u = measuring height of u_0.

With the similarity profiles defined in Eqs. (7-4), (7-5), and (7-6), the following effective cloud characteristics can be defined and are used in the code:

$$B_{eff} = \frac{1}{c(x,0,z)} \int_0^\infty c(x,y,z)\, dy = b + \frac{\sqrt{\pi}}{2} S_y \ , \tag{7-7}$$

$$H_{eff} = \frac{1}{c(x,y,0)} \int_0^\infty c(x,y,z)\, dz = \frac{\Gamma(\frac{1}{1+\alpha})}{1+\alpha} S_z \ , \tag{7-8}$$

$$u_{eff} = \frac{1}{\int_0^\infty c(x,y,z)dz} \int_0^\infty u\, c(x,y,z)\, dz = u_0 (\frac{S_z}{z_0})^\alpha \frac{1}{\Gamma(\frac{1}{1+\alpha})} \ , \tag{7-9}$$

where

B_{eff} = effective cloud half-width,
H_{eff} = effective cloud height,
u_{eff} = effective cloud speed.

The HEGADAS code is based on the following six governing equations:

1. Conservation of mass
2. Empirical relation describing the vertical entrainment of air into the top of the cloud
3. Empirical relation describing gravity spreading
4. Empirical relation describing crosswind dispersion
5. Heat transfer from the surface
6. Water vapor transfer from the surface

Except for the equation for mass conservation, all other equations are in differential form. The equation for the crosswind gravity spreading applies only to the region where the central core of the cloud exists (i.e., where b is finite). The differential equation for the crosswind dispersion is based on the Briggs (1973) algorithms for passive crosswind dispersion. Both the vertical entrainment law and the crosswind gravity spreading law converge to the passive dispersion limit in the far field. Consequently, the HEGADAS formulation yields results similar to those from conventional Gaussian dispersion models for passive dispersion. The formulas that apply to the far-field passive limits for HEGADAS are similar to the formulas in PGPLUME.

Concentrations for different species predicted by the UF_6 thermodynamics and chemistry modules should be interpreted as "plume-averages" since they are calculated as ratios of the plume-integrated molar flow rates of the species to the total plume-integrated molar flow rate of the mixture. Corresponding "ground-level" concentrations for each species can be calculated using the assumed similarity profiles in HEGADAS.

Conservation of mass requires that

$$\dot{m} = \int_0^{\infty} \int_{-\infty}^{\infty} c(x,y,z)\, u(z)\, dy\, dz \quad , \tag{7-10}$$

where $\dot{m}$ is the mass flux of the species. Substituting Eqs. (7-4), (7-5), and (7-6) into Eq. (7-10) yields

$$\dot{m} = c_A(x)\, \frac{2\,(\, b + \frac{\sqrt{\pi}}{2}\, S_y\,)\, S_z^{1+\alpha}\, u_0}{(1+\alpha)\, z_u^{\alpha}} \quad . \tag{7-11}$$

Equation (7-11) is used to calculate ground-level concentrations, in kg/m^3, for each species at the end of each integration step when values of $\dot{m}$, b, S_y, and S_z are known.

As described in Sect. 7.1, the basic approach of the UF_6 version of the model is that the host model, through its dispersion calculations at any step, provides the air entrainment rate to the chemistry module; the chemistry module calculates the new mixture composition resulting from chemical reactions; and the thermodynamics module then updates the equilibrium temperature and density of the mixture. These output variables are in turn used by the host model to perform dispersion calculations for the next step. Because HEGADAS-S does not directly output the air entrainment rate, the following formulas were used to retrieve the air entrainment rate from the code. The air entrainment rate, in kmoles/s/m, used in HEGADAS (Witlox, 1993c) can be described as

$$\frac{d}{dx}\left[M_{eff}^{mol}\right] = 2\, B_{eff}\left[u_e(u_T) \,/\, v_0 + Q_{wv}\right] \quad , \tag{7-12}$$

where

$$M_{eff}^{mol} = 2 B_{eff}\, H_{eff}\, u_{eff} \,/\, v_m \tag{7-13}$$

is the effective molar flow of the cloud (kmole/s of mixture passing through a vertical plane at downwind distance x),

and

B_{eff} = effective cloud half-width (see Eq. 7-7),
H_{eff} = effective cloud height (see Eq. 7-8),
u_{eff} = effective cloud speed (see Eq. (7-9),
v_m = molar volume of the mixture,
v_0 = molar volume of ideal gas at 0°C and 1 atm = 22.4 m^3/kmole,
u_e = vertical air-entrainment velocity,
u_T = modified friction velocity after taking into account the effect of thermal convection,
Q_{wv} = molar water-vapor flux from the surface.

Equation (7-12) can be rewritten as

$$\frac{d}{dx}\left[2\, B_{eff}\, u_{eff}\, H_{eff} / \nu_m\right] = (ET + EM)\, 2\, B\, \frac{u_0\, z_u}{\nu_0\, L\, (1+\alpha)} \quad , \tag{7-14}$$

where

ET = entrainment due to ambient turbulence,
EM = entrainment due to molecular motions,
B = source half-width
L = source length, specified by the user,
z_u = measuring height of the reference wind speed u_0,
S_z = vertical dispersion parameter.

The entrainment rate calculated above should be multiplied by the molecular weight of air to convert to kg/m/s—the units required by the UF_6 chemistry and thermodynamics routines.

In the original HEGADAS-S, the user can specify the integration step via the DXFIX parameter in the input file. In HEGADAS-S/UF_6, DXFIX is hardwired to ensure DXFIX is small enough to account for fast UF_6 chemical reactions. (Note that the original AEROPLUME also has the integration step hardwired in the code.) The current implementation assumes that DXFIX equals 0.01 m for downwind distances < 25 m. The value of DXFIX gradually increases as x increases (e.g., DXFIX = 0.025 m for x < 50 m; DXFIX = 0.05 m for x < 100 m). To suppress excessive output resulting from the small values of DXFIX, HEGADAS-S/UF_6 prints out results every meter when DXFIX is ≤ 1 m, and every 5·DXFIX when DXFIX > 1 m.

7.6 HEGADAS-T/UF_6

HEGADAS-T is used to describe the dispersion of releases where the source emission rate is transient or varies with time. Transient behavior of the dense plume is approximated by a series of quasi-steady state solutions in which so-called observers are released over the source at a series of times, and each observer sees the source emission rate as steady state. Because one HEGADAS-S/UF_6 run is performed for each "observer," the algorithms described above for HEGADAS-S/UF_6 also apply to HEGADAS-T/UF_6.

To run HEGADAS-T/UF_6, the user needs to specify a number of times after release where output is desired. These output times should be chosen in a way such that concentration values for intermediate output times can be approximated using linear interpolation. The final time series of the concentration predictions as a function of downwind distance are obtained by merging the results for each observer or steady state solution at each output time (Witlox, 1993c).

The integration step in HEGADAS-T/UF_6 is calculated by the model as a function of the spacing of the observers and output times and is not directly controlled by the user. To obtain the high downwind resolution required to account for fast UF_6 chemical reactions, original limits on the numbers of the observers and output times hardwired in the code have been changed. The current HEGADAS-T/UF_6 can handle up to 321 observers (increased from 161) and 200 output times (increased from 50). These limits are specified by parameters MAXOBS and MAXNTST, which can be easily changed if necessary.

For instantaneous releases, the HEGABOX module (to be described later) should be run first. HEGABOX then generates enough information for HEGADAS-T to complete the far-field calculations. One of the files generated by HEGABOX and read by HEGADAS-T is the "HBO" observer file where the starting location, cloud width, cloud height, pollutant mole fraction, ground heat flux, and pollutant temperature associated with each observer at the transition point are listed. However, information concerning the source strength is not included in the HBO file. Since the UF_6 thermodynamics and chemistry modules require the input of source strength, it was necessary to derive an equivalent mass flux for each observer generated at the end of a HEGABOX run before HEGADAS-T can be run. This derivation begins with an estimate of the equivalent vertical dispersion coefficients [refer to Eq. (7-8)]:

$$S_z = \frac{(1+\alpha)\ H}{\Gamma\left(\frac{1}{1+\alpha}\right)} \quad , \tag{7-15}$$

where

α = wind profile exponent,
H = cloud height.

The equivalent volume flux seen by the observer is

$$\dot{V} = 2\ B\ H\ u_{eff} = \frac{2\ B\ S_z^{1+\alpha}\ u_0}{(1+\alpha)\ z_u^{\alpha}} \quad , \tag{7-16}$$

where

B = cloud radius,
u_{eff} = effective cloud velocity as defined in Eq. (7-9),
u_0 = reference wind speed,
z_u = measuring height of u_0.

The equivalent mass flux for the observer can then be calculated as

$$\dot{m} = \dot{V}\ \rho \quad , \tag{7-17}$$

where ρ = cloud density calculated by HEGABOX.

In HEGADAS-T/UF_6, an equivalent mass flux is assigned to each observer according to Eq. (7-17) before the thermodynamics and chemistry calculations are begun. Currently, plume lift-off is not treated in HEGADAS-T/UF_6. Since each observer may see the plume lifting off at different times, results cannot be merged in a straightforward manner.

7.7 HEGABOX/UF_6

Puttock (1987; 1988) originally developed the HEGABOX model to describe the gravity-dominated phase of the dispersion of ground-level, cylindrical-shaped instantaneous releases of heavy gases with no momentum effect. The implementation of the HEGABOX module in HGSYSTEM is discussed in Post (1993a). HEGABOX assumes a uniform pollutant concentration within the cloud, which always retains a cylindrical shape. The entrainment of air into the cloud is assumed to be through the cloud edges due to lateral slumping of the cloud and through the top of the cloud due to vertical entrainment. Since cloud density always exceeds ambient density in HEGABOX, plume lift-off does not apply to the algorithm.

HEGABOX makes a transition to HEGADAS-T when gravity-spreading no longer dominates the dispersion. This occurs when the spreading of cloud material caused by gravity slumping becomes less important than the spreading caused by the cloud's own speed, which should approach the ambient wind speed as time increases. In the HEGABOX code, this transition formally takes place when the internal puff Richardson number becomes less than 10. To run HEGABOX, the user must provide source data such as the mass and the radius of the release.

The dispersion and thermodynamics subsystems are completely separated in HEGABOX/UF_6, following the same principles adopted in AEROPLUME/UF_6 and HEGADAS/UF_6. The dispersion subsystem calculates the air entrainment within one integration step; the chemistry subsystem uses the entrainment information to update the cloud composition due to chemical reactions; and the thermodynamics subsystem calculates the corresponding cloud temperature and density, which are used in turn by the dispersion subsystem for the next step.

The air entrainment rate, in kg/s, to be communicated to the chemistry subsystem of HEGABOX is 0.028966 E, where E is the rate of change of the moles of moist air in the cloud as directly calculated by HEGABOX [as the variable $F(2)$ in the subroutine DERIV], and 28.966 is the molecular weight, in kg/kmole, of air.

7.8 OUTPUT

Main output files for the original HGSYSTEM were the APR file for AEROPLUME, HSR file for HEGADAS-S, HTR file for HEGADAS-T, and HBR file for HEGABOX. These files have been modified so that concentrations (in mass fractions) for UF_6, UO_2F_2, HF, water vapor, and air are printed separately. This is different from the original

HGSYSTEM, which printed only the concentrations for the pollutant as a whole. Since all mass concentrations are derived as ratios of the source strength for each species to the total source strength of the mixture, they should be interpreted as plume averages. These plume averages represent the actual predictions of the AEROPLUME/UF_6 and HEGABOX/UF_6 modules, where a uniform distribution is assumed within the plume. However, because a similarity concentration profile is assumed in HEGADAS/UF_6, equivalent "ground-level" concentrations (in g/m^3) for UF_6, UO_2F_2 and HF are also printed (refer to Sect. 7.4).

Because most of the generic enhancements to HGSYSTEM (see Chap. 6) were implemented as post-processors, their presence does not influence the original calculations in the model. As a result, all outputs from these additional options are not written to the original model output file. Instead, whenever one (or more) option is selected by the user, AEROPLUME/UF_6, HEGADAS-S/UF_6, and HEGABOX/UF_6 will generate an additional output file with enough information to allow the user to calculate the final concentrations after accounting for the effects of all the options chosen. For each downwind distance (or time), this output file lists (1) original ground-level mass concentrations, in kg/m^3, predicted by the model; (2) dry and wet deposition velocities, in m/s; and (3) concentration correction factors (described in Sect. 7.1) corresponding to the effects of canyons, concentration fluctuations, and variations of concentration with averaging time. It is assumed that these effects are independent and their associated correction factors should be multiplied to obtain final results.

8. EVALUATIONS

8.1 OBJECTIVES OF MODEL EVALUATION EXERCISE

The primary objective of the work described in this chapter has been to evaluate the hybrid HGSYSTEM/UF_6 model with data from full-scale field experiments. The model's performance has been compared with the performance of other hazardous gas models for limiting cases, such as nonbuoyant inert gases and nonreactive dense gases. In addition, HGSYSTEM/UF_6 model predictions have been compared with a few UF_6 field experiments. As a result, typical accuracies and relative uncertainties of the model can be estimated. A secondary objective of the model evaluation exercise has been to compare the equilibrium chemical solutions for UF_6 mixtures with solutions presented by Rodean (1989).

8.2 EVALUATIONS WITH FIELD DATA FROM EIGHT SITES (NO UF_6)

8.2.1 Models to be Included

The new hybrid HGSYSTEM/UF_6 model has been included in all evaluations. Nine independent dense gas models had already been evaluated with the field data sets that were used: DEGADIS, SLAB, AIRTOX, CHARM, FOCUS, GASTAR, PHAST, TRACE, and Britter and McQuaid (1988). Therefore, performance statistics for HGSYSTEM/UF_6 could be directly compared with performance statistics that existed in our files for these nine models (Hanna et al., 1993).

8.2.2 Description of Field Data Sets

The set of field data used for this portion of the evaluations includes the eight experiments used by Hanna et al. (1993) in their evaluation of 14 hazardous gas models. Characteristics of these data sets are summarized in Table 8-1. Data include the following:

- **Nonbuoyant releases:** Prairie Grass and Hanford
- **Continuous dense gas releases:** Burro, Coyote, Desert Tortoise, Goldfish, Maplin Sands, and part of the Thorney Island tests
- **Instantaneous dense gas releases:** Thorney Island

The three Goldfish trials involved releases of HF (about 4000 kg per trial). There are 41 separate field trials involving dense gases. These data are stored on Sigma's computer files in a so-called Modelers Data Archive (MDA) that has been widely distributed to interested scientists and engineers throughout the world. We do not describe details of these data sets here. Refer to the article by Hanna et al. (1993, Sect. 3) or to the project report prepared for the U.S. Air Force and API by Hanna et al. (1991, Vol. II).

Table 8-1. Summary of characteristics of the data sets used by Hanna, Chang, and Strimaitis in their model evaluations[a]

Characteristics	Burro	Coyote	Desert Tortoise	Goldfish	Hanford ^{85}Kr (Continuous)	Maplin Sands	Prairie Grass	Thorney Island (Instantaneous)	Thorney Island (Continuous)
Number of trials	8	3	4	3	5	4,8	44	9	2
Material	LNG	LNG	NH_3	HF	^{85}Kr	LNG,LPG	SO_2	Freon & N_2	Freon & N_2
Type of release	Boiling liquid (dense gas)	Boiling liquid (dense gas)	2-Phase jet (dense gas)	2-Phase jet (dense gas)	Gas (nonbuoyant)	Boiling liquid (dense gas)	Gas jet (nonbuoyant)	Gas (dense gas)	Gas (dense gas)
Total mass (kg)	10700-17300	6500-12700	10000-36800	3500-3800	11-24[b]	LNG: 2000-6600 LPG: 1000-3800	23-63	3150-8700	4800
Duration (s)	79-190	65-98	126-381	125-360	598-1191	60-360	600	Instantaneous	460
Surface	Water	Water	Soil	Soil	Soil	Water	Soil	Soil	Soil
Roughness (m)	0.0002	0.0002	0.003	0.003	.03	.0003	.006	.005-.018	.01
Stability class	C-E	C-D	D-E	D	C-E	D	A-F	D-F	E-F
Max. distance (m)	140-800	300-400	800[c]	3000	800	400-650	800	500-580	472
Min. averaging time (s)	1	1	1	66.6-88.3	38.4	3	Dosage	0.06	30
Max. averaging time (s)	40-140	50-90	80-300	66.6-88.3	270-845	3	600	0.06	30
Reference	Koopman et al. 1982	Goldwire et al. 1983	Goldwire et al. 1985	Blewitt et al. 1987	Nickola et al. 1970	Puttock et al., 1984	Barad, 1958	McQuaid and Roebuck, 1985	McQuaid and Roebuck, 1985

[a] *Source:* (Hanna et al., 1993)
[b] Curies rather than kilograms are used as a measure of the amount of this radioactive tracer released.
[c] Concentrations are measured beyond 800 m, but there are not well-instrumented measurement arcs.

The Hanna et al. (1993) model evaluation exercise included the 1990 Version 1.0 of HGSYSTEM (Witlox et al., 1990), which was applied to the eight field data sets listed in Table 8-1. Our new hybrid HGSYSTEM/UF_6 model, intended to reduce to HGSYSTEM for chemicals other than UF_6, is based on a more recent version (3.0) of HGSYSTEM, as developed by Shell under support of API over the past three years. The changes to components of the model are described in a series of reports from Shell, as outlined in the following references:

- Witlox (1993a) — HF thermodynamics model
- Witlox (1993b) — Two-phase thermodynamics models for a nonreactive multi-component pollutant
- Post (1993a) — New HEGABOX (for instantaneous releases) module
- Post (1993b) — New AEROPLUME (for pressurized jet releases) module
- Witlox (1993c) — Updated technical description of the HEGADAS module

The new HGSYSTEM 3.0 technical documentation (Post, 1994c) combines these earlier reports into a comprehensive final report. HGSYSTEM has been reevaluated with the eight sets of field data because one new module has been added to HGSYSTEM: HEGABOX for instantaneous sources; the PLUME module has been superseded by the AEROPLUME module; and most parts of the model have changed slightly. The HGSYSTEM component modules listed below have been applied to these data in our new model evaluation exercise.

Field Experiment and Source Type	HGSYSTEM Module to be Applied
Burro (evaporation area source of LNG)	HEGADAS-S
Coyote (evaporation area source of LNG)	HEGADAS-S
Desert Tortoise (NH_3 aerosol horizontal jet)	AEROPLUME/HEGADAS-S
Goldfish (HF aerosol horizontal jet)	HFPLUME/HEGADAS-S
Hanford ^{85}Kr (trace gas from point)	HEGADAS-S (orifice diameter unknown)
Maplin Sands (evaporation area source of LNG & LPG)	HEGADAS-S
Prairie Grass (trace gas (SO_2) from point)	AEROPLUME/PGPLUME
Thorney Island (instantaneous volume source of Freon & N_2)	HEGABOX/HEGADAS-T
Thorney Island (continuous area source of Freon & N_2)	HEGADAS-S

The existing MDA contained sufficient input data (e.g., mass emission rate, wind speed) to carry out the HGSYSTEM runs described. The MDA also contained the concentration observations that were necessary for the statistical evaluations.

8.2.3 Model Output Parameters That Were Evaluated

Of primary interest in the evaluation is the maximum near-ground-level concentration at each downwind distance; a measure (e.g., the standard deviation) of the plume width and height at each downwind distance; and geometric characteristics of particular contours of

concentration or dosage. For a module (i.e., AEROPLUME) in which uniform crosswind and vertical profiles are assumed, the average plume concentration is the same as the maximum centerline concentration.

8.2.4 Statistical Model Evaluation Procedures to be Used

The statistical model evaluation software, BOOT, applied in the study described by Hanna et al. (1993) was used. BOOT has been well tested in a wide range of studies and currently is in use by groups in the United States, Europe, and Australia. This software involves use of the relative mean bias, normalized mean-square-error, correlation coefficient, and fraction of predictions within a factor-of-two of observations. Confidence intervals on these performance measures are generated by bootstrap resampling. Hanna et al. (1993, Sect.4) describe these procedures in detail.

8.2.5 Standards for Accepting or Rejecting Model Performance

Air quality modelers have not yet agreed upon the magnitude of standards for accepting or rejecting model performance. In most cases, a model is considered acceptable if most of its predictions are within a factor-of-two of the observations. However, in dense gas models, the study by Hanna et al. (1993) demonstrated that the performance measures for several models were within a range of acceptability, as shown in Fig. 8-1. Most models fall in a cluster of fair performance, with $0.7 <$ geometric mean bias < 1.5 and $1.3 <$ geometric variance < 2.5. Consequently, to be acceptable, the performance measures for the new model would be expected to at least fall within this same range.

8.2.6 Results of Model Evaluation at Eight Field Sites

The BOOT model evaluation software produces many tables and figures. We have selected a set of figures in which geometric variance VG is plotted versus geometric mean bias MG for each model. These performance measures are calculated from the following formulas:

$$VG = \exp\overline{(\ln(C_o/C_p))^2} \quad , \tag{8-1}$$

$$MG = \exp\overline{(\ln(C_o/C_p))} \quad . \tag{8-2}$$

Therefore, a ***perfect*** model would have $VG = MG = 1.0$.

Five figures are presented in this section. Figures 8-2a, b, and c consist of a set of results for concentration predictions for three groups of data: continuous dense gas field data, continuous passive gas field data, and instantaneous dense gas field data. Figures 8-3a and b are concerned with predictions of plume width for groups 1 and 2.

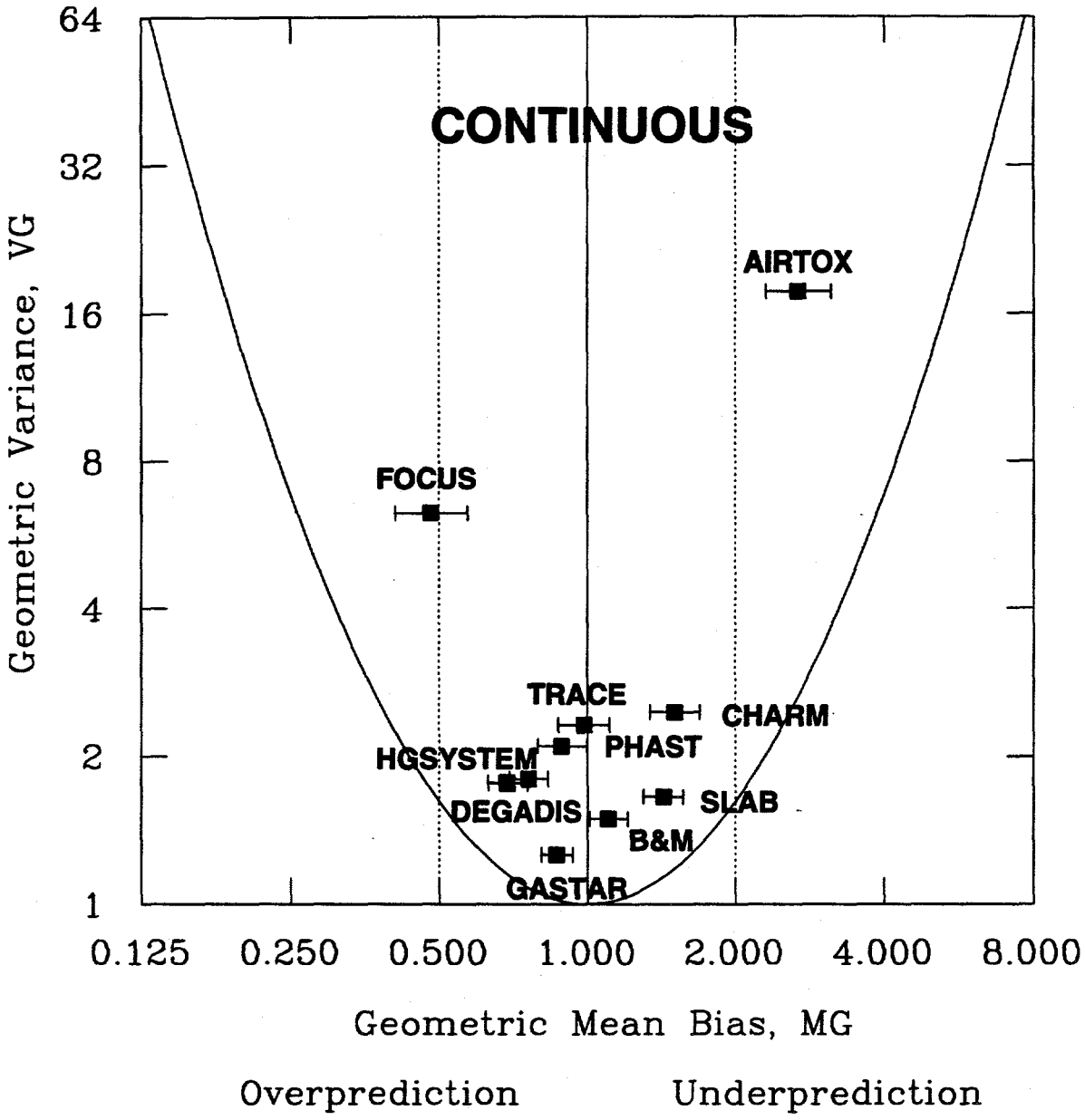

Fig. 8-1. Example of presentation of model evaluation results (Hanna et al., 1993, Fig 1a).

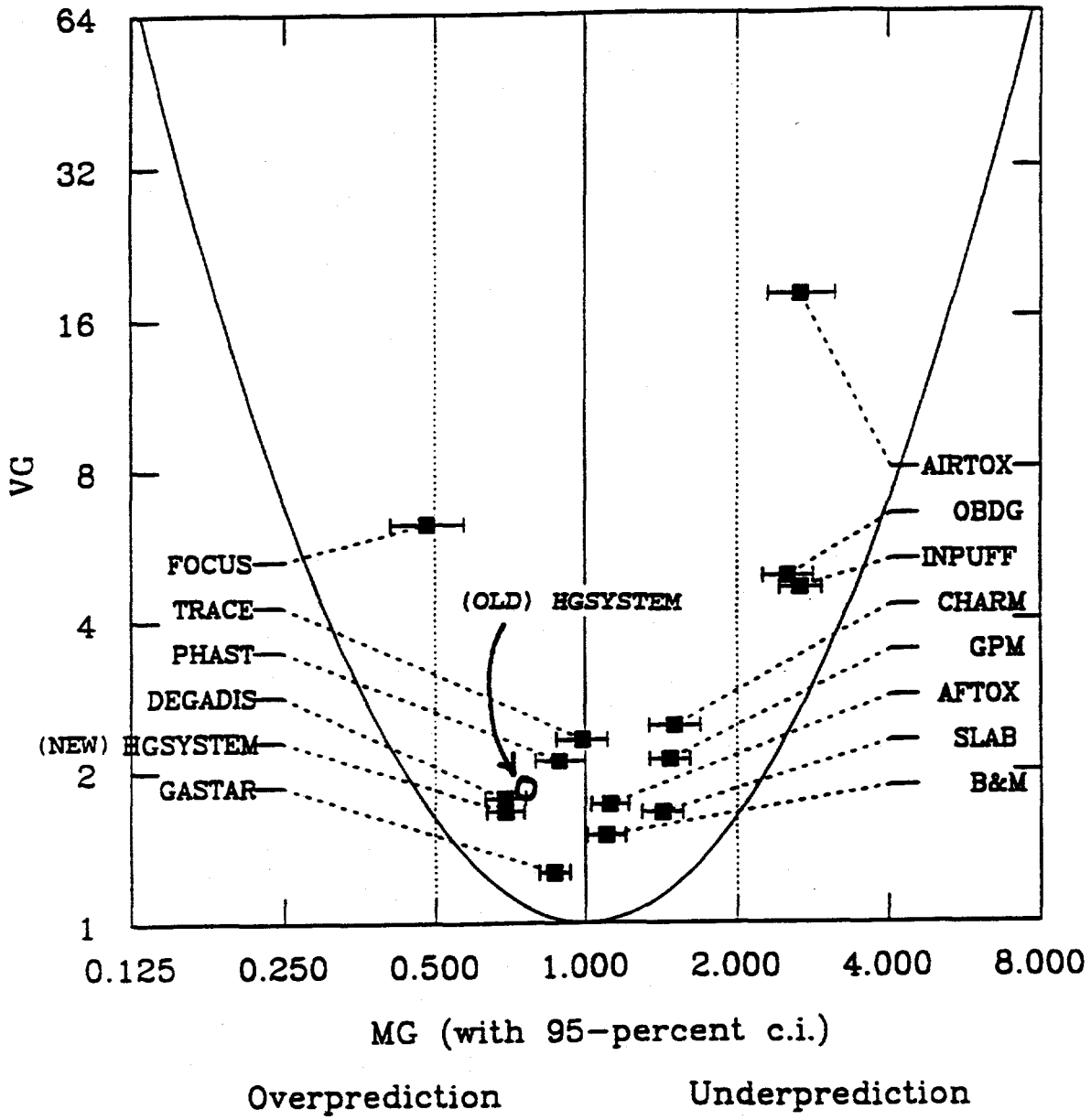

Fig. 8-2a. Group 1: Burro, Coyote, Desert Tortoise, Goldfish, Maplin Sands, and Thorney Island — continuous dense gas field data (N = 123) concentrations.

Model performance measures, geometric mean bias $MG = \exp\overline{(\ln C_o - \ln C_p)}$ and geometric variance $VG = \exp\overline{(\ln C_o - \ln C_p)^2}$, for maximum plume centerline concentration predictions and observations. Horizontal lines indicate 95% confidence intervals on MG; solid parabola is "minimum VG" curve; vertical dotted lines represent a factor-of-two agreement between mean predictions and observations. Group 1 continuous dense gas data sets involve 32 trials and 123 points, for the shortest available instrument averaging times.

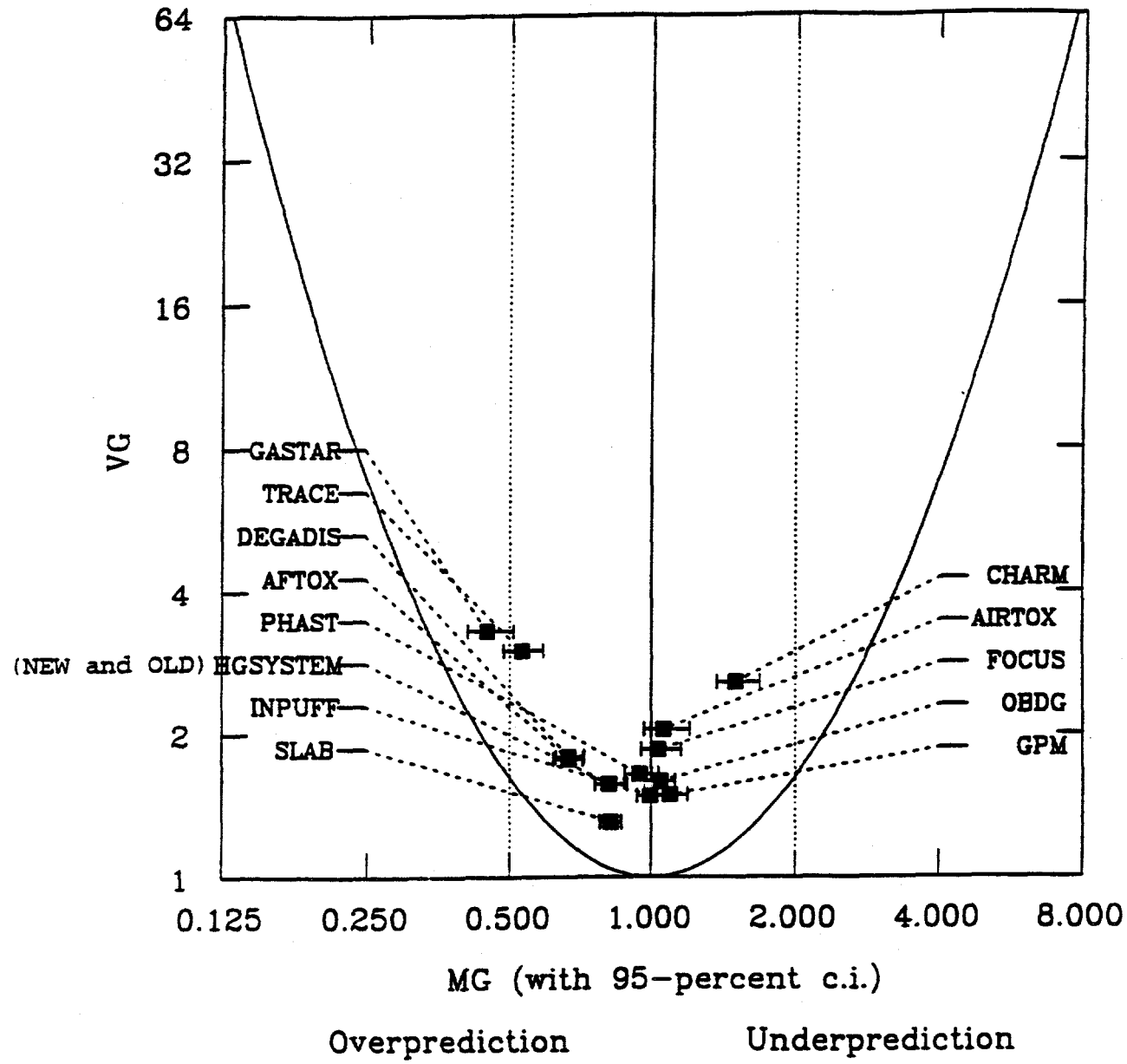

Fig. 8-2b. Group 2: Prairie Grass and Hanford — continuous passive gas field data (N=222) concentrations.

Model performance measures, geometric mean bias $MG = \exp\overline{(\ln C_o - \ln C_p)}$ and geometric variance $VG = \exp\overline{(\ln C_o - \ln C_p)^2}$, for maximum plume centerline concentration predictions and observations. Horizontal lines indicate 95% confidence intervals on MG; solid parabola is "minimum VG" curve; vertical dotted lines represent factor-of-two agreement between mean predictions and observations. Group 2 continuous passive gas data sets involve 49 trials and 222 points for the shortest available instrument averaging times.

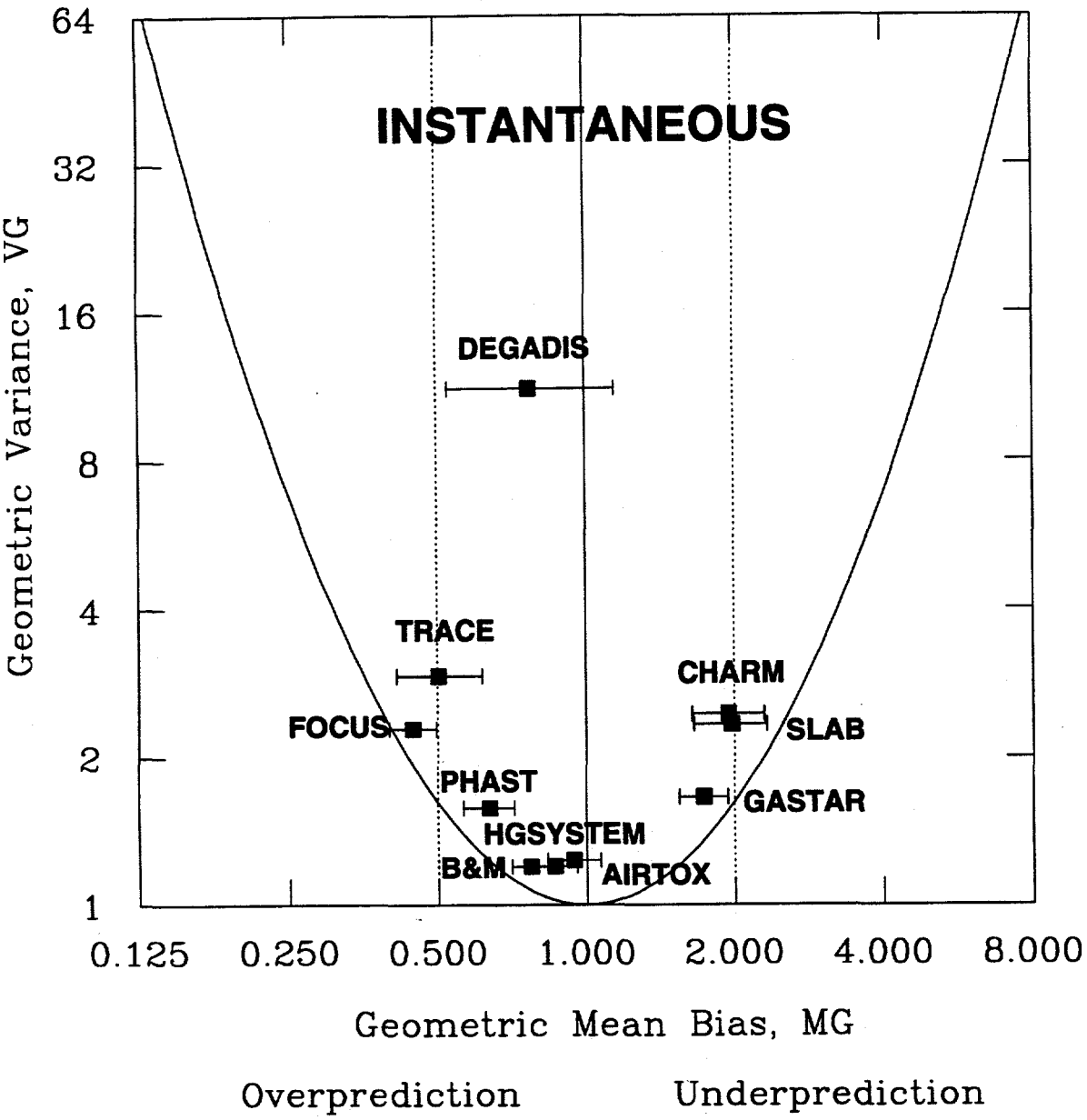

Fig. 8-2c. Group 3: Thorney Island — instantaneous dense gas field data (N = 61) concentrations.

Model performance measures, geometric mean bias $MG = \exp\overline{(\ln C_o - \ln C_p)}$ and geometric variance $VG = \exp\overline{(\ln C_o - \ln C_p)^2}$, for maximum plume centerline concentration predictions and observations. Horizontal lines indicate 95% confidence intervals on MG; solid parabola is 'minimum VG" curve; vertical dotted lines represent factor-of-two agreement between mean predictions and observations. Group 3 instantaneous dense gas data set involves 9 trials and 61 points for the shortest available instrument averaging times.

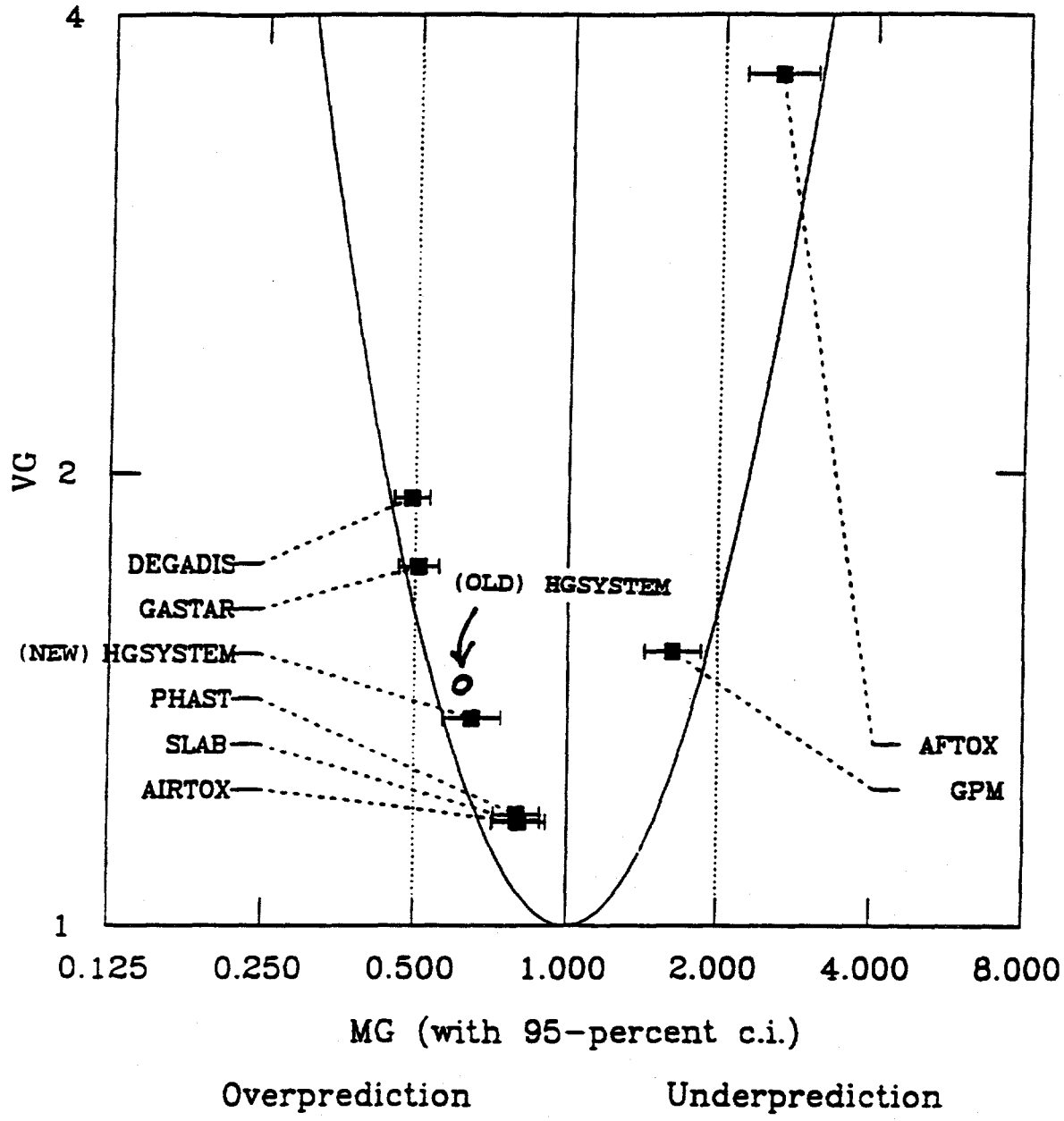

Fig. 8-3a. Group 1: Burro, Coyote, Desert Tortoise, and Goldfish — continuous dense field data (N = 30) widths.

Model performance measures, geometric mean bias $MG = \exp\overline{(\ln W_o - \ln W_p)}$ and geometric variance $VG = \exp\overline{[(\ln W_o - \ln W_p)^2]}$, for plume width predictions and observations. Horizontal lines indicate 95% confidence intervals on MG; solid parabola is "minimum VG" curve; vertical dotted lines represent factor-of-two agreement between mean predictions and observations. Group 1 continuous dense gas data sets involve 18 trials and 30 points.

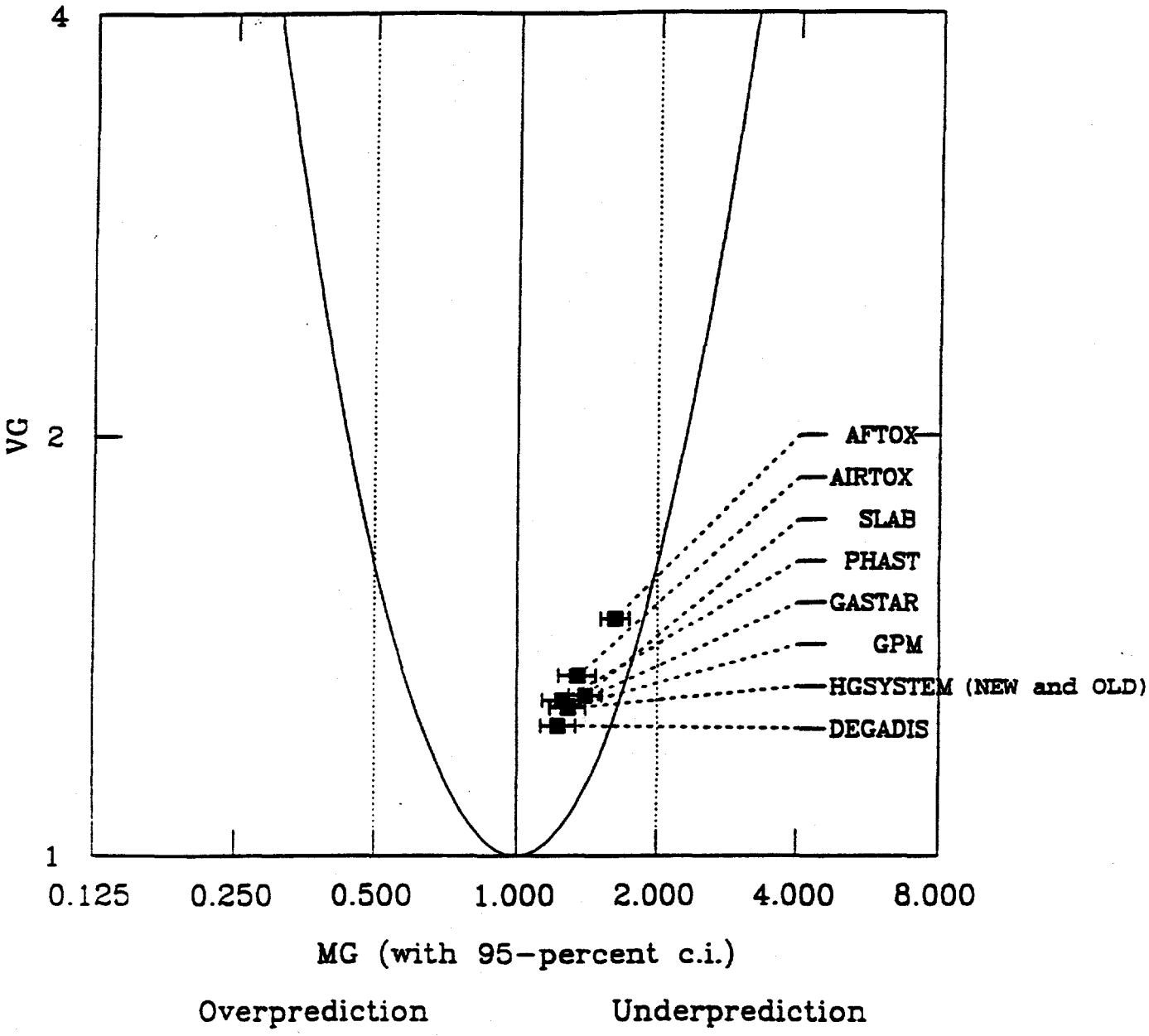

Fig. 8-3b. Group 2: Prairie Grass and Hanford — continuous passive field data (N = 85) widths.

Model performance measures, geometric mean bias $MG = \exp\overline{(\ln W_o - \ln W_p)}$ and geometric variance $VG = \exp\overline{[(\ln W_o - \ln W_p)^2]}$, for plume width predictions and observations. Horizontal lines indicate 95% confidence intervals on MG; solid parabola is "minimum VG" curve; vertical dotted lines represent factor-of-two agreement between mean predictions and observations. Group 2 continuous passive gas data sets involve 49 trials and 85 points.

Figure sets (a) and (b) show that there is very little difference between the results for the **old** (Version 1.0) and the **new** (Version 3.0) HGSYSTEM models. Both versions overpredict the mean by about 20 to 40%, with a geometric variance of about 2, and both versions are within the cloud of the five or six best-performing models. The biggest difference occurs for Fig. 8-2c (instantaneous dense gas field data). Here, the old model did not apply at all, while the new model (with the addition of HEGABOX) now applies and is one of the three best performing models, along with AIRTOX and the Britter and McQuaid (1988) nomograms.

Like other dense gas models, HGSYSTEM overpredicts the dense gas plume widths by approximately 50% (see Fig. 8-3a) and underpredicts the passive gas plume widths by about 30% (see Fig. 8-3b). The conclusion is that the new version of HGSYSTEM is among the better performing models, with a typical mean bias of about 20 to 40% and a typical scatter less than a factor-of-two.

8.3 EVALUATION WITH THE FRENCH UF_6 DATA

UF_6 gas was released in three experiments in France in 1986, 1987, and 1989. These are the only field data available for UF_6. The French data are reported by Crabol et al. (1991), Just (1986), Just and Bloom (1989), and Bloom and Just (1993). The last two reports describe applications of the PLM89A model to these experiments. Release conditions are given in Table 8-2. Approximately 80 g/s of UF_6 was released from a 5-cm-diam opening at about a 3-m height. UF_6 particle evaporation was not a factor since the release was in the gas phase. The release was two orders-of-magnitude less than that from the postulated 14-ton cylinder rupture in Chap. 3; therefore, the effects of the chemical reactions and thermodynamics were minor. Consequently, these data represent a passive gas release. When HGSYSTEM/UF_6 is applied, the model quickly *transitions* from AEROPLUME/UF_6 (dense gas jet module) to PGPLUME (passive gas module). For this reason, the standard Gaussian Plume Model (GPM) used by the EPA for passive gas releases was also applied to the three field tests, and the results were included in the evaluation exercise.

Tables 8-3, 8-4, and 8-5 list observed and predicted concentrations from PLM89A, HGSYSTEM/UF_6, and GPM at downwind distances ranging from 10 m to 500 m. Observations were made at a 1-m height (2 m below release height); therefore, the models predict the plume is mostly passing above the observing instrument for the first few tens-of-meters of plume travel. To attempt to bracket the observations, predictions are given at both 1 m (instrument height) and 3 m (source height).

The tables clearly suggest the PLM89A, HGSYSTEM/UF_6, and GPM predictions are in fair agreement with each other. At the 3-m height, usually the models are within ± 20% of each other. All models tend to overpredict when compared with observations in the far-field (distances of 50 m or greater), where concentrations at 1-m and 3-m heights are nearly equal. The amount of the overprediction is about a factor-of-three for the 1986 test, factor- of-two for the 1987 test, and 10 to 20% for the 1989 test.

Table 8-2. Characteristics of the three UF_6 releases			
Characteristics	**First release**	**Second release**	**Third release**
Date	04.10.1986	04.18.1987	06.05.1989
UF_6 Flow Rate g/s	75.7	80.9	81.2
Duration (mn)	10	30	15
Release Quantity (kg)	45.8	146.2	73.1
Meteorological Conditions			
Wind Velocity (m/s)	6.9 @ 10 m	3.3 @ 10 m	4.8 @ 10 m
Direction	306 to 308°	305°	315.8°
Humidity (%)	100	72.2	54.3
Ambient Temperature (°C)	8.8 @ 10 m	13 @ 2 m	17.7 @ 2 m
Temperature Gradient (C°/100 m)	-	- 1.9	- 2.6
Estimated Stability Class	D	C	B
Ground Temperature (°C)	N/A	13.3	21.2
Ground Level Sampling			
Location of samplers (m)	10, 20, 40, 100, 500, 1000, 2200	10, 20, 40, 70, 100, 200, 500	10, 20, 40, 70, 100, 200
Number of dynamic samplers	110	116	112
Number of static samplers	110	138	9
Number of SF_6 analyses	65	62	52
Sampling in Altitude			
Number of US samplers	19	19	19
Altitude (m)	1,3,8 (5 masts) 1,3,8,15 (1 mast)	1,3,8 (5 masts) 1,3,8,15 (1 mast)	1,3,6 (3 masts) 1,3,8 (2 masts) 1,3,8,15 (1 mast)

Source: (Crabol et al., 1991)

Table 8-3. Observed and predicted uranium concentrations for the French 1986 field test[a]							
Downwind distance (m)	Observed (mg/m^3)	PLM89A (mg/m^3)		HGSYSTEM/UF_6 (mg/m^3)		GPM (mg/m^3)	
	1-m ht	1-m ht	3-m ht	1-m ht	3-m ht	1-m ht	3-m ht
10	434	0.051	1800	0.034	1474	7.6	2131
20	262	43	610	0.16	660	128	582
40	93	100	170	71	229	135	159
100	10	46	42	54	38	44	41
500	1.5	3.2	3.1	4.7	4.7	2.6	2.6

Source: (Just, 1986)

[a] The release height was 3.15 m. Observed concentrations were measured at 1 m; concentrations for PLM89A, HGSYSTEM/UF_6, and GPM were predicted at 1-m and 3-m heights. When HGSYSTEM/UF_6 was applied, a ***transition*** from AEROPLUME/UF_6 to PGPLUME was made at a distance prior to the first measuring distance (10 m) in the table.

Table 8-4. Observed and predicted uranium concentrations for the French 1987 field test[a]							
Downwind distance (m)	Observed (mg/m^3)	PLM89A (mg/m^3)		HGSYSTEM/UF_6 (mg/m^3)		GPM (mg/m^3)	
	1-m ht	1-m ht	3-m ht	1-m ht	3-m ht	1-m ht	3-m ht
10	543	161	1560	2.4	1215	106	2693
20	281	248	479	69	519	333	715
40	112	163	160	114	179	228	214
70	43	82	75	79	62	103	94
100	24	49	46	51	44	55	53
200	7.4	15	15	16	16	15	15
500	1.2	2.4	2.4	3.1	3.0	2.6	2.6

Source: (Just and Bloom, 1989)

[a] Release height was 3.15 m. Observed concentrations were measured at 1 m; concentrations for PLM89A, HGSYSTEM/UF_6, and GPM were predicted at 1-m and 3-m heights. When HGSYSTEM/UF_6 was applied, a ***transition*** from AEROPLUME/UF_6 to PGPLUME was made at a distance prior to the first measuring distance (10 m) in the table.

Table 8-5. Observed and predicted uranium concentrations for the French 1989 field test[a]					
Downwind distance (m)	Observed (mg/m^3)	HGSYSTEM/UF_6 (mg/m^3)		GPM (mg/m^3)	
	1-m ht	1-m ht	3-m ht	1-m ht	3-m ht)
10	231	14	676	203	884
20	154	78	220	210	239
40	61	70	48	93	85
70	27	36	32	36	34
100	16	21	19	18	18
200	4.9	6.0	5.9	4.7	4.7

Source: (Bloom and Just, 1993)

[a] Release height was 3.15 m. Observed concentrations were measured at 1 m; concentrations for HGSYSTEM/UF_6 and GPM were predicted at 1-m and 3-m heights. When HGSYSTEM/UF_6 was applied, a ***transition*** from AEROPLUME/UF_6 to PGPLUME was made at a distance prior to the first measuring distance (10 m) in the table.

Observed and predicted lateral dispersion parameters σ_y were also compared for the three French UF_6 tests. An estimate of σ_y was made from the observations by calculating the square root of the second moment of crosswind distributions at each downwind monitoring arc. Each resulting observed σ_y is listed in Table 8-6 along with the predictions of HGSYSTEM and the GPM. In the 1986 test, each predicted σ_y is about a factor-of-two less than each observed σ_y at all distances except the farthest distance (500 m), where each predicted σ_y is about 50% higher than each observed value. In the 1987 test, agreement is better at all distances, with HGSYSTEM showing only 15% underpredictions at small distances and near-perfect agreement at large distances. In the 1989 test, HGSYSTEM σ_y predictions are still fairly good, with an average underprediction of about 15%. The conclusion is that over the three French UF_6 tests, HGSYSTEM tended to show slight underpredictions of σ_y, ranging from 15% to a factor-of-two.

Conclusions from the tables are difficult to generalize in the near-field because the observing instrument is located 2 m below the plume release height, and the model predictions are strong functions of the vertical distance from the plume axis. The slight overpredictions found for the French UF_6 tests are not consistent with the Hanna et al. (1993) results for the Prairie Grass passive gas experiments, in which both the GPM and original HGSYSTEM model had little bias.

Table 8-6 Observed and predicted cloud widths (σ_y, m) for the three French UF_6 field tests				
Field test	Downwind distance (m)	Observed σ_y (at 1 m)	HGSYSTEM/UF_6 σ_y	GPM σ_y
1986	10	2.2	1.1	0.8
	20	3.7	2.0	1.6
	40	6.8	3.7	3.2
	100	13	8.3	8.0
	500	26	36	39
1987	10	2.5	2.1	1.1
	20	4.3	3.7	2.2
	40	8.4	6.9	4.4
	70	14	11	7.7
	100	19	16	11
	200	30	30	22
	500	65	68	54
1989	10	2.6	2.6	1.6
	20	5.4	4.8	3.2
	40	11	9.1	6.4
	70	19	15	11
	100	24	21	16
	200	49	39	32

8.4 COMPARISON WITH RODEAN'S RESULTS

Rodean (1989) solved the set of thermodynamics and chemistry equations for mixtures of UF_6 and moist air for equilibrium conditions. That is, he assumed a certain amount of UF_6 was mixed with a certain amount of moist air and allowed to reach equilibrium. Then, the characteristics (e.g., temperature and density) of the final state of the mixture were determined. The graph on the right side of Fig. 8-4 and Fig. 8-5 contain Rodean's solutions for temperature and density as a function of the mass fraction of uranium and fluoride in the mixture. Rodean assumed (1) the UF_6 release had an initial temperature of 82°C and was

50% gas and 50% solid, and (2) ambient temperature was 25° C, with a relative humidity of 100% (specific humidity, q, of 0.02). He defined the following normalized variables:

- β: (mass of initial UF_6)/(mass of initial UF_6 + mass of entrained dry air)
- α: mass of fraction of UF_6 vaporized
- η: mass fraction of UF_6 converted to UO_2F_2 and HF via chemical reactions
- ρ/ρ_o: ratio of mixture density to ambient density at equilibrium

For comparison, the simulations of our new HGSYSTEM/UF_6 model are plotted on the left side of Fig. 8-4 and Fig. 8-5. Because the model assumes finite reaction rates (i.e., the solution is ***not*** in equilibrium), some differences are expected. When the AEROPLUME/UF_6 module in HGSYSTEM/UF_6 was applied, the values listed below were assumed for the input data; these were set as close to the conditions used by Rodean as possible.

Nozzle diameter	0.02 m
Nozzle elevation	15.0 m
Emission rate	15 kg/s
Storage temperature	82° C
Storage pressure	2 Atm
Ambient temperature	25° C
Ambient relative humidity	100%
Ambient wind speed	5.6 m/s
Pasquill-Gifford stability class	C

Upon exit from the nozzle, liquid UF_6 flashes to about 50% vapor and 50% solid, in agreement with Rodean's assumptions concerning the initial mass fraction vaporized, α.

Figure 8-4 shows the HGSYSTEM/UF_6 and Rodean equilibrium curves are in good agreement for variation of mixture temperature with mass fraction, β. Both curves show a cooling to about 15° C or 18° C as the solid UF_6 evaporates (Region I). Because of the time delay, the evaporation predicted by HGSYSTEM/UF_6 is not completed until $\beta = 0.5$ (Rodean curve indicates the evaporation is completed at $\beta = 0.6$). Both curves show an increase in temperature in Region II, where UF_6 gas is reacting with water vapor. The maximum temperature reached is less for HGSYSTEM/UF_6 (62° C) than for the Rodean model (75° C), possibly due to the increase in the mixing timescale as the plume becomes larger. Finally, the curves follow each other in Region III, where all the UF_6 has been used up and the UO_2F_2 and HF products are merely being diluted by the entrainment of ambient air.

Figure 8-5 shows the predictions of relative density ρ/ρ_o are also in good agreement for the HGSYSTEM/UF_6 model and the Rodean (1989) equilibrium model. Note that ρ/ρ_o drops below 1.0 (i.e., the plume is positively buoyant) at values of mixture mass fraction of about 0.08. Consequently, the plume may lift-off the ground at that point if the Briggs lift-off criterion is satisfied (see Sect. 6.2).

The conclusion is that the new HGSYSTEM/UF_6 model predictions agree well with the equilibrium solutions of Rodean (1989) except for minor differences that may be caused by the use of a finite reaction timescale in HGSYSTEM/UF_6.

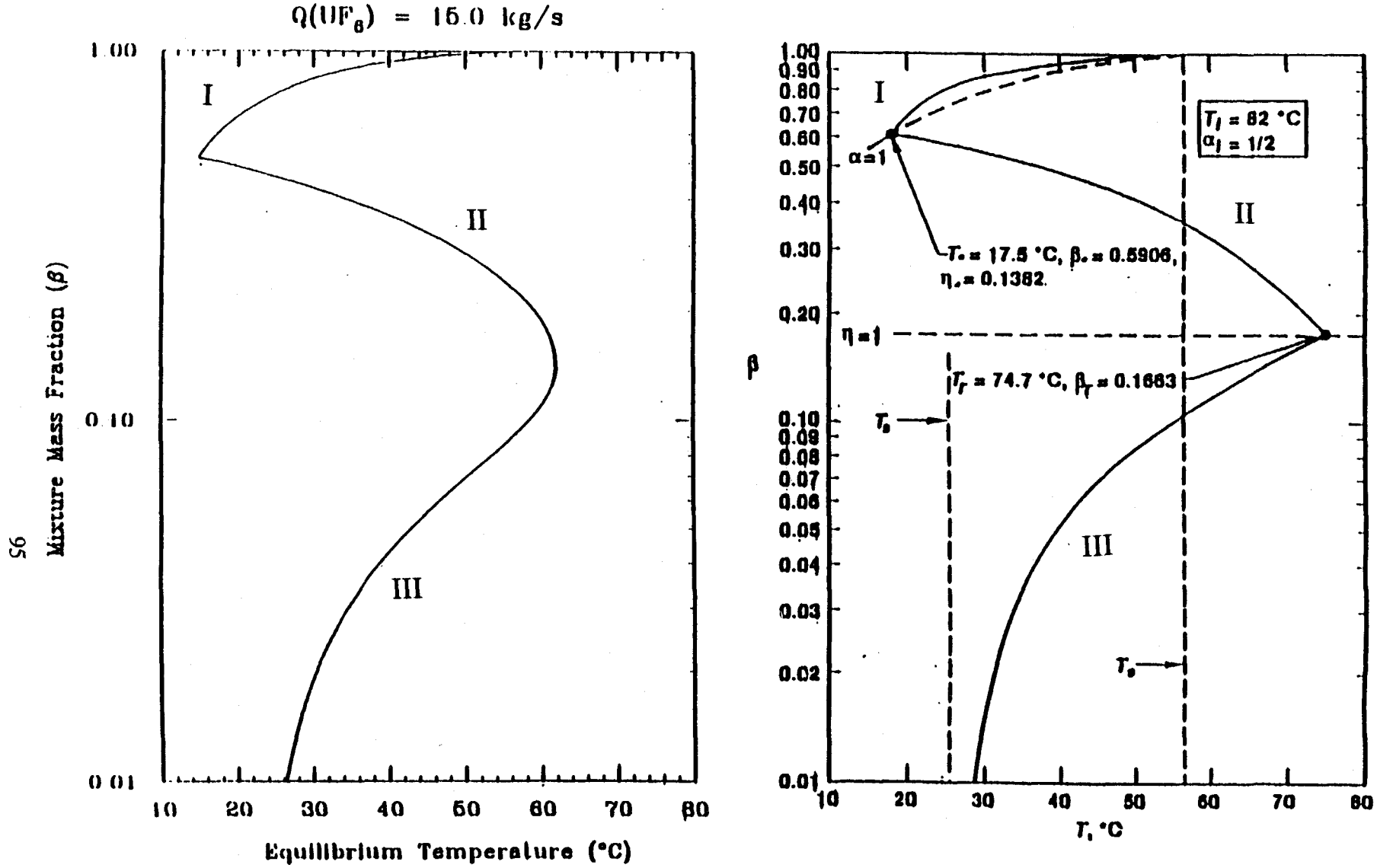

Fig. 8-4. Mixture mass fraction β for HGSYSTEM/UF_6 predictions (left side) and for Rodean's (1989) equilibrium solution (right side). Three regions are seen: (I) cooling due to evaporation of solid UF_6; (II) warming due to reaction of UF_6 vapor with water vapor; and (III) dilution of products (HF and UO_2F_2) by entrainment.

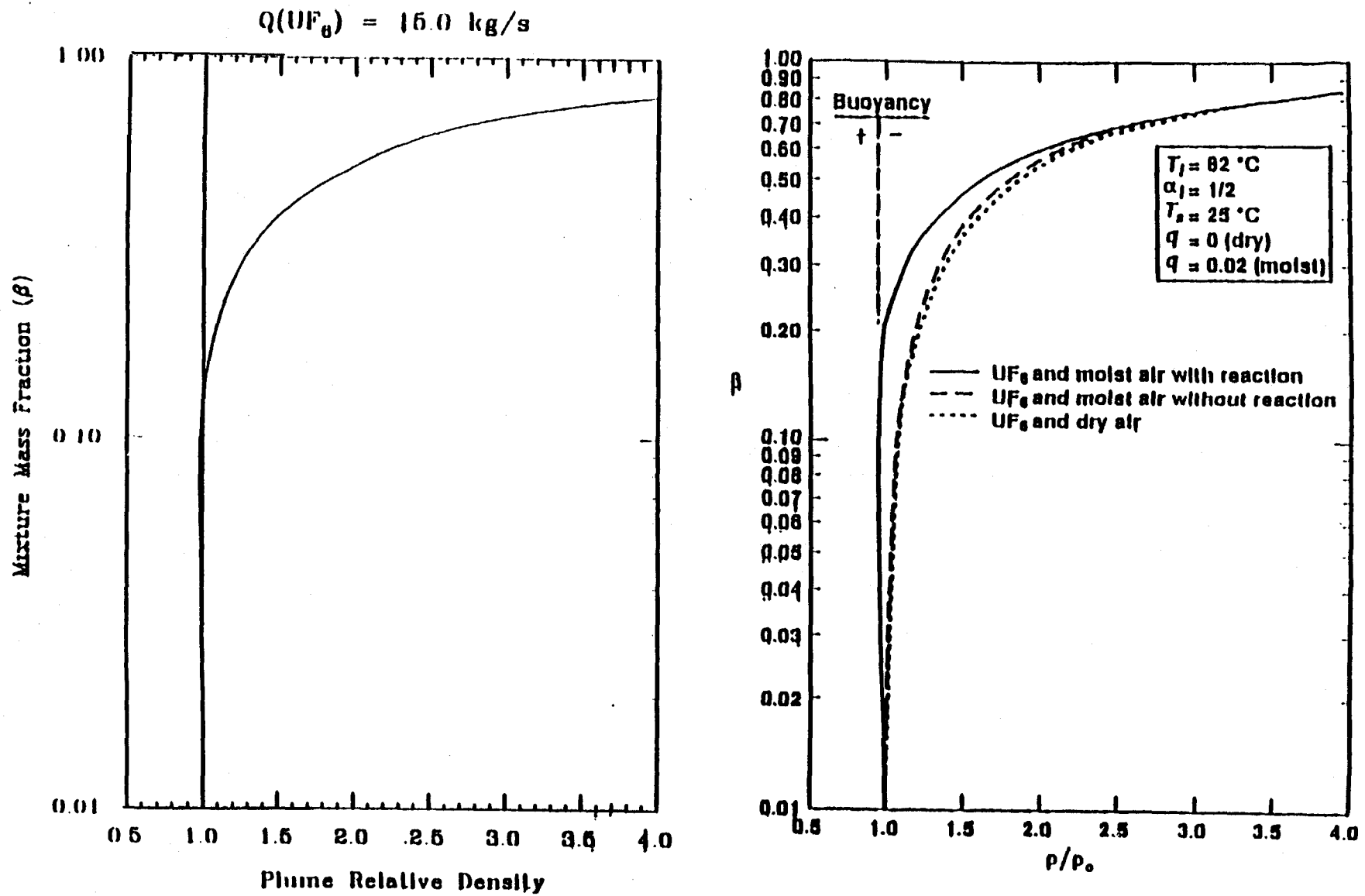

Fig. 8-5. Plume relative density ρ/ρ_a for HGSYSTEM/UF_6 predictions (left side) and for Rodean's (1989) equilibrium solution (right side).

REFERENCES

Armstrong, D. P., W. D. Bostick, and Fletcher. 1991. "An FT-IR Study of the Atmospheric Hydrolysis of Uranium Hexafluoride," *Applied Spectroscopy*, 45, pp. 1008-1016.

Barber, E. J. 1994, Martin Marietta Utilities Services, K-25 Site, Oak Ridge, Tennessee; personal communication with The Earth Technology Corp., Concord, Mass.

Barad, M. L. 1958. *Project Prairie Grass, a Field Program in Diffusion*, Vol. I, AFCRC-TR-58-235(I), AD 15272, AFGL, Hanscom Air Force Base, Mass.

Bayne, C. K., and W. D. Bostick. 1985. *Particle Size Distributions Formed by Atmospheric Hydrolysis of Uranium Hexafluoride*, ORNL/CSD/TM-9387, ORNL., Energy Systems, Oak Ridge, Tenn.

Blewitt, D. N., J. F. Yohn, R. P. Koopman, and T. C. Brown. 1987. "Conduct of Anhydrous Hydrofluoric Acid Spill Experiment," *Proceedings, International Conference on Vapor Cloud Modeling*, AIChE, New York.

Bloom, S. G., and R. A. Just. 1993. *Analysis of the June 5, 1989, UF_6 Release Test*, K/D-6092, Energy Systems, Oak Ridge K-25 Site, Oak Ridge, Tenn.

Bloom, S. G., R. A. Just, and W. R. Williams. 1989. *A Computer Program for Simulating the Atmospheric Dispersion of UF_6 and Other Reactive Gases Having Positive, Neutral, or Negative Buoyancy*, K/D-5694, Energy Systems, ORGDP, Oak Ridge, Tenn.

Briggs, G. A. 1973. *Lift-off of Buoyant Gas Initially on the Ground*, draft; available from ATDD/NOAA, P.O. Box 2456, Oak Ridge, TN 37831-2456.

Briggs, G. A. 1975. "Plume Rise Predictions," *Lectures on Air Pollution and Environmental Impact Analyses*, pp. 59-111, D. A. Haugen, Ed., Amer. Meteorol. Soc., Boston.

Brighton, P. W. M. 1989. *The Effects of Natural and Man-Made Obstacles on Heavy Gas Dispersion*, Safety and Reliability Directorate, UK Atomic Energy Authority, Wigshaw Lane, Culceth, Warrington, WA3 4NE, United Kingdom.

Britter, R. E. 1989. *Experiments on Some Effects of Obstacles on Dense Gas Dispersion*, SRD R 407, UKAEA, Wigshaw Lane, Culceth, Warrington, WA3 4NE, United Kingdom.

Britter, R. E. and J. McQuaid. 1988. *Workbook on the Dispersion of Dense Gases*, HSE Contract Research Report No. 17/1988, Health and Safety Executive, Sheffield, United Kingdom.

Carruthers, D., D. Thomson, R.E. Britter, and J.C.R. Hunt. 1992. "Description of the United Kingdom Atmospheric Dispersion Modeling System (ADMS)"; pub. in *Proceedings for CEC Workshop on Objectives for Next Generation of Practical Short-Range Atmospheric Dispersion Models*, Riso Nat. Lab., Denmark.

Chorin, A. J. 1973. "Numerical Study of Slightly Viscous Flow," *J. Fluid Mech.*, 57, pp. 785-796.

Colenbrander, G. W. 1980. "A Mathematical Model for the Transient Behavior of Dense Vapor Clouds"; pub. in proceedings of *3rd International Symposium on Loss Prevention and Safety Promotion in the Process Industries.*

Crabol, B., C. Geisse, L. Iacona, D. Boulaud, and G. Deville-Cavelin. 1991. "Presentation and Interpretation of Field Experiments of Gaseous UF_6 Releases in the Atmosphere"; pub. in *Proceedings, OECD/NEA/CSNI/Specialist Meeting on Safety and Risk Assessment in Fuel Cycle Facilities*, pp. 320-350, Tokyo, Japan.

DeWitt, R. 1960. *Uranium Hexafluoride: A Survey of the Physico-Chemical Properties*, Report GAT-280, USAEC.

Ermak, D. L., 1990. *User's Manual for SLAB: An Atmospheric Dispersion Model for Denser-Than-Air Releases*, UCRL-MA-105607, LLNL, Livermore, Calif.

Fauske, H. K., and M. Epstein. 1988. " Source Term Considerations in Connection with Chemical Accidents and Vapour Cloud Modelling," *I. Loss Prev. Process Ind.*, 1.

Goldwire, H. C., et al. 1983. *LLNL/NWS 1981 LNG Spill Tests: Dispersion, Vapor Burn, and Rapid Phase Transition*, UCID-199953, LLNL, Livermore, Calif.

Goldwire, H. C., et al. 1985. *Desert Tortoise Series Data Report: 1983 Pressurized Ammonia Spills*, UCID-20562, LLNL, Livermore, Calif.

Golder, D. 1972. "Relations Among Stability Parameters in the Surface Layer," *Bound. Lay. Meteorol.*, 3, pp. 56-65.

Hall, D. J., and R. A. Waters. 1986. *Further Experiments on a Buoyant Emission from a Building*, Report No. LR 567 PAISBN 0 85624 425 2, Warren Spring Lab., Gunnels Wood Road, Stevenage, Hertfordshore SG1 3BX, United Kingdom.

Hanna, S. R. 1984. "The Exponential Probability Density Function and Concentration Fluctuations in Smoke Plumes," *Bound. Lay. Meteorol.*, 29, pp. 361-375.

Hanna, S. R., and J. C. Chang. 1992. "Boundary-Layer Parameterizations for Applied Dispersion Modeling over Urban Areas. *Bound. Lay. Meteorol.*, 58, pp. 229-259.

Hanna, S. R., and J. C. Chang. 1993. "Hybrid Plume Dispersion Model (HPDM) Improvements and Testing at Three Field Sites." *Atmos. Environ.*, 27A, pp. 1491-1508.

Hanna, S. R., G. A. Briggs, and R. F. Hosker Jr. 1982. *Handbook on Atmospheric Diffusion*, DOE/TIC-11223, TIC, USDOE, Oak Ridge, Tenn.

Hanna, S. R., J. C. Chang, and D. G. Strimaitis. 1993. "Hazardous Gas Model Evaluation with Field Observations. *Atmos. Environ.*, 27A, pp. 2265-2285.

Hanna, S. R., D. G. Strimaitis and J. C. Chang. 1991. *Hazard Response Modeling Uncertainty (A Quantitative Method) Vol. II, Evaluation of Commonly-Used Hazardous Gas Dispersion Models*, Sigma Research Corp., Concord, Maine.

Hicks, B. B., W. W. Lewellen, and J. C. Weil. 1985. *Atmospheric Components of the Oak Ridge UF_6 Dispersion Model* (PP D-8-5), Energy Systems, Oak Ridge, Tenn.

Hicks, B. B., et al. 1989. *TRIAD: A Puff-Trajectory Model for Reactive Gas Dispersion with Application to UF_6 Releases Into the Atmosphere*, TM ERL ARL-168, NOAA, Air Resources Lab., Silver Spring, Md.

Just, R. A. 1986. *Analysis of the April 18, 1986, UF_6 Release Test*, K/D-5720, Energy Systems, ORGDP, Oak Ridge, Tenn.

Just, R. A., and S. G. Bloom. 1989. *Analysis of the April 10, 1987, UF_6 Release Test*, K/D-5806, Energy Systems, ORGDP, Oak Ridge, Tenn.

Konig, G. 1987. 'Windkanalmodellierung der Ausbreilung Stofallartig Freigesetzter Gase Schwerer als Luft," *Hanburger Geophysikalische Einzelschriften, Series A*, No. 85.

Koopman, R. P. et al. 1982. *LLNL NWC 1980 LNG Spill Tests*, UCID 19075, LLNL, Livermore, Calif.

Leitnaker, J. M. 1989. *Possible Temperature Changes when Uranium Hexafluoride Reacts with Water or Iron*, Energy Systems, ORGDP, Oak Ridge, Tenn.

Marotzke, K. 1988. "Wind Tunnel Modeling of Density Current Interaction with Surface Obstacles"; meeting of CEC Project BA at TNO in Apeldoorn, Sept. 29-30, 1988, The Netherlands.

McFarlane, K., A. Prothero, J. S. Puttock, P. T. Roberts, and H. W. M. Witlox. 1990. *Development and Validation of Atmospheric Dispersion Models for Ideal Gases and Hydrogen Fluoride*, TNER.90,015, Shell Research Ltd., Chester, United Kingdom.

McQuaid, J., and B. Roebuck. 1985. *Large-Scale Field Trials on Dense Vapour Dispersion*, Safety Eng. Lab., Research and Lab Services Div., Broad Lane, Sheffield, England.

Meroney, R. N. 1979. "Lift-Off of Buoyant Gas Initially on the Ground. *J. Industrial Aerodynamics*, 5, pp. 1-11.

Meroney, R.N. 1982. "Turbulent Diffusion near Buildings,"*Engineering Meteorology*, Chap. 11, pp. 481-525, E.J. Plate, Ed., Elsevier Sci. Publ. Co., Amsterdam.

Nickola, P. W., J. V. Ramsdell Jr., and J. D. Ludwick. 1970. *Detailed Time Histories of Concentrations Resulting from Puff and Short-Period Releases of Inert Radioactive Gas: A Volume of Atmospheric Diffusion Data*, BNWL-1272, UC-53, BNWL, Richland, Wash.

Pleim, J., A. Venkatram, and R. Yamartino. 1984. *ADOM/TADAP Model Development Program, Vol. 4, The Dry Deposition Module*, Ontario Ministry of the Environment, Rexdale, Ontario, Canada.

Poreh, M., and J. E. Cermak. 1986. *Experimental Study of Aerosol Plume Dynamics—Wind Tunnel Study of Buoyant Horizontal Emissions*, Report CER86-87MP-JEC5, Fluid Dynamics and Diffusion Lab., Colorado State Univ., Fort Collins, CO 80523.

Post, L. 1993a. *Implementation of the HEGABOX Model for the Simulation of Gravity-Dominated Dispersion of Dense Clouds*, TNER.93.023, Thornton Research Centre, Shell Research Ltd.

Post, L. 1993b. *Implementation of the AEROPLUME Model of Atmospheric Dispersion of Pressurized Jets*, TNER.93.024, Thornton Research Centre, Shell Research Ltd.

Post, L. 1994a. Thornton Research Centre, Shell Research Ltd., private communication with The Earth Technology Corporation, Concord, Mass.

Post, L. 1994b. *Implementation of the SPILL Model for Transient Pressurized Liquid Releases*, Draft. Thornton Research Centre, Shell Research Ltd.

Post, L. 1994c. *HGSYSTEM 3.0 Technical Reference Manual*, TNER.94.059, Thornton Research Centre, Shell Research Ltd.

Post, L. 1994d. *HGSYSTEM 3.0 User's Manual*, TNER.94.058, Thornton Research Centre, Shell Research Ltd.

Puttock, J. S. et al. 1984. *Spill Tests of LNG and Refrigerated Liquid Propane on the Sea, Maplin Sands, 1980: Experimental Details of the Dispersion Tests*, TNER.84.046, Shell Research, Ltd., Thornton Research Centre, Combustion Div.

Puttock, J. S. 1987. "Comparison of Thorney Island Data with Predictions of HEGABOX/HEGADAS," *J. Haz. Materials*, **16**, pp. 439-455.

Puttock, J. S. (Ed.) 1988. "A Model for Gravity-Dominated Dispersion of Dense-Gas Clouds," *Proceedings of the Stably Stratified Flow and Dense Gas Dispersion Conference*, Clarendon Press, Oxford.

Raj, P. K., and J. A. Morris. 1987. *Source Characterization of Heavy Gas Dispersion Models for Reactive Chemicals*, AFGL-TR-88-0003, Vol. 1, Technology and Management Systems, Inc., Burlington, Maine.

Ramsdell, J. V. Jr., C. A. Simonen, and K. W. Burk. 1993. *Regional Atmospheric Transport Code for Hanford Emission Tracking (RATCHET)*, CDC Cont. No. 200-92-0503(CDC)/18620(BNW), Battelle, PNL, Richland, WA 99352.

Rodean, H. C. 1989. *Toward More Realistic Material Models for Release and Dispersion of Heavy Gases*, UCRL-53902, DE 900 12015, LLNL, Livermore, CA 94551.

Schotte, W. 1987. "Fog Formation of Hydrogen Fluoride in Air," *Ind. Eng. Chem. Res.*, **26**, pp. 300-306.

Schotte, W. 1988. "Thermodynamic Model for HF Fog Formation"; letter to C. A. Soczek, E.I. DuPont deNemours & Co., DuPont Experimental Station, Eng. Dept., Wilmington, Del.

Schulman, L. L., S. R. Hanna, and R. E. Britter. 1990. *Effects of Structures on Toxic Vapor Dispersion, Final Report*, Cont. No. F08635-90-C-397, ESL/AFESC, Tyndall Air Force Base, Fla.

Sehmel, G. A. 1984. "Deposition and Resuspension,"*Atmospheric Science and Power Production*, Chap. 12, pp. 533-583, DIE/TIC-27601, DE84005177, NTIS, USDOC, Springfield, VA 22161.

Slade, D. H. 1968. "Diffusion from Instantaneous Sources," *Meteorology and Atomic Energy, 1968*, TID-24190, pp. 163-175, USAEC.

Slawson, P. R., G. J. Hitchman, and L. E. Hawker. 1990. "The Characteristic Behavior of Finite Length Line Sources of Heat in a Crossflow," *J. Heat Transfer*, 112, pp. 349-355.

Slinn, W. G. N. 1984. "Precipitation Scavenging," *Atmospheric Science and Power Production*, Chap. 11, pp. 466-532, DOE/TIC-27601, DE84005177, NTIS, USDOC, Springfield, VA 22161.

Sykes, R.I., and W. S. Lewellen. 1992. *Review of Potential Models for UF_6 Dispersion*, K/GDP/SAR-19, Energy Systems, Oak Ridge K-25 Site, Oak Ridge, Tenn.

Varma, A.A. 1982. *Development of Models for the Analysis of Atmospheric Releases of Pressurized Uranium Hexafluoride*, ARAP Report No. 482, prepared for Union Carbide Corp., Nuclear Div., Oak Ridge, TN 37830.

Weil, J. C. 1988. "Plume Rise," *Lectures on Air Pollution Modeling*, pp. 119-166, Amer. Meteorol. Soc., Boston.

Weil, J.C. 1992. *Updating the ISC Model Through AERMIC*, 85th Annual Meeting of Air and Waste Management Assoc., Kansas City.

Williams, W. R. 1985a. *Calculational Methods for Analysis of Postulated UF_6 Releases*, ORNL/ENG/TM-31/V1, Energy Systems, ORNL, Oak Ridge, Tenn.

Williams, W. R. 1985b. *Calculational Methods for Analysis of Postulated UF_6 Releases*, ORNL/ENG/TM-31/V2, Energy Systems, Inc., ORNL, Oak Ridge, Tenn.

Williams, W. R. 1986. *Computer Programs for Developing Source Terms for a UF_6 Dispersion Model to Simulate UF_6 Releases from Buildings*, K/D-5695, Energy Systems, ORGDP, Oak Ridge, Tenn.

Wilson, D. J., and R. E. Britter. 1982. " Estimates of Building Surface Concentrations from Nearby Point Sources. *Atmos. Environ.*, 16, pp. 2631-2646.

Wilson, D. J., and B. W. Simms. 1985. *Exposure Time Effects on Concentration Fluctuations in Plumes*, Report No. 47, Dept. of Mech. Eng., Univ. of Alberta, Edmonton, Alberta, Canada.

Witlox, H.W.M. 1993a. *Thermodynamics Model for Mixing of Moist Air with Pollutant Consisting of HF, Ideal Gas and Water*, TNER.93.021, Shell Research Ltd., Thornton Research Centre, Chester, United Kingdom.

Witlox, H. W. M. 1993b. *Two-Phase Thermodynamic Model for Mixing of a Non-Reactive Multi-Component Pollutant with Moist Air*, TNER.93.022, Shell Research Ltd., Thornton Research Centre, Chester, United Kingdom.

Witlox, H. W. M. 1993c. *Technical Description of the Heavy-Gas Dispersion Program HEGADAS*, TNER.93.032, Shell Research Ltd., Thornton Research Centre, Chester, United Kingdom.

Witlox, H.W.M., K. McFarlane, F.J. Rees, and J.S. Puttock. 1990. *Development and Validation of Atmospheric Dispersion Models for Ideal Gases and Hydrogen Fluoride, Part II, HGSYSTEM Program User's Manual*, TNER.90.016, Shell Research Ltd., Thornton Research Centre, Chester, United Kingdom.

APPENDIX A

Nomenclature

A	(1) plume cross-sectional area (m^2); (2) building side area (m^2)
B	source half-width (m)
B_{eff}	effective plume (cloud) width (m)
c_p^{HFV}	specific heat of HF vapor (kj/kmole/° C)
c_p^{wv}	specific heat of water vapor (kJ/kmole/° C)
c_p^{a}	specific heat of dry air (kJ/kmole/° C)
c_{UO2F2}	specific heat of UO_2F_2 solid (kJ/kmole/° C)
C	local pollutant concentration
C_A	ground-level (peak) concentration
C_{cl}	centerline concentration
D	(1) lateral plume length scale (m); (2) molecular diffusivity (cm^2/s)
D_B	Brownian viscosity (cm^2/s)
D_p	particle diameter (μm)
$\dot{E}$	excess energy flux (J/s)
Entr	aAir entrainment rate (kg/s/m)
ET	entrainment due to ambient turbulence
EM	entrainment due to molecular motion
F	local buoyancy flux (m^4/s^3)
f_1	fugacity of HF-monomer (atm)
f_v	fraction of UF_6 which is vapor
F_1	rate of entrainment of water vapor into the plume within one integration step (kmole/s)
F_2	rate of entrainment of dry air into the plume within one integration step (kmole/s)
F_{Dp}	local particle deposition flux to the ground
F_{wet}	precipitation-induced flux of material to the ground
g	gravitational acceleration (m/s^2)
H	(1) specific enthalpy (J/kg in AEROPLUME, kJ/s in UF6THRM); (2) plume (cloud) height (m)
H_B	obstacle height (m)
$H^{\Delta HF}$	enthalpy departure of HF vapor from the ideal monomer gas at the plume temperature (kJ/kmole)
H_{atm}	ambient specific enthalpy (kJ/kmole)
H_{chem}	enthalpy flow rate associated with UF_6 chemical reactions (kJ/s)
H_{subl}	enthalpy flow rate associated with the sublimation solid UF_6 (kJ/s)
H_{poly}	enthalpy flow rate associated with the polymerization of HF (kJ/s)
H_{entr}	enthalpy flow rate associated with the entrainment of ambient air (kJ/s)
H_{HF}	enthalpy flow rate for the HF in the plume mixture (kJ/s)
H_a	enthalpy flow rate for the dry air in the plume mixture (kJ/s)
H_{UF6}	enthalpy flow rate for the UF_6 in the plume mixture (kJ/s)
H_{UO2F2}	enthalpy flow rate for the UO_2F_2 in the plume mixture (kJ/s)

H_w	enthalpy flow rate for the water vapor in the plume mixture (kJ/s)
H_{tot}	total enthalpy flow rate of the plume mixture (kJ/s)
H_{eff}	effective plume (cloud) height (m)
H_{UF6}^{s}	specific enthalpy of UF_6 solid (kJ/kmole)
H_{UF6}^{l}	specific enthalpy of UF_6 liquid (kJ/kmole)
H_{UF6}^{v}	specific enthalpy of UF_6 vapor (kJ/kmole)
I	intermittency of concentrations
K	dimensionless concentration
$K_i(T)$	equilibrium constants at temperature T for dimer (i=2), hexamer (i=6), and octamer (i=8) formation (atm^{-i+1})
$K_c(T)$	equilibrium constant at temperature T for the formation of $HF{\cdot}H_2O$ complex, (atm^{-1})
L	(1) Monin-Obukhov length (m); (2) source length (m)
l_b	buoyancy length scale (m)
L_{min}	minimum Monin-Obukhov length under stable conditions (m)
LAI	leaf area index
$\dot{m}$	total mass flow rate (kg/s)
M_{ma}	equivalent molecular weight of moist air (kg/kmole)
M_a	molar flow rate of dry air (kmole/s)
M_{HF}	molar flow rate of HF assuming all HF to be HF-monomer (kmole/s)
M_{sol}	total molar flow rate of the solid phase of the mixture (kmole/s)
M_{tot}	total molar flow rate of the plume mixture (kmole/s)
M_{UF6}	molar flow rate of UF_6 (both vapor and solid) (kmole/s)
M_{UF6}^{v}	molar flow rate of UF_6 vapor (kmole/s)
M_{UF6}^{s}	molar flow rate of UF_6 solid (kmole/s)
M_{UO2F2}	molar flow rate of UO_2F_2 solid (kmole/s)
M_{vap}	total molar flow rate of the vapor phase of the mixture (kmole/s)
M_w	molar flow rate of water (kmole/s)
M_{eff}^{mol}	effective molar flow rate of the plume
N	cloud cover in fractions
P	total pressure of the plume mixture (atm in UF6THRM, Pa in AEROPLUME)
Pr	precipitation rate (mm/hr)
P_{UF6}^{Sat}	saturation vapor pressure of UF_6 (atm)
$P_v(T)$	saturation vapor pressure of water at temperature T (atm)
P_{atm}	ambient pressure (atm)
$\dot{P}_x$	excess horizontal momentum flux (kg m/s^2)
$\dot{P}_z$	excess vertical momentum flux (kg m/s^2)
P_{wt}	partial pressure of water vapor (atm)
q	square root of the turbulent kinetic energy (m/s)
R	universal gas constant, = 0.082 (atm m^3/K/kmole); (2) plume(cloud) radius (m)
$\dot{R}$	finite reaction rate for the chemical reactions of UF_6 with water vapor (kmole/s^2)

r	the shortest distance along the surface between the source and receptor (m)
r_a	aerodynamic resistance (s/m)
r_{cut}	cuticle resistance (s/m)
r_g	resistance to transfer across nonvegetated ground or water surface (s/m)
r_s	surface or laminar layer resistance (s/m)
r_f	stomate resistance (s/m)
r_t	transfer resistance, functions of surface characteristics (s/m)
r_H	relative humidity of the ambient air (fractions; $0 \le r_H \le 1$).
$\dot{R}_{UF6}$	heat release due to the chemical reactions of UF_6 with water vapor (same as H_{chem})
$\dot{R}_{th}$	heat release/absorption due to thermodynamic effects (kJ/s)
s	distance along the plume axis (m)
Sc	Schmidt number
St	Stokes number
S_{CF}	slip correction factor for large particles
S_z	vertical dispersion parameter (m) used in HEGADAS
S_y	lateral dispersion parameter (m) used in HEGADAS
t	time (s)
T^*	reference temperature, = 25°C
T_{atm}	ambient temperature (°C)
T_F	plume mixture temperature (°F)
T_I	integral scale for the turbulent fluctuations in the concentrations (s)
T	plume mixture temperature (°C)
U	total plume velocity (m/s)
U_{amb}	ambient wind speed (m/s)
u_{eff}	effective cloud speed (m/s)
u_H	wind speed at the height of the building in the flow upwind of the building (m/s)
u_*	friction velocity (m/s)
v_d	deposition velocity (m/s)
V_e	entrainment velocity (m/s)
v_s	gravitational settling speed (m/s)
$\dot{V}$	volume flow rate (m^3/s)
W_c	canyon width (m)
X	horizontal plume displacement (m)
y	molar fraction of water vapor in the ambient air
y_α	molar fraction of species α in the vapor phase, α = a (dry air), w (H_2O), c ($HF{\cdot}H_2O$), UF_6 (UF_6), 11 (HF monomer), 12 (HF dimer), 16 (HF hexamer) or 18 (HF octamer)
Z	plume centroid height (m)
Z_d	reference height for the deposition calculations, = 10m
Z_0	surface roughness (cm)

Greek Symbols

Φ_1	fugacity coefficient of HF in the gas phase
ϕ	plume inclination angle with respect to horizontal (°)
ρ	plume density (kg/m^3)
ΔH_{UF6}^{CHEM}	heat release from UF_6 chemical reactions within one integration step (kJ/s)
Δs	integration step size along the plume centerline (m)
ΔH_e^n	vertical heat flux from the ground to the plume within the nth integration step (kJ/s)
ΔH_α	enthalpy of association for HF species α, α=2 (dimer), 6 (hexamer), 8 (octamer), c (HFH2O)
Λ	(1) turbulent macro-scale (m); (2) scavenging scale (s^{-1})
ρ_p	particle density (g/m^3)
ρ_{air}	air density (g/m^3)
μ	air viscosity (g/cm/s)
ν	(1) molecular viscosity (cm^2/s); (2) solar elevation angle
α	(1) wind-profile power-law exponent; (2) surface moisture availability
σ_y	lateral dispersion coefficient (m) for a Gaussian distribution
Γ	exposed circumference of the plume cross section (m)

Subscripts and Superscripts

atm	ambient atmosphere
n	index for integration step
n+a	state of the plume mixture after the calculations of the dispersion subprocess at the nth integration step
n+b	state of the plume mixture after the calculations of the chemical reaction subprocess at the nth integration step
n+1	state of the plume mixture after the calculations of the thermodynamic subprocess at the nth integration step, equals the plume state at the beginning of the n+1th step
v	vapor (gas) phase
s	solid phase

APPENDIX B

Old and New HGSYSTEM Predictions and Observations for Modelers Data Archive

Versions 3.0 and 1.0 of HGSYSTEM

Tabulation of the observed concentrations (ppm) and the concentrations (ppm) predicted by Versions 3.0 and 1.0 of HGSYSTEM for the Burro (BU), Coyote (CO), Desert Tortoise (DT), Goldfish (GF), Hanford (HC for continuous; HI for instantaneous), Maplin Sands (MS), Prairie Grass (PG), and Thorney Island (TC for continuous; TI for instantaneous) field experiments.

TRIAL	x(m)	z(m)	OBSERVED	HGSYSTEM v 3.0	HGSYSTEM v 1.0
BU2	57	1.0	152540	581600	514300
	140	1.0	55000	163000	112000
BU3	57	1.0	224380	603900	539100
	140	1.0	89850	156000	108000
BU4	57	1.0	177030	360700	283900
	140	1.0	71620	72200	57100
BU5	57	1.0	190410	378400	309100
	140	1.0	96000	82800	64100
BU6	57	1.0	178690	359400	286200
	140	1.0	60970	74100	58500
BU7	57	1.0	179390	537700	527300
	140	1.0	71320	219000	213000
	400	1.0	38560	59127	59000
BU8	57	1.0	558740	1000000	1000000
	140	1.0	164110	868000	865000
	400	1.0	35810	149190	151420
	800	1.0	21160	48617	50842
BU9	57	1.0	********	313000	789700
	140	1.0	105560	118070	299000
	400	1.0	39640	33785	118000
	800	1.0	13950	32675	32675
CO3	140	1.0	106820	209000	139000
	200	1.0	48620	136000	68300
	300	1.0	19050	40000	20900
CO5	140	1.0	115330	94700	75900
	200	1.0	80920	41800	32400
	300	1.0	31740	12900	10400
	400	1.0	23040	5665	4680
CO6	140	1.0	126980	363000	350000
	200	1.0	85000	230000	222000
	300	1.0	41830	154000	150000
	400	1.0	32910	118070	117000
DT1	100	1.0	63260	114490	263470
	800	1.0	10950	9205	11933
DT2	100	1.0	109580	120940	276160
	800	1.0	18590	14722	17252

Versions 3.0 and 1.0 of HGSYSTEM

Tabulation of the observed concentrations (ppm) and the concentrations (ppm) predicted by Versions 3.0 and 1.0 of HGSYSTEM for the Burro (BU), Coyote (CO), Desert Tortoise (DT), Goldfish (GF), Hanford (HC for continuous; HI for instantaneous), Maplin Sands (MS), Prairie Grass (PG), and Thorney Island (TC for continuous; TI for instantaneous) field experiments.

TRIAL	x(m)	z(m)	OBSERVED	HGSYSTEM	HGSYSTEM v 1.0
DT3	100	1.0	97250	145170	299950
	800	1.0	15630	14836	17311
DT4	100	1.0	84260	98466	243920
	800	1.0	20910	19100	22789
GF1	300	1.0	25473	18816	22263
	1000	1.0	3098	2373	2575
	3000	1.0	411	208	270
GF2	300	1.0	19396	11101	11497
	1000	1.0	2392	1342	1391
GF3	300	1.0	18596	9555	9168
	1000	1.0	2492	1031	1080
	3000	1.0	224.0	86.4	105
HC1	200	1.5	49.7	119.4	124.2
	800	1.5	3.39	11.84	12.42
HC2	200	1.5	4.90	3.71	3.57
	800	1.5	0.420	0.124	0.122
HC3	200	1.5	7.24	********	4.61
	800	1.5	0.440	********	0.157
HC4	200	1.5	14.0	12.1	11.6
	800	1.5	1.170	0.392	0.395
HC5	200	1.5	13.8	43.8	45.2
	800	1.5	1.95	4.06	4.22
HI2	200	1.5	363	********	*******
	800	1.5	38.4	********	*******
HI3	200	1.5	90.5	********	*******
	800	1.5	7.39	********	*******
HI5	200	1.5	172	********	*******
	800	1.5	6.81	********	*******
HI6	200	1.5	189	********	*******
	800	1.5	5.54	********	*******
HI7	200	1.5	173	********	*******
	800	1.5	2.00	********	*******
HI8	200	1.5	153	********	*******
	800	1.5	9.47	********	*******

Versions 3.0 and 1.0 of HGSYSTEM (continued)

Tabulation of the observed concentrations (ppm) and the concentrations (ppm) predicted by Versions 3.0 and 1.0 of HGSYSTEM for the Burro (BU), Coyote (CO), Desert Tortoise (DT), Goldfish (GF), Hanford (HC for continuous; HI for instantaneous), Maplin Sands (MS), Prairie Grass (PG), and Thorney Island (TC for continuous; TI for instantaneous) field experiments.

TRIAL	x(m)	z(m)	OBSERVED	HGSYSTEM	HGSYSTEM v 1.0
MS27	89	0.9	123100	140300	135100
	131	0.9	94900	97600	94740
	324	0.9	35600	23786	23880
	400	0.9	29100	14183	14100
	650	0.9	5700	4414	4365
MS29	58	0.9	141500	227600	218000
	90	0.9	114300	123000	118000
	130	0.9	61900	81100	77700
	182	0.9	54300	50680	49340
	252	0.9	20400	31120	31020
	324	0.9	16500	20043	20020
	403	0.9	13500	13067	13020
MS34	87	0.9	118100	110800	104150
	179	0.9	45500	34670	33140
MS35	129	0.9	77400	73450	70180
	250	0.9	30700	24000	23900
	406	0.9	22800	9784	9724
MS42	28	0.9	113200	665600	662000
	53	0.9	110900	328000	323300
	83	0.9	66700	167900	165900
	123	0.9	41500	97970	97150
	179	0.9	21700	60740	60640
	247	0.9	21800	40730	40730
	398	0.9	10500	22370	22340
MS43	88	0.9	56500	114400	113400
	129	0.9	35100	72120	72100
	249	0.9	18900	31340	31340
	400	0.9	7500	12303	12200
MS46	34	0.9	97600	339200	335000
	91	0.9	57200	117700	116700
	130	0.9	37600	78800	78900
	182	0.9	26100	46100	46020
	250	0.9	18500	25300	25300
	322	0.9	16700	15200	15220
	401	0.9	7200	9684	9611
MS47	90	0.9	80900	150000	148000
	128	0.9	40200	97920	97240
	182	0.9	31300	64200	64300
	250	0.9	15500	44100	44200
	321	0.9	14400	31639	31630
	400	0.9	9500	21043	21000

Versions 3.0 and 1.0 of HGSYSTEM (continued)

Tabulation of the observed concentrations (ppm) and the concentrations (ppm) predicted by Versions 3.0 and 1.0 of HGSYSTEM for the Burro (BU), Coyote (CO), Desert Tortoise (DT), Goldfish (GF), Hanford (HC for continuous; HI for instantaneous), Maplin Sands (MS), Prairie Grass (PG), and Thorney Island (TC for continuous; TI for instantaneous) field experiments.

TRIAL	x(m)	z(m)	OBSERVED	HGSYSTEM	HGSYSTEM v 1.0
MS49	90	0.9	72100	104000	103000
	129	0.9	46700	67570	67160
	180	0.9	43500	45300	45300
	250	0.9	25000	29100	29100
	322	0.9	14800	18057	18080
	400	0.9	7600	11777	11700
MS50	59	0.9	103300	227100	225000
	93	0.9	57100	136200	135200
	182	0.9	30800	63520	63620
	400	0.9	11900	15530	15600
MS52	61	0.9	56300	257500	255600
	95	0.9	33800	151500	151500
	178	0.9	26000	73200	73380
	249	0.9	11200	49350	49540
	398	0.9	11800	21800	21720
	650	0.9	7500	8023	7920
MS54	56	0.5	226900	296000	293600
	85	0.5	120000	157000	156000
	178	0.5	53400	58360	58460
	247	0.5	49500	38700	38700
PG7	50	1.5	36.3	35.0	97.3
	100	1.5	8.50	25.02	16.83
	200	1.5	1.60	4.88	2.76
	400	1.5	0.300	1.163	0.438
	800	1.5	0.0300	0.2731	0.0695
PG8	50	1.5	154.9	61.6	171
	100	1.5	41.8	44.6	33.6
	200	1.5	9.30	8.91	6.13
	400	1.5	1.50	2.20	1.05
	800	1.5	0.260	0.580	0.174
PG9	50	1.5	71.7	66.5	117.9
	100	1.5	20.3	24.2	23.4
	200	1.5	5.00	5.76	4.30
	400	1.5	1.00	1.51	0.739
	800	1.5	0.190	0.406	0.123
PG10	50	1.5	66.2	34.9	89.8
	100	1.5	15.8	22.2	15.6
	200	1.5	4.10	4.43	2.57
	400	1.5	1.00	1.07	0.408
	800	1.5	0.0600	0.2518	0.0646
PG13	400	1.5	46.7	62.7	73.5
	800	1.5	37.1	21.1	23.9

Tabulation of the observed concentrations (ppm) and the concentrations (ppm) predicted by Versions 3.0 and 1.0 of HGSYSTEM for the Burro (BU), Coyote (CO), Desert Tortoise (DT), Goldfish (GF), Hanford (HC for continuous; HI for instantaneous), Maplin Sands (MS), Prairie Grass (PG), and Thorney Island (TC for continuous; TI for instantaneous) field experiments.

TRIAL	x(m)	z(m)	OBSERVED	HGSYSTEM	HGSYSTEM v 1.0
PG15	50	1.5	147	214	71.1
	100	1.5	38.8	19.9	11.5
	200	1.5	7.80	2.43	1.80
	400	1.5	1.700	0.341	0.278
	800	1.5	0.2000	0.0562	0.0433
PG16	50	1.5	67.4	248.7	76.0
	100	1.5	12.7	21.9	12.2
	200	1.5	2.30	2.59	1.90
	400	1.5	0.200	0.349	0.294
	800	1.5	0.0200	0.0628	0.0458
PG17	50	1.5	235	156	324
	100	1.5	98.2	78.7	78.6
	200	1.5	30.8	19.0	19.2
	400	1.5	9.50	5.09	4.78
	800	1.5	3.48	1.44	1.22
PG18	50	1.5	231	223	543
	100	1.5	94.8	120.1	154.9
	200	1.5	35.1	30.7	45.7
	400	1.5	11.70	8.21	13.9
	800	1.5	5.17	2.19	4.37
PG19	50	1.5	78.4	78.2	157.9
	100	1.5	19.7	33.3	31.2
	200	1.5	4.70	7.68	5.70
	400	1.5	0.700	1.996	0.977
	800	1.5	0.130	0.536	0.162
PG20	50	1.5	61.9	153.9	207.9
	100	1.5	19.1	51.4	52.0
	200	1.5	5.60	13.44	13.04
	400	1.5	1.20	3.64	3.29
	800	1.5	0.280	1.025	0.841
PG21	50	1.5	104	118	146
	100	1.5	36.2	37.6	36.4
	200	1.5	10.80	9.53	9.12
	400	1.5	3.30	2.58	2.30
	800	1.5	1.170	0.724	0.588
PG22	50	1.5	85.2	100.1	131.2
	100	1.5	30.8	30.0	32.7
	200	1.5	10.10	7.80	8.20
	400	1.5	3.20	2.12	2.07
	800	1.5	0.910	0.596	0.529
PG23	50	1.5	63.4	97.6	118.9
	100	1.5	22.0	29.1	29.6
	200	1.5	6.90	7.54	7.42
	400	1.5	2.20	2.04	1.87
	800	1.5	0.740	0.575	0.478

Versions 3.0 and 1.0 of HGSYSTEM (continued)

Tabulation of the observed concentrations (ppm) and the concentrations (ppm) predicted by Versions 3.0 and 1.0 of HGSYSTEM for the Burro (BU), Coyote (CO), Desert Tortoise (DT), Goldfish (GF), Hanford (HC for continuous; HI for instantaneous), Maplin Sands (MS), Prairie Grass (PG), and Thorney Island (TC for continuous; TI for instantaneous) field experiments.

TRIAL	x(m)	z(m)	OBSERVED	HGSYSTEM	HGSYSTEM v 1.0
PG24	50	1.5	56.1	89.9	113.2
	100	1.5	18.2	26.6	28.3
	200	1.5	6.00	6.91	7.08
	400	1.5	2.00	1.87	1.78
	800	1.5	0.680	0.526	0.457
PG25	50	1.5	109	390	97.1
	100	1.5	14.7	29.5	15.3
	200	1.5	2.30	3.32	2.37
	400	1.5	0.500	0.422	0.364
	800	1.5	0.0800	0.0499	0.0567
PG28	50	1.5	184	634	548
	100	1.5	73.0	157.4	154.0
	200	1.5	22.0	43.8	45.0
	400	1.5	7.90	12.91	13.63
	800	1.5	3.19	4.02	4.28
PG29	50	1.5	86.6	145.4	216.2
	100	1.5	32.8	49.2	52.9
	200	1.5	10.2	13.0	13.1
	400	1.5	3.40	3.54	3.26
	800	1.5	0.960	0.994	0.831
PG32	200	1.5	100.1	95.9	107
	400	1.5	42.1	30.6	33.8
	800	1.5	20.59	9.96	11.0
PG33	50	1.5	75.3	144.7	193.6
	100	1.5	23.1	48.0	48.4
	200	1.5	6.90	12.34	12.14
	400	1.5	1.40	3.37	3.06
	800	1.5	0.270	0.950	0.784
PG34	50	1.5	72.8	140.3	189.9
	100	1.5	24.9	46.4	47.4
	200	1.5	6.90	11.93	11.88
	400	1.5	1.80	3.25	2.99
	800	1.5	0.460	0.915	0.766
PG36	50	1.5	299	845	1296
	100	1.5	195	328	390
	200	1.5	72.4	104.3	119.8
	400	1.5	22.8	33.6	37.7
	800	1.5	13.9	11.1	12.2
PG37	50	1.5	83.5	119.1	151.7
	100	1.5	29.1	38.0	37.6
	200	1.5	8.40	9.66	9.38
	400	1.5	2.70	2.62	2.36
	800	1.5	0.770	0.735	0.603

Versions 3.0 and 1.0 of HGSYSTEM (continued)

Tabulation of the observed concentrations (ppm) and the concentrations (ppm) predicted by Versions 3.0 and 1.0 of HGSYSTEM for the Burro (BU), Coyote (CO), Desert Tortoise (DT), Goldfish (GF), Hanford (HC for continuous; HI for instantaneous), Maplin Sands (MS), Prairie Grass (PG), and Thorney Island (TC for continuous; TI for instantaneous) field experiments.

TRIAL	x(m)	z(m)	OBSERVED	HGSYSTEM	HGSYSTEM v 1.0
PG38	50	1.5	133	137	195
	100	1.5	57.0	45.3	48.1
	200	1.5	19.0	11.7	11.9
	400	1.5	6.90	3.19	2.99
	800	1.5	2.380	0.901	0.764
PG41	50	1.5	164	220	321
	100	1.5	69.0	73.9	92.2
	200	1.5	24.5	19.1	27.3
	400	1.5	8.90	5.06	8.33
	800	1.5	3.58	1.34	2.62
PG42	50	1.5	100	130	168
	100	1.5	36.8	42.0	41.7
	200	1.5	11.5	10.7	10.4
	400	1.5	2.90	2.91	2.63
	800	1.5	0.780	0.819	0.672
PG43	50	1.5	89.4	60.6	183.8
	100	1.5	20.7	46.6	36.1
	200	1.5	5.80	9.22	6.57
	400	1.5	0.900	2.279	1.124
	800	1.5	0.190	0.597	0.186
PG44	50	1.5	69.0	80.8	163.7
	100	1.5	18.2	36.2	32.3
	200	1.5	5.20	8.22	5.90
	400	1.5	1.10	2.12	1.01
	800	1.5	0.210	0.568	0.168
PG45	50	1.5	132	186	300
	100	1.5	41.5	72.6	74.5
	200	1.5	14.4	18.5	18.6
	400	1.5	3.10	5.04	4.67
	800	1.5	1.02	1.42	1.19
PG46	50	1.5	203	201	351
	100	1.5	72.2	85.7	86.6
	200	1.5	21.9	21.6	21.5
	400	1.5	7.50	5.91	5.39
	800	1.5	2.28	1.67	1.38
PG48	50	1.5	80.7	156.1	220.1
	100	1.5	23.6	54.9	55.0
	200	1.5	6.10	13.86	13.78
	400	1.5	1.70	3.76	3.47
	800	1.5	0.470	1.058	0.888
PG49	50	1.5	77.1	74.8	142.2
	100	1.5	24.1	29.5	28.1
	200	1.5	6.70	6.91	5.16
	400	1.5	1.20	1.81	0.885
	800	1.5	0.210	0.485	0.147

Versions 3.0 and 1.0 of HGSYSTEM (continued)

Tabulation of the observed concentrations (ppm) and the concentrations (ppm) predicted by Versions 3.0 and 1.0 of HGSYSTEM for the Burro (BU), Coyote (CO), Desert Tortoise (DT), Goldfish (GF), Hanford (HC for continuous; HI for instantaneous), Maplin Sands (MS), Prairie Grass (PG), and Thorney Island (TC for continuous; TI for instantaneous) field experiments.

TRIAL	x(m)	z(m)	OBSERVED	HGSYSTEM	HGSYSTEM v 1.0
PG50	50	1.5	87.0	73.7	139.8
	100	1.5	27.9	28.8	27.7
	200	1.5	6.60	6.77	5.08
	400	1.5	1.40	1.77	0.872
	800	1.5	0.210	0.475	0.145
PG51	50	1.5	100	184	301
	100	1.5	26.3	71.9	74.7
	200	1.5	6.70	18.26	18.64
	400	1.5	1.10	4.99	4.68
	800	1.5	0.160	1.414	1.196
PG53	50	1.5	339	916	1067
	100	1.5	192	299	326
	200	1.5	83.1	92.1	101.1
	400	1.5	30.4	29.1	31.9
	800	1.5	12.19	9.41	10.3
PG54	50	1.5	155	136	190
	100	1.5	61.4	44.9	46.8
	200	1.5	22.3	11.5	11.6
	400	1.5	8.10	3.14	2.91
	800	1.5	3.450	0.888	0.743
PG55	50	1.5	77.3	112.5	141.9
	100	1.5	30.3	35.5	35.3
	200	1.5	9.70	8.98	8.82
	400	1.5	2.80	2.43	2.22
	800	1.5	1.010	0.680	0.568
PG56	50	1.5	113	135	184
	100	1.5	39.9	44.3	45.3
	200	1.5	13.2	11.4	11.3
	400	1.5	4.60	3.10	2.83
	800	1.5	1.700	0.876	0.723
PG57	50	1.5	102	180	273
	100	1.5	29.2	66.0	68.0
	200	1.5	10.4	17.0	17.0
	400	1.5	3.10	4.64	4.27
	800	1.5	0.790	1.310	1.092
PG58	200	1.5	111	108	124
	400	1.5	49.9	34.7	38.9
	800	1.5	20.7	11.4	12.6
PG59	50	1.5	267	861	932
	100	1.5	193	264	285
	200	1.5	84.5	81.2	88.4
	400	1.5	35.7	25.5	27.9
	800	1.5	13.79	8.24	9.02

Tabulation of the observed concentrations (ppm) and the concentrations (ppm) predicted by Versions 3.0 and 1.0 of HGSYSTEM for the Burro (BU), Coyote (CO), Desert Tortoise (DT), Goldfish (GF), Hanford (HC for continuous; HI for instantaneous), Maplin Sands (MS), Prairie Grass (PG), and Thorney Island (TC for continuous; TI for instantaneous) field experiments.

TRIAL	x(m)	z(m)	OBSERVED	HGSYSTEM	HGSYSTEM v 1.0
PG60	50	1.5	110	112	138
	100	1.5	42.5	33.7	34.2
	200	1.5	15.50	8.78	8.53
	400	1.5	5.30	2.39	2.15
	800	1.5	2.160	0.673	0.549
PG61	50	1.5	70.3	159.6	226.3
	100	1.5	20.1	56.5	56.5
	200	1.5	6.00	14.28	14.16
	400	1.5	1.50	3.88	3.57
	800	1.5	0.340	1.098	0.913
PG62	100	1.5	40.9	47.6	35.5
	200	1.5	11.50	9.43	6.46
	400	1.5	2.80	2.32	1.11
	800	1.5	0.720	0.610	0.183
TC45	40	0.4	200000	263700	263700
	53	0.4	129000	147330	147330
	72	0.4	89000	75734	75834
	90	0.4	62000	50443	50543
	112	0.4	37900	35640	35740
	158	0.4	26200	21476	21576
	250	0.4	7600	11587	11687
	335	0.4	5000	7911	7996
	472	0.4	3600	5127	5197
TC47	50	0.4	159000	462530	461530
	90	0.4	74000	92378	92478
	212	0.4	14700	17034	17131
	250	0.4	6700	12944	13039
	335	0.4	4800	8040	8135
	472	0.4	2400	4570	4644
TI6	71	0.4	90400	105480	*******
	141	0.4	36700	39348	*******
	180	0.4	26200	25975	*******
	283	0.4	9760	10884	*******
	424	0.4	5290	3995	*******
TI7	71	0.4	132000	101340	*******
	100	0.4	59200	64183	*******
	150	0.4	33800	35942	*******
	180	0.4	25400	26980	*******
	224	0.4	19800	18579	*******
	361	0.4	11900	7316	*******
	500	0.4	6020	3292	*******
TI8	71	0.4	92500	104090	*******
	100	0.4	61100	66362	*******
	150	0.4	40300	37722	*******
	200	0.4	28100	24110	*******
	364	0.4	10800	7864	*******
	412	0.4	6920	5576	*******
	510	0.4	4260	3276	*******

Versions 3.0 and 1.0 of HGSYSTEM (continued)

Tabulation of the observed concentrations (ppm) and the concentrations (ppm) predicted by Versions 3.0 and 1.0 of HGSYSTEM for the Burro (BU), Coyote (CO), Desert Tortoise (DT), Goldfish (GF), Hanford (HC for continuous; HI for instantaneous), Maplin Sands (MS), Prairie Grass (PG), and Thorney Island (TC for continuous; TI for instantaneous) field experiments.

TRIAL	x(m)	z(m)	OBSERVED	HGSYSTEM	HGSYSTEM v 1.0
TI9	71	0.4	123000	85853	*******
	100	0.4	70600	52830	*******
	141	0.4	35800	32464	*******
	180	0.4	26500	22787	*******
	224	0.4	20700	16400	*******
	316	0.4	11400	9200	*******
	503	0.4	5450	3700	*******
TI12	71	0.4	116000	87535	*******
	150	0.4	31700	30071	*******
	200	0.4	18500	19089	*******
	361	0.4	9990	6139	*******
	500	0.4	3680	2488	*******
TI13	71	0.4	73300	131030	*******
	100	0.4	64600	86768	*******
	224	0.4	25400	21971	*******
	316	0.4	12500	13924	*******
	361	0.4	9260	10599	*******
	412	0.4	7290	9407	*******
TI17	40	0.4	127000	206520	*******
	50	0.4	85100	149680	*******
	71	0.4	47600	92751	*******
	100	0.4	31900	58262	*******
	141	0.4	14900	35480	*******
	224	0.4	6520	16208	*******
	500	0.4	3330	2425	*******
TI18	40	0.4	242000	262180	*******
	60	0.4	86100	167500	*******
	70	0.4	62700	141020	*******
	80	0.4	52500	121080	*******
	100	0.4	40800	92645	*******
	200	0.4	16100	24627	*******
	224	0.4	11000	24393	*******
	300	0.4	8060	14783	*******
	400	0.4	4870	7474	*******
	510	0.4	3490	5083	*******
TI19	40	0.4	184000	244060	*******
	60	0.4	82400	149070	*******
	71	0.4	72200	121850	*******
	100	0.4	53900	80881	*******
	224	0.4	13600	16874	*******
	361	0.4	6770	10051	*******
	583	0.4	2990	5197	*******

APPENDIX C

Addendum to the HGSYSTEM User's Manual So That UF_6 Modules Can Be Applied

Addendum to the HGSYSTEM User's Manual so that UF_6 Modules can be Applied

The current User's Manual for HGSYSTEM, prepared by Post (1994a) of Shell's Thornton Research Centre, does not include any information concerning how to apply the three UF_6 modules - AEROPLUME/UF_6, HEGADAS/UF_6, and HEGABOX/UF_6. The software distributed by Shell does contain these modules, but no written guidance is given by Shell for their use.

The purpose of this addendum is to provide sufficient information for a person to apply the three UF_6 modules. It is assumed that the reader has the HGSYSTEM User's Manual (Post, 1994a) and is able to refer back-and-forth from that document to this document. To aid in this process, the section numbers below correspond to the section numbers in the HGSYSTEM User's Manual (i.e., Section 10 describes AEROPLUME, section 12 describes HEGABOX, and Section 13 describes HEGADAS).

10.A. Addendum to the User's Manual for AEROPLUME/UF_6

Refer to Section 10 of the HGSYSTEM User's Manual by Post (1994a).

10.A.1 Input

The main input data file (the API file) for the UF_6 version of AEROPLUME (AEROPLUME/UF_6) is similar to that for the original model. The reader is referred to the User's Manual (Post, 1994a) for the original AEROPLUME for detailed descriptions of the input parameters included in the API file. Some deviations from the original API file are required, however, in order to run AEROPLUME/UF_6. The deviations are mainly related to the parameters in the GASDATA data block where the properties of the pollutant are defined. In the following, deviations from the original API file and the additional required information for AEROPLUME/UF_6 are discussed:

MWGAS: This parameter always refers to the molecular weight for UF_6, regardless of the composition of the mixture.

CPGAS: The value of the parameter, although mandatory for AEROPLUME, is not used for UF_6 releases.

SPECIES: This parameter does not apply to AEROPLUME/UF_6, since the physical properties for all species participating in the UF_6 chemical reactions have been "hard-wired" in the code.

WATERPOL: This parameter does not apply to AEROPLUME/UF_6.

CDG: This parameter does not apply to AEROPLUME/UF_6.

CDL: This parameter does not apply to AEROPLUME/UF_6.

CPOLST: This parameter refers to the plume-averaged mass concentration (kg/m^3) for UF_6 at the termination of an AEROPLUME/UF_6 run.

VPOLST: This parameter refers to the plume-averaged mass fraction (%) for UF_6 at the termination of an AEROPLUME/UF_6 run.

VCMIN: This parameter does not apply to AEROPLUME/UF_6.

VCMAX: This parameter does not apply to AEROPLUME/UF_6.

When running AEROPLUME/UF_6, the user must specify either the RESERVOIR or the RELEASE data block in the API file. If the RESERVOIR data block is specified, it is assumed that the release is pure liquid UF_6. The AEROPLUME/UF_6 code then calculates the partitioning of the vapor and solid phases of UF_6 upon flashing. The pollutant temperature at the point of flashing is assumed to be the sublimation point of UF_6, 56.56°C. (This temperature is different from the storage temperature specified in the API file.)

If the RELEASE data block is specified in the API file, the release can be any of combination of UF_6 (vapor and solid, but not liquid), UO_2F_2, HF, water vapor, and air, whose corresponding mass fractions are specified in the FRC file (i.e., a file whose file name is the same as the run name, and whose extension is FRC). The FRC file is read with free-format. There must be one entry per line. The mass fractions for total UF_6, UO_2F_2, HF, water vapor, and air must add up to one. The format of the FRC file is specified below:

Line No.	Real/ Integer	Remarks
1	R	Mass fraction of air
2	R	Mass fraction of HF
3	R	Mass fraction of UF_6 gas
4	R	Mass fraction of total UF_6
5	R	Mass fraction of UO_2F_2
6	R	Mass fraction of water vapor

Note that when the RELEASE data block is used in the API file, the release temperature specified in the API file should be as close as possible to the equilibrium temperature corresponding to the mixture composition specified in the FRC file. Otherwise, the thermodynamics routines may have difficulties finding a convergent solution.

As an option, when running AEROPLUME/UF_6, the user can also specify for the SPRINT solver package the values of (1) SSTEP, the external integration step size; (2) RWORK(6), the

maximum internal integration step size; (3) RWORK(7), the minimum internal integration step size; (4) RTOL, the relative error tolerance for each of the 14 governing equations; and (5) ATOL, the absolute error tolerance for each of the 14 governing equations, via an STP input file (i.e., a file whose file name is the same as the run name, and whose extension is STP). If the STP file does not already exist, AEROPLUME/UF_6 uses the existing default values in the code for the above control parameters. These default values have been set to what we believe are their optimal values after making a large number of sensitivity runs. It is strongly recommended that the option of specifying the control parameters via the STP file only be used by expert users who are familiar with SPRINT and AEROPLUME. The main purpose of this implementation is to avoid the need to re-compile the code for special, troublesome cases when the default values do not lead to a successful completion of an AEROPLUME/UF_6 run.

10.A.2 Output

The main output data file (the APR file) for AEROPLUME/UF_6 is similar to that for the original AEROPLUME model, but includes the following additional information: (1) mass fractions (%) for total UF_6, UO_2F_2, HF, water vapor, and air; (2) mass concentrations (mg/m^3) for uranium and fluorine; (3) the fraction of UF_6 that is in the vapor phase, and (4) the Briggs plume lift-off parameter (see Section 6.2 of Hanna et al., 1995). Note that because the AEROPLUME model assumes a top-hat (uniform) concentration profile, all concentrations refer to plume-averages.

10.A.3 Guidance for Use

The AEROPLUME/UF_6 model is used to simulate pressurized jet releases of UF_6. The model should not be applied to the following scenarios:

(1) an unpressurized release, or when the jet exit velocity is small compared to the ambient wind speed (e.g., an ambient wind speed of 5.0 m/s and a exit velocity of 2.5 m/s),

(2) a very large orifice size (e.g., diameter > 1.0 m) where a "jet" configuration is not clearly defined,

(3) a high-speed, downward-pointing jet that hits the ground with a steep angle (e.g., > 30° from the horizontal), and

(4) a very low release height (e.g., elevation lower than 0.3 m) where the initial momentum effects associated with the jet are quickly destroyed after the impact with the ground.

Before AEROPLUME/UF_6 performs any dispersion calculations, it will verify whether the jet speed is lower than the ambient wind speed. If so, the program will pause and issue a message warning the user that the source configuration may violate the model assumptions. The user then decides whether to abort or to carry on the calculations.

AEROPLUME is frequently used to predict concentrations near the source. The model then makes a transition to a module such as HEGADAS or PGPLUME to perform calculations of concentrations farther downwind. The interface between AEROPLUME and HEGADAS is established through the HSL file generated by AEROPLUME. The interface between AEROPLUME and PGPLUME is established through the PGL file generated by AEROPLUME. For UF_6 releases, the interface between AEROPLUME/UF_6 and HEGADAS/UF_6 requires another LNK file (i.e., a file whose file name is the same as the run name, and whose extension is LNK) generated by AEROPLUME/UF_6. The LNK file contains parameters that are used to ensure the continuity of the UF_6 thermodynamic and chemistry calculations between the two modules. The LNK file is not used by PGPLUME since that module does not treat thermodynamics and chemistry.

The MATCH data block in AEROPLUME contains parameters that govern the timing of the transition from AEROPLUME to either HEGADAS or PGPLUME. These parameters include: RULST (a function of the excess velocity ratio), RELST (a function of the entrainment ratio), RGLST (a function of the buoyancy effect for advection), RNLST (a function of the buoyancy effect for passive diffusion), and RALST (a function of the plume aspect ratio). The parameters are used for various transition criteria. A transition is made only when all transition criteria are met. The reader is referred to the Technical Reference Manual of HGSYSTEM (Post, 1994b) for more detailed discussions. The user normally does not need to change the values of the above five parameters. However, if the user decides to speed the transition of AEROPLUME to either HEGADAS or PGPLUME, he can accomplish this by increasing the values for RULST, RELST, RGLST and RNLST, and by decreasing the value for RALST. Conversely, the transition can be delayed by decreasing the values for RULST, RELST, RGLST and RNLST, and by increasing the value of RALST. It is strongly suggested that the values for the above five parameters not be changed. Any changes should be made only by experienced users.

In the original AEROPLUME code, if the termination criteria for AEROPLUME are met prior to the satisfaction of the transition criteria, the module will halt its execution without generating the HSL link file for HEGADAS, or the PGL link file for PGPLUME. In order to increase the flexibility of the AEROPLUME/UF_6 model, the procedure is modified so that when the termination criteria are

met prior to the transition criteria, the PGL or HSL file will nonetheless still be generated (depending on whether or not the plume is close to the neutral limit). However, we recommend that the information contained in the link file only be used with extreme caution, since the information is derived from a premature AEROPLUME/UF_6 transition to a far-field module.

In the PGL interface file generated by AEROPLUME/UF_6 for PGPLUME, CMASS (pollutant mass concentration in kg/m^3 at the transitional plane) and MMPOL (pollutant molecular weight in kg/kmole) for UF_6, UO_2F_2, HF, uranium, and fluorine are all included. However, only the entries for UF_6 are "activated", and the entries for other species are all commented out (by asterisks). This procedure is followed because PGPLUME is a passive dispersion program with no thermodynamic and chemistry calculations. It can treat only one pollutant at a time. AEROPLUME/UF_6, HEGADAS/UF_6 and HEGABOX/UF_6, on the other hand, can keep track of UF_6, UO_2F_2, HF, uranium, and fluorine simultaneously. Therefore, if the user needs to estimate the far-field concentrations for multiple species, PGPLUME has to be run multiple times, each time with the entries for CMASS and MMPOL for the species of interest activated.

As a user option, AEROPLUME/UF_6 can treat the possible lift-off of a ground-hovering plume (see Section 6.2 of Hanna et al., 1995). As a first-order approximation, when the plume lift-off criterion is met, the plume regime will change from either "touchdown", where a circular segment plume geometry is assumed, or "slumped", where a half-elliptic plume geometry is assumed, to "airborne", where a circular plume geometry is assumed. Because the change of the plume regime is instantaneous, in order to conserve mass, a discontinuity in the plume lateral length scale, D, might occur. Furthermore, although the plume regime after lift-off is "airborne", it is possible that the combination of the plume centroid height and the plume diameter implies that the plume is still intersecting the ground. In this case, the entrainment rate calculated internally by the module is scaled by the ratio of the exposed plume circumference to the total plume circumference.

If the user decides not to use the meteorological processor described in Section 6.3 of Hanna et al. (1995), it is important that the Pasquill-Gifford stability class and the ambient wind speed, both specified in the API file, should be consistent. For example, a high ambient wind speed (> 5.0 m/s) indicates neutral conditions. If the user decides to use the meteorological processor, then the value of the stability class specified in the API file will not be used, and will be replaced by a value internally calculated by the code.

The AEROPLUME/UF_6 code is reasonably robust. However, the module does occasionally encounter numerical difficulties. When this occurs, the user can slightly alter the ambient conditions (e.g., changing stability class from "F" to "E", or increasing the ambient wind speed by 0.1 m/s), or the source conditions (e.g., increasing the source elevation by 0.1 m). These techniques usually

overcome the numerical difficulties. Another remedy is to specify customized stepping control parameters for the SPRINT solve package via the STP file, as mentioned previously. For example, the user can decrease the external step size, and relax the error tolerance in order for SPRINT to find convergent solutions. However, the execution time may be increased and the accuracy of the results may be decreased as a result. Consequently, we strongly suggest that this method only be used by expert users who have an in-depth understanding of SPRINT and AEROPLUME.

12.A Addendum to the User's Manual for HEGABOX/UF_6

Refer to Section 12 of the HGSYSTEM User's Manual by Post (1994a).

12.A.1 Input

The main input data file (the HBI file) for the UF_6 version of HEGABOX (HEGABOX/UF_6) is similar to that for the original model. The reader is referred to the User's Manual (Post, 1994a) for the original HEGABOX code for detailed descriptions of the input parameters included in the HBI file. Some deviations from the original HBI file are required in order to run HEGABOX/UF_6. These deviations are primarily related to the parameters in the GASDATA data block where the properties of the pollutant are defined. In the following, deviations from the original HBI file and the additional required information for HEGABOX/UF_6 are discussed:

WATERPOL: This parameter does not apply to HEGABOX/UF_6.

EXGASPOL: This parameter does not apply to HEGABOX/UF_6.

WPICKUP: This parameter does not apply to HEGABOX/UF_6.

INICONC: This parameter does not apply to HEGABOX/UF_6.

MWGAS: This parameter always refers to the molecular weight for UF_6, regardless of the composition of the mixture.

CPGAS: The value of this parameter, although mandatory for HEGABOX, is not used for UF_6 releases.

SPECIES: This parameter does not apply to HEGABOX/UF_6, since the physical properties for all species participating in the UF_6 chemical reactions have been "hard-wired" in the code.

When running HEGABOX/UF_6, the user will be prompted to indicate whether the release is (1) a pure liquid UF_6 release, or (2) a mixture of any combination of UF_6 (vapor and solid, but not

liquid), UO_2F_2, HF, water vapor, and air. For release scenario (1), the HEGABOX/UF_6 code calculates the partitioning of the vapor and solid phases of UF_6 upon flashing. The pollutant temperature at the point of flashing is assumed to be the sublimation point of UF_6, 56.56°C (this temperature is different from the initial pollutant storage temperature specified in the HBI file). For release scenario (2), the user must provide the FRC file (see the AEROPLUME/UF_6 section for a description of the FRC file) where the initial composition of the mixture is specified. In this case, it is important that the initial pollutant temperature specified in the HBI file should be as close as possible to the equilibrium temperature corresponding to the mixture composition specified in the FRC file. Otherwise, the thermodynamics routines may have difficulties finding a convergent solution.

12.A.2 Output

The main output data file (the HBR file) for HEGABOX/UF_6 is similar to that for the original HEGABOX model, but includes the following additional information: (1) mass fractions (%) for total UF_6, UO_2F_2, HF, water vapor, and air; (2) mass concentrations (mg/m^3) for uranium and fluorine; and (3) the fraction of UF_6 that is in the vapor phase. Note that all concentrations predicted by HEGABOX refer to cloud-averages.

12.A.3 Guidance for Use

HEGABOX/UF_6 is designed to simulate the initial spreading of an initially stagnant, dense cloud of a cylindrical shape. The release is assumed to be instantaneous. Therefore, it is important to ensure that the source scenario of interest conforms to the configuration assumed by HEGABOX.

HEGABOX is frequently used near the source to describe the initial phase of an instantaneous release. The module then makes a transition to the HEGADAS-T module to calculate concentrations farther downwind. The interface between HEGABOX and HEGADAS-T is established through the HTL and HBO files generated by HEGABOX. For UF_6 releases, the interface between HEGABOX/UF_6 and HEGADAS-T/UF_6 requires another LNK file (i.e., a file whose file name is the same as the run name, and whose extension is LNK) generated by HEGABOX/UF_6. The LNK file contains parameters that are used to ensure the continuity of the UF_6 thermodynamic and chemistry calculations between the two modules.

If the user decides not to use the meteorological processor described in Section 6.3 of Hanna et al. (1995), it is important that the Pasquill-Gifford stability class and the ambient wind speed, both specified in the HBI file, should be consistent. For example, a high ambient wind speed (> 5.0 m/s) indicates neutral conditions. If the user decides to use the meteorological processor, then the value of the stability class specified in the HBI file will not be used, and will be replaced by a value internally calculated by the code.

The HEGABOX/UF_6 code is robust. Our tests have not revealed any cases where the code encounters numerical difficulties. In order to properly account for the fast UF_6 chemical reactions, it is recommended that the parameter DTMAX (maximum time step for numerical integration) be kept small (e.g., ≤ 0.25 second). Consequently, the values of the parameters ARSIZE and ARST10 specified in the include file ARSIZE.INC must be large enough to hold program results. The values of ARSIZE and ARST10 for the original HEGABOX code were 200 and 2000, respectively. It is recommended that the values be increased to 8000 and 80000 for HEGABOX/UF_6. As a result, the program must be compiled using 32-bit FORTRAN compilers where the DOS 640 KB limit of the program size does not apply.

13.A. Addendum to the User's Manual for HEGADAS/UF_6

Refer to Section 13 of the HGSYSTEM User's Manual by Post (1994a).

The HEGADAS module has a steady-state version called HEGADAS-S, and a transient version called HEGADAS-T. In the following, the term "HEGADAS" refers to both the HEGADAS-S and HEGADAS-T models. The terms "HEGADAS-S" and "HEGADAS-T" are used when the description specifically applies to the steady-state or the transient version of HEGADAS, respectively.

13.A.1 Input

The main input data files (the HSI file for HEGADAS-S and the HTI file for HEGADAS-T) for the UF_6 version of HEGADAS (HEGADAS/UF_6) are similar to that for the original model. The reader is referred to the original HEGADAS User's Manual (Post, 1994a) for detailed descriptions of the input parameters included in the HSI and HTI files. Some deviations from the original HSI and HTI files are required in order to run HEGADAS/UF_6. Changes are made to (1) the parameters in the GASDATA data block where the properties of the pollutant are defined, (2) the parameters in the CONTROL data block where the output cloud contour information is defined, (3) the parameters in the CLOUD data block where the integration step size is defined for HEGADAS-S, (4) the parameters in the TIMEDATA data block where the time-dependent plume information at a break-point is defined for HEGADAS-T, and (5) the parameters in the AUTOTIM data block by which an optimal set of output times is decided internally by HEGADAS-T. The rationale for the above changes are given below in the "Guidance for Use" section.

Deviations from the original HSI and HTI files and the additional required information for HEGADAS/UF_6 are discussed below.

FLUX: This parameter does not apply to HEGADAS-S, i.e., the user must specify the dry pollutant emission rate in kg/s, rather than kg/s/m^2.

WATERPOL: This parameter does not apply to HEGADAS/UF_6.

EXGASPOL: This parameter does not apply to HEGADAS/UF_6.

WPICKUP: This parameter does not apply to HEGADAS/UF_6.

ENTPOL: This parameter does not apply to HEGADAS/UF_6.

MWGAS: This parameter always refers to the molecular weight for UF_6, regardless of the composition of the mixture.

CPGAS: The value of this parameter, although mandatory for HEGADAS, is not used for UF_6 releases.

SPECIES: This parameter does not apply to HEGADAS/UF_6, since the physical properties for all species participating in the UF_6 chemical reactions have been "hard-wired" in the code.

DXFIX: This parameter does not apply to HEGADAS-S/UF_6. The information is hard-wired in the code.

NFIX: This parameter does not apply to HEGADAS-S/UF_6. The information is hard-wired in the code.

XGEOM: This parameter does not apply to HEGADAS-S/UF_6.

CU: This parameter does not apply to HEGADAS/UF_6.

CL: This parameter does not apply to HEGADAS/UF_6.

CUV: This parameter does not apply to HEGADAS/UF_6.

CLV: This parameter does not apply to HEGADAS/UF_6.

CAMIN: This parameter refers to the ground-level, center-line mass concentrations (kg/m^3) for UF_6 at the termination of a HEGADAS run.

COMIN: This parameter refers to the plume-averaged mass fraction (%) for UF_6 at the termination of a HEGADAS run.

AUTOTM: The AUTOTM data block and its associated parameters do not apply to HEGADAS-T/UF_6.

ITYPBR: This parameter does not apply to HEGADAS-T/UF_6, i.e., break-point simulations are not supported.

RBUND: This parameter does not apply to HEGADAS-T/UF_6.

H: This parameter does not apply to HEGADAS-T/UF_6.

BRKDATA: This parameter does not apply to HEGADAS-T/UF_6.

ZRS: This parameter does not apply to HEGADAS-T/UF_6.

When running HEGADAS/UF_6, the user must also provide the FRC file (see the AEROPLUME/UF_6 section for a description of the FRC file), where the initial composition of the mixture is specified. It is important that the release temperature specified in the HSI or HTI file be as close as possible to the equilibrium temperature corresponding to the mixture composition specified in the FRC file as possible. Otherwise, the thermodynamics routines may have difficulties finding a convergent solution.

13.A.2 Output

The main output data file (the HSR file) for HEGADAS-S/UF_6 is similar to that for the original HEGADAS-S model, but includes the following additional information: (1) plume-averaged mass fractions (%) for total UF_6, UO_2F_2, HF, water vapor, and air; (2) equivalent ground-level center-line mass concentrations (mg/m^3) for UF_6, UO_2F_2, HF, uranium, and fluorine; (3) the fraction of UF_6 that is in the vapor phase, (4) the Briggs plume lift-off parameter (see Section 6.2 of Hanna et al., 1995); (5) plume rise (m) if plume lift-off has taken place; (6) the air entrainment rate; and (7) the mixture density relative to air. Currently, when the Briggs lift-off parameter exceeds 20, it is assumed that the whole plume bodily lifts off the ground without changing its original shape, and the location of the maximum concentration remains at the "base" of the plume. As a result, after plume lift-off has occurred, the so-called "ground-level" concentrations listed in the HSR file in fact refer to the maximum concentrations observed at the elevated base of the plume, and the concentrations between the base of the plume and the ground are assumed to be zero.

The main output data file (the HTR file) for HEGADAS-T/UF_6 is similar to that for the original HEGADAS-T model, but includes the following additional information: (1) plume-averaged

mass fractions (%) for total UF_6, UO_2F_2, and HF; and (2) equivalent ground-level center-line mass concentrations (mg/m^3) for UF_6, UO_2F_2, and HF.

13.A.3 Guidance for Use

HEGADAS/UF_6 is used to simulate the dispersion of a ground-based area source that is initially heavier than air. The source should not possess any initial momentum of its own.

Because the physical properties for all species participating in the UF_6 chemical reactions with water vapor are specified in the HEGADAS/UF_6 code, there is no need to specify this information in the input file. Output information concerning cloud contours is disabled in HEGADAS/UF_6, since it is not practical to print out the contour information for each of the many species (e.g., UF_6, HF, uranium, etc.) Moreover, the integration step size is hard-wired in the HEGADAS-S/UF_6 code, assuring that sufficiently small step sizes are used to account for the relatively fast UF_6 chemical reactions.

So-called "break-point" simulations are not supported in HEGADAS-T/UF_6. Instead, the user must specify the time-varying information concerning the source (located at zero downwind distance) in the HTI file. The only exception occurs for the case when HEGABOX/UF_6 is run first, and a transition to HEGADAS-T/UF_6 is made at some time after the release. In addition, the automatic selection of output times is not supported in HEGADAS-T/UF_6, since the automatically-selected output times do not provide adequate resolution for the fast UF_6 chemical reactions.

HEGADAS-T/UF_6 is computationally intensive. The time-varying behavior of the release is simulated through the release of many the so-called "observers", where each observer is characterized by a single steady-state HEGADAS-S/UF_6 simulation. In the steady-state version of HEGADAS, the integration step size is directly specified by the user; however, in the transient version of HEGADAS, the integration step size is indirectly controlled through the specification of output times in the HTI file. In order to guarantee sufficiently small integration step sizes, it is necessary to specify a large number of closely-spaced output times in the HTI file. It is recommended that the output times not be more than a few seconds apart when the thermodynamic effects of UF_6 chemical reactions are important (i.e., when the UF_6 mass fraction is higher than, say, 10%). In addition, the program needs to simulate the release of many observers to ensure sufficient resolution. This combination of large numbers of output times and large numbers of observers leads to relatively long execution times for HEGADAS-T/UF_6. While the original HEGADAS-T code allowed a maximum of 20 output times and 161 observers, the new HEGADAS-T/UF_6 code can handle a maximum of 200 output times and

321 observers. (The limits on output times and observers are specified in the PARAMS.INC include file, and can be easily changed.) As a result, the program must be compiled using 32-bit FORTRAN compilers where the DOS 640 KB limit of the program size does not apply.

A plume lift-off mechanism (see Section 6.2 of Hanna et al., 1995) is implemented in HEGADAS-S/UF_6. However, the user is warned that, because the implementation is a first-order attempt to describe how the plume lifts off the ground, the results should be interpreted with caution. The HEGADAS model assumes an exponential variation of concentration with height, with the maximum concentration at the ground or the bottom of the plume. When the plume lift-off criterion is met, the plume bodily lifts off the ground without changing its shape. The vertical concentration distribution keeps its exponential shape, but the base of the plume is elevated, with zero concentration in the region between the ground and the plume.

If the user decides not to use the new meteorological processor described in Section 6.3 of Hanna et al. (1995), it is important that the Pasquill-Gifford stability class and the ambient wind speed, both specified in the HSI and HTI files, should be consistent. For example, a high ambient wind speed (> 5.0 m/s) indicates neutral conditions. If the user decides to use the meteorological processor, then the value of the stability class specified in the HSI and HTI files will not be used, and will be replaced by a value internally calculated by the code.

The HEGADAS-S/UF_6 code is robust. We have not found any cases where the model failed to run to completion. However, if any numerical difficulties do occur, users are advised to slightly alter the input ambient or source conditions.

The HEGADAS-T/UF_6 code is also robust, since it involves multiple runs with the HEGADAS-S/UF_6 code. However, HEGADAS-T/UF_6 implements various convergence checks to ensure that the predicted concentrations from each observer can be merged together to yield a smooth description of the time-varying behavior of the release. These convergence checks sometimes cause the program to stop before its normal completion. If this occurs, the input conditions (e.g., output time and the time-varying source data) should be slightly altered and the code rerun.

19. User's Manual for VENT, A Program to Calculate Concentrations on Building Faces

A stand-alone FORTRAN program, "VENT.FOR", was coded to calculate the concentrations on building faces due to releases from vents (Hanna et al., 1995). To run this program, the user is prompted to provide the following information:

- source emission rate (kg/s),
- source volume flux (m^3/s),
- upwind wind speed at the height of the building (m/s),
- distance between the receptor and the vent (m),
- building area (m^2), and
- whether the receptor is located on the upper 2/3 of the building,

The program then calculates the value of the maximum concentration (kg/m^3) on building faces.

References

Hanna, S.R., J.C. Chang, and J.X. Zhang, 1995: Technical documentation of HGSYSTEM/UF_6 model. Prepared for Lockheed Martin Energy Systems, Oak Ridge, TN 37831, by EARTH TECH Inc., 196 Baker Avenue, Concord, MA 01742.

Post, L., 1994a: HGSYSTEM 3.0 User's Manual. Shell Research Limited, Thornton Research Centre, Chester, England, TNER.94.058.

Post, L. (Ed.), 1994b: HGSYSTEM 3.0 Technical Reference Manual. Shell Research Limited, Thornton Research Centre, Chester, England, TNER.94.059.